ABSTRACT

FLEMING, AARON JOHN. Towards Neural Control of Powered Prosthetic Ankles for Enhanced Postural Control: Investigation of Muscle Coordination in Individuals with Transtibial Amputation. (Under the direction of Dr. He (Helen) Huang).

The loss of a lower-limb impairs an individual's mobility and independence since the design of current prostheses are focused primarily on restoring basic functions, like walking. Modern powered prostheses can provide active support to individuals; however, these devices are limited by their ability to sense the user's environment. Individuals with amputation are forced to relearn to navigate their world with a device that provides limited assistance, leading to significantly decreased balance confidence, increased energy consumption and risk of falls. While individuals with amputation lose agency over their missing limb, they retain the ability to communicate intent via efferent motor commands to the intact nerves and muscles within the residual limb. These neuromuscular signals can be observed through electromyography (EMG) and used as control inputs to the prosthesis. One method, termed direct EMG control, measures EMG activity from the residual muscle to continuously and proportionally change prosthetic joint mechanics (i.e., joint torque, stiffness). Early work with this control paradigm investigated the ability for amputees to use residual muscle activity to drive prosthetic device behavior, however these studies have been limited. These studies used a single residual muscle, have only attempted cyclic behavior like walking. Thus, it is unclear 1) whether individuals can coordinate the activity from multiple previously antagonistic residual muscles to improve prosthesis function and 2) whether dEMG control using previously antagonistic residual muscles can improve activities outside of steady state walking like standing postural control. This work sought to investigate the ability for individuals with transtibial amputation to coordinate previously antagonistic residual muscle activity for the enhancement of standing stability.

In Chapter 1, I reviewed the literature on the research conducted on EMG control of lower-limb prostheses. This chapter demonstrated the potential for dEMG as a control paradigm and show the need for volitional control to restore activities, like standing postural control, that would be especially challenging for autonomous control paradigms.

In Chapter 2, I analyzed the ability for individuals with transtibial amputation to coordinate residual muscle activity to control a virtual inverted pendulum. In this study I observed that individuals with transtibial amputation are capable of adapting activity from their previously antagonistic residual muscles to improve performance. Participants varied in the amount they improved performance over time, demonstrating the need for further study to uncover the potential mechanisms that allows some individuals to learn more rapidly than others. This study demonstrated the promise for individuals with transtibial amputation to use dEMG control of a powered prosthetic ankle to improve standing postural control.

In Chapter 3, I investigated the ability for individuals with transtibial amputation to use their residual muscles in dEMG control of a prosthetic ankle to improve prosthetic control during expected perturbation. The results demonstrated the ability for transtibial amputees to restore postural control mechanisms (i.e., anticipatory and compensatory postural adjustments) with dEMG control after guided, extended training. Individuals significantly improved balance metrics and improved symmetry between their intact and residual limb behavior.

In Chapter 4, I investigated the potential neural mechanisms (via muscle mode analysis) that individuals with transtibial amputation employ while learning to use dEMG control of a powered prosthetic ankle. After participants trained with dEMG controlled prosthetic ankle I observed significant changes in the potential neural structure of control. Participants restructured muscle modes, coordinating homologous intact and residual muscles. Amputees improved

proficiency of muscle module recruitment and efficiency of the recruited muscle modules. This study of residual-intact muscle coordination during standing postural sway tasks demonstrated the flexibility of amputees to shift neural structures for improved control. Future study should investigate if these developed muscle modes can be generalized to improve function across multiple activities.

Towards Neural Control of Powered Prosthetic Ankles for Enhanced Postural Control: Investigation of Muscle Coordination in Individuals with Transtibial Amputation.

by
Aaron John Fleming

A dissertation submitted to the Graduate Faculty of
North Carolina State University
in partial fulfillment of the
requirements for the degree of
Doctor of Philosophy

Biomedical Engineering

Raleigh, North Carolina
2022

APPROVED BY:

Dr. He Huang Committee Chair	Dr. Michael Lewek
Dr. Jason Franz	Dr. Jonathan Stallrich

Dr. Nitin Sharma

DEDICATION

This dissertation is dedicated to my Mom, Dad, Joshua, and Kayla. I love you and I'm thankful for your unconditional love and support.

BIOGRAPHY

Aaron John Fleming was born in Philadelphia, PA to Robert and Judith Fleming. He grew up in Wake Forest, NC with his brother and sister, Joshua and Kayla. Aaron and his siblings were homeschooled by his Father, Robert for all their schooling until college. Aaron attended North Carolina State University where he earned his B.S. in Mechanical Engineering. Shortly after graduating Aaron worked in the Neuromuscular Rehabilitation Engineering Lab (NREL) under Dr. Huang, part-time, assisting graduate students with studies. Aaron then lived close to 2 years in Senegal where he taught English, learned French and built relationships with friends around faith and God. Aaron returned to the states to pursue his PhD in the Joint Department of Biomedical Engineering at NC State University and UNC Chapel Hill in the NREL Lab. During his time in the program, Aaron has been awarded a NIH pre-doctoral fellowship. Aaron also co-founded a startup company, OpenGait Prosthetics, with the aim of developing prosthetic socket technology that improves access for individuals with amputation in low-resource settings. Aaron's next plans are best by summarized by a scene from the movie "Night at the Museum":

Teddy Roosevelt to Larry: "It's time for your next adventure."

Larry replies, "I have no idea what I'm going to do tomorrow."

Teddy whispers back, "How exciting!"

ACKNOWLEDGEMENTS

I want to thank Dr. He (Helen) Huang. Thank you, Helen, for believing in me and giving me countless opportunities to succeed in the pursuit of this PhD. You have challenged me more than I have ever been before. I have become a better researcher, writer, and student because of it. Because of you I have a voice in my head that always says “so what” challenging me to look beyond and understand the bigger picture of my work. For all of it I am thankful.

I must thank Stephanie Huang, my second mentor. Thank you for your patience with my early grad school years and your countless points of feedback that has made my work and, more importantly, my thinking better. You perceive and understand the world around you better than most and I hope I can one day have a fraction of the quality of work that you put into everything you do.

Thank you to my lab mates, current and past, who have helped me at many points. I truly believe NREL has had one of the healthiest, and supportive lab dynamics between grad students and I do not take that for granted. Thank you to Ming, who first interviewed me as a fresh undergrad trying to work in the NREL Lab in 2014. From every point since then you have only ever been helpful.

To my family – thank you for always supporting me and being there whenever I needed to talk about research. My family and homeschooling are the reason I had many of the tools to succeed in graduate school.

To the participants of these studies (and now friends of mine) – Thank you for your time and patience. Without you this work would not be possible. It is my hope and expectation that this work will be a step towards making prostheses that empower you to achieve your goals.

To my partner and best friend Ashlyn Young – thank you being there in the highs and lows of grad school. You make life better, and I can't wait to see what the next phase of life has for us.

Lastly, I want to thank God. I cannot escape the fact that arriving at this point has been a combination of not only hard work, but many fortunate events. I am convinced that without my relationship with God I would not be the man I am today.

I say to the LORD, "You are my Lord; I have no good apart from you." – Psalm 16:2

TABLE OF CONTENTS

LIST OF FIGURES

Appendix B

LIST OF TABLES

CHAPTER 1

Fleming, Aaron, et al. “Myoelectric control of robotic lower limb prostheses: a review of electromyography interfaces, control, paradigms, challenges and future directions.” *Journal of Neural Engineering.* 2021. (Used in section 1.2-1.4)

1.1 Background on Individuals with Lower Limb Amputation

The loss of a limb drastically changes the life of an individual. After lower-limb amputation, individuals typically are prescribed a prosthesis that is passive, where the dynamics of the prosthetic knee and/or ankle joint are fixed. These devices allow individuals to return to basic activities of daily life such as standing and walking, however these tasks now require more effort [1, 2], cognitive load [3, 4], and are inherently more dangerous due to the increased risk of fall [5-7]. Through rehabilitation, individuals with amputation can adapt movements *around* their new prosthetic limb mechanics to improve many of these factors [2, 8, 9]. Though, even with rehabilitation, individuals with lower-limb amputation have low balance confidence and still high risk for falling [6, 10, 11].

In recent years, powered prostheses have become commercially available, where ankle and knee joints can produce active joint torque which could be used to restore function in many daily-life activities. While the design of these devices allows for the potential to use this power, the control of prosthetic ankle and knee joints are still in their infancy. The EmPower prosthetic ankle (Ottobock, Germany), for example, provides active torque assistance during different various steady state walking conditions (uphill, downhill, level ground etc.). This device, however, provides no assistance to other activities like standing balance, squatting, reaching, turning and many other activities which make up for the whole of movements that individuals

with amputation make daily. Further, this and other devices are only capable of making reactive changes based on the information available to the onboard prosthesis sensors. This means that the prosthesis does not adapt behavior in situations of expected perturbation (i.e., catching a door that is swinging open, releasing an object) where the device is naïve to need for anticipatory action. Truly there are a myriad of activities for which prosthesis control has yet to evolve to adequately assist amputee users. One potential path to drastically expand the capability of lower-limb prosthesis control is by taking advantage of the retained ability of amputees to communicate intent of movement of the missing limb (often termed 'phantom limb') via efferent motor commands to their residual limb.

1.2 Review of EMG Control of Lower Limb Prostheses

A human controlling a prosthetic limb as if it were their own biological limb has fascinated biomedical researchers for many decades [12-17]. At the centre of this idea is a direct link between the human nervous system and the prosthesis actuators, allowing for commands from the user to the prosthetic limb. Electromyography (EMG) provides an additional way to decode peripheral efferent signals from muscles in the residual limb [18]. EMG signals are common control signals for powered upper limb prostheses and have been in use for over 50 years [19]. In contrast, EMG control of robotic lower limb prostheses is still in its infancy. This is largely because: (1) motorized, robotic lower limb prostheses have only been practical as devices in the past decade, and (2) autonomous control of robotic lower limb prostheses has been sufficient to support basic locomotive activities in amputee users [20-26].

The time is ripe to develop myoelectric control of lower limb prostheses to maximally restore motor function of individuals with lower limb amputations. The mechatronics of robotic lower limb prostheses have become more mature, practical, and accessible [26-28], yet these

modern, robotic devices are still limited in function, partly because the devices are pre-programed autonomous machines [21, 22, 29-33] unable to directly take user input. Current autonomous prosthesis controllers are sufficient to actively assist cyclic stepping motions in predictable environments (e.g. a clean floor in clinics), however they are inadequate to actively assist *versatile daily tasks* that require coordination with user intent (e.g. anticipatory postural adjustments in standing or walking, performing leisure activities) [34, 35]. They also do not provide adaptation to varying, unconstructed environments and task contexts (e.g. change of load carriage or walking on uneven terrains) [36, 37]. While increasingly complex autonomous control designs are being developed to incrementally address these drawbacks, myoelectric control, on the other hand, can be a simple and viable solution to resolve these limitations because the human motor control system is highly flexible and adaptable to changing tasks and environments.

Publications on EMG control of robotic lower limb prostheses have started to emerge and accumulate in the last decade [16, 38-41]. Decoding algorithms and control frameworks have significantly advanced since the early foundational EMG control analysis [12, 42, 43]. These pioneering studies explored different EMG decoding algorithms and control frameworks, brought forth novel functionality in robotic prosthetic legs which cannot be easily achieved by autonomous control, and showed feasibility and promise in amputee testing. However, none of these existing methods have been adopted by commercial lower-limb prostheses so far. Thus, this chapter aims to summarize the literature related to EMG control of robotic lower-limb prostheses. One goal of this review is to highlight the factors affecting EMG control of lower limb prosthetic devices. A second goal is to evaluate current EMG control paradigms. And third is to identify opportunities for improving prosthesis function through the restoration of volitional

control of a missing joint. To address our goals, we first review the different surgical approaches/muscle nerve configurations and how they could influence EMG control. We then summarize the current methods for measuring EMG and the existing EMG control paradigms. Finally, we address current opportunities for EMG control to improve dynamic autonomous prosthetic control. The resulting knowledge may provide a novel control framework for robotic lower limb prostheses, shared by both autonomy and humans, to maximize the mobility of individuals with lower limb amputations.

1.3 Relevant Factors affecting Electromyographic Control of Prosthetic Limbs

Considerations of the biological configuration of residual muscles, existing sensor technology and current control strategies will be needed to advance the field of EMG prosthetic control. This section reviews the current state of each of those areas to provide a full perspective of the state of EMG control in lower limb prosthetics. We start with residual muscle configurations to summarize existing amputation procedures and how they could impact EMG residual muscle signal quality. Section 1.2.1 reviews current methods for measuring residual muscle EMG inside the prosthetic socket. Section 1.2.2 summarizes current EMG control paradigms, in which we focus on supervisory control (i.e., hierarchical combination of an EMG decoder for locomotion mode recognition with state-machine-based autonomous control) and direct control (i.e. continuous EMG control of prosthetic joint mechanics). Within each control paradigm, we layout considerations/approaches as well as evaluation methods and reported results. Tables A1 and A2 (Appendix A) provide additional information about study methods and controller information for the reviewed studies.

1.3.1 Amputated Muscle/Nerve Configuration

The configuration of the muscle-nerve attachment (i.e., to bone or tendon) in the residual limb determines how existing biological signaling pathways can be used for prosthetic feedback and neuromuscular control [44-46]. Many factors, such as the cause of amputation (e.g., traumatic or dysvascular), residual limb length and shape, and subsequent muscle atrophy, can influence existing number of motor units, proprioceptors, and afferent neurons, which alter muscle fiber function and quality [47-50]. The type of surgical technique used for limb amputation is crucial for preservation of muscle tone and length, motor unit recruitment, and proprioception. For example, residual muscles must be stabilized to either muscle or bone at appropriate tensions [51, 52] because insufficient or too high tension can lead to atrophy, contractures, and/or pain. These resulting issues can affect residual muscle activity [51-53] and the quality of EMG signals in prosthesis control.

Traditional surgical techniques for lower limb amputations have had little evolution and do not consider the neural interface for prosthesis control [54]. The most common surgery for transtibial and transfemoral amputees discards distal tissue around the amputation site and fixes isolated muscle bellies through a combination of myodesis and myoplasty [51, 55, 56]. Myoplasty sews opposing muscle groups together while myodesis attaches muscles directly to bone [51]. The nerves are transected and positioned in soft tissue away from scar tissue, the incision, or areas subject to prosthetic socket irritation, with the goal of minimizing painful neuromas [51]. Residual muscles after traditional amputation surgery can still be activated by the brain and spinal cord, but the EMG patterns during walking are often different from the patterns in physically intact humans [57-59].

Recently, novel surgical techniques have been developed that consider the human-machine interface of a powered lower limb prosthesis. The goal of the surgical techniques is not just to reshape the residual limb, but to improve the neural interface for adaptable, reliable neuromuscular control of lower limb prostheses in dynamic real-world environments.

One surgical technique, the Agonist-Antagonist Myoneural Interface (AMI), attempts to use the body's natural mechanisms for proprioceptive feedback to enhance prosthetic control and embodiment. In the AMI, surgeons reconnect agonist-antagonist residual muscle pairs to restore reciprocal muscle function [60]. When the agonist contracts, the mechanical linkage stretches the antagonist and vice versa. Such reciprocal contractions engage length and force receptors in both muscle-tendon units, resulting in a more natural sensation of position and velocity for improved motor control of residual muscles [44, 60, 61]. One individual who received the AMI procedure produced more isolated contractions of antagonist residual muscles and improved stability in gait-related tasks when using an EMG controlled 2-degree-of-freedom prosthetic ankle compared to amputees without the AMI [44]. The individual also exhibited reflexive prosthesis motions indicating a higher level of embodiment. In order to produce this antagonist mechanical linkage for individuals who have already received a 'traditional' amputation surgery, a regenerative neural interface has been proposed to implement AMI through the use of targeted muscle reinnervation and muscle grafts [62, 63].

Targeted Muscle Reinnervation (TMR) is a surgical technique that aims to restore neuromuscular control sources in amputees by transferring residual nerves to muscles that are no longer biomechanically functional [45, 46, 64]. The reinnervated muscles act as a biological amplifier to restore EMG recording sites for the missing joint control [45, 46]. For example, the tibial nerve branch for transfemoral amputees can be connected to the *semitendinosis* and the

common peroneal nerve branch can be inserted into the long head of the *biceps femoris* [65]. The EMG signals from these reinnervated thigh muscles can convey neuromuscular control signals for the prosthetic ankle joint. Combining peripheral nerve surgery with EMG based control strategies for prosthetics has led to more coordinated control of multi-jointed prosthetic devices. The majority of studies using TMR have been on individuals with upper limb amputations [45, 66, 67], but there is increasing focus on shifting to individuals with lower limb amputations [65].

1.3.2 Neural Interfaces

One of the most critical aspects of neural prosthesis control is the accurate and robust sensing of neuromuscular activity (i.e., the control input). The limb-socket interface of lower-limb prostheses, which are subject to weight bearing forces, sweat accumulation, changes in limb volume, make EMG sensing challenging (discussed more in Section 3). A majority of existing studies on myoelectric control of lower limb prostheses have used bipolar surface EMG electrodes to record neuromuscular control signals. One major challenge with this approach is the attachment of EMG electrodes within the prosthetic socket or liner for reliable EMG recordings without compromising socket suspension or user comfort. One study developed several socket-EMG interfaces that integrated commercial EMG electrodes on the prosthesis socket directly [68]. Additionally, fluctuations in residual limb volume over time, can compromise reliable skin contact with the sensor inside the socket. Recent studies have used low profile, neonatal EMG sensors within the prosthetic socket for successful myoelectric prosthesis ankle control [69, 70]. A novel prosthetic liner with embedded dome electrodes and conductive textile fibers [71] can ease the sensor placement and wire management and yield reliable skin-electrode contact. Furthermore, new flexible, low-profile EMG sensors [72] have the potential to

be fabricated directly within the prosthetic liner, ensuring comfort and reducing skin contact problems that arise from limb volume fluctuations.

Another challenge with myoelectric control of lower limb prostheses can be the placement of bipolar EMG electrodes to target specific residual muscles. Although the volume of lower limb muscles is relatively large compared to those in the upper limbs, identifying specific muscles is often challenged by atrophy of residual musculature and lack of knowledge on amputation procedure. Fite et al. used principal component analysis of surface EMG to reduce the effect of variation in measured residual muscle activity caused by differences in sensor placement across days [39]. This provided some success at standardizing the myoelectric signals for prosthetic control.

Implantable EMG sensor interfaces can mitigate limitations accompanying bipolar surface electrodes. Wireless intramuscular EMG sensors have been developed recently to transmit muscle activity signals from residual muscles to the prosthesis without any transcutaneous leads [73-78]. This interface has significant potential to target specific residual muscles not reachable with surface EMG and could be surgically implanted in parallel with other surgical procedures such as osseointegration or never reinnervation. These invasive neural interfaces have been, however, primarily tested in upper limb amputees to date. We are aware of only one study that implanted wireless intramuscular EMG sensors in lower limb amputees for prosthesis control [76]. Another promising technology is high-density, flexible surface EMG. It may provide more information and greater resolution of residual muscle activations for prosthesis control. High-density EMG was first used with amputees to confirm reinnervation of residual muscles [79, 80]. Other studies have used high-density EMG to remove motion artifacts [81, 82] in walking and measure muscular activity from ankle flexors/extensors and

invertors/evertors for prosthetic control [83]. High-density EMG shows significant potential for future prosthetic control development through integration of individual motor unit activations with prosthetic control, targeting specific muscle locations more easily, and removing artifacts caused by movement.

1.4 EMG Control Paradigms

Current commercialized robotic prosthetic legs (e.g. e.g. PowerKnee^{TM}, Össur, Iceland; EmPower, Otto bock, Germany) do not rely on active neuromuscular human input for control but instead use onboard kinetic/kinematic sensing to drive autonomous controllers for pre-programmed activities [84]. These commercial devices employ finite-state machines to adjust knee and/or ankle joint impedance or position the joints based on predefined states such as the gait phase (e.g. swing and stance) and locomotion mode (e.g. stair ascent and level-ground walking) [21, 22, 29]. Transitions between gait phases can be triggered by measurements of intrinsic sensors (e.g. a load cell or motion sensor) in the prosthesis, while transitions between locomotion modes often requires input from the human user (e.g. specific body motions measured by sensors) [25, 85-87]. Existing autonomous control approaches are sufficient to assist amputees walking in well-defined environments, but they are inadequate for unconstrained tasks that require dynamic user intent and/or adaptation with varying environments (e.g. trail hiking, jumping, catching objects, etc.). These limitations have sparked interest in the research community to develop neural/EMG control that might improve adaptability and versatility of robotic lower limb prostheses. There have been two prominent approaches to integrate amputee users' efferent neural signals (i.e. EMG signals) for lower limb prosthesis control in the current literature: supervisory EMG control and direct EMG control (Figure 1 & 2).

1.4.1 Supervisory EMG Control

In current commercial robotic lower limb prostheses, transitions between locomotion modes are achieved manually, which is cumbersome. Instead, supervisory EMG control automatically recognizes the user's locomotion mode by EMG pattern recognition (Figure 1). By monitoring EMG patterns, prostheses can hierarchically adjust low-level autonomous control (e.g., finite state machine) to switch control based on recognized task modes [13, 37, 41, 88, 89]. Essentially, supervisory EMG controllers are built upon autonomous locomotion-mode-dependent prosthesis control, where the joint mechanics in each task are dominated by the low-level autonomous control. In this manner, the supervisory EMG controller acts as a part of a finite-state machine and it adjusts the mechanics of prosthesis joints only at the locomotion mode transitions.

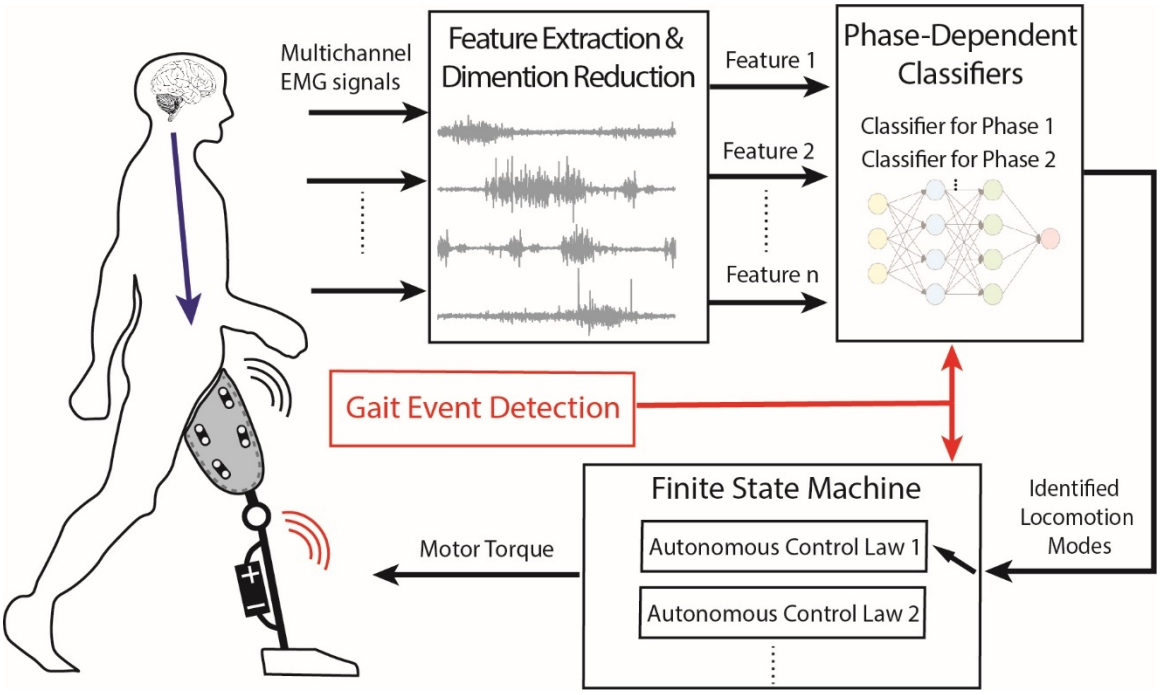

Figure 1-1 Supervisory EMG control paradigm for robotic lower limb prosthesis. In supervisory EMG control, EMG signals and gait events are used to classify the user's locomotion mode (such as level-ground walking, stair ascent/descent, ramp ascent/descent). The classifier's decision determines transitions between the predefined finite-states and thus the specified low-level control prosthesis operation associated with the state. In this paradigm the user's residual EMG activity has no effect on the prosthesis dynamics within locomotion modes since the autonomous control law is predetermined by the finite state machine. In the case of prosthesis error, adaptations in efferent neuromuscular signals (blue arrow) do not directly modulate prosthesis dynamics. Thus, the user is not encouraged to adapt residual muscle activity while using supervisory EMG control. However, changes in EMG activity over time could lead to improvements in classification accuracy of the available locomotion modes.

1.4.1.1 Input Signals

In past studies, researchers used EMG signals recorded from residual limb muscles as neural inputs for locomotion mode recognition [41, 90-93]. EMG electrodes are typically placed on the residual limb based on intact muscle anatomical location, palpation, and visual inspection of EMG signals [22, 41, 94]. Because EMG pattern recognition classified the locomotion mode based on multi-channel signal pattern, cross-talk in EMG recordings did not significantly

influence classification performance. Within the existing studies, as many as nine EMG electrodes on a residual thigh [37] or four electrodes on a residual shank [92] were used. Groups also experimented with augmenting classifier inputs with muscles above the amputation level (e.g. the *gluteus maximus* on transfemoral amputees or the thigh muscles of transtibial amputees) [37, 95, 96]. However, adding sensors to intact muscles requires additional sensors outside the prosthetic socket, increasing the complexity for daily use and sensor setup. Another group found TMR surgery on a transfemoral amputee enhanced myoelectric control information recorded from reinnervated residual muscles, improving prosthesis control [41, 97]. The participants with TMR surgery had around a 40% error reduction rate during virtual movements compared to the amputee participants without TMR [41]. Furthermore, pattern recognition that combined EMG signals with intrinsic mechanical measures (neuromuscular-mechanical fusion) further improved the accuracy and reliability of locomotion mode recognition [38, 85, 97]. This fusion-based approach outperformed the algorithm that solely used EMG or only used mechanical measurements as system inputs [38]. With this, a source selection study showed EMG signals were essential for accurate prediction of user locomotion mode transitions compared to mechanical measurements alone [90].

1.4.1.2 EMG Feature Extraction and Phase-Dependent EMG Pattern Classification

EMG pattern recognition has been widely used for upper limb prosthesis control [14, 19, 98-101], but adjustments are necessary for lower limb prosthesis control. For control of upper limb prosthesis movements (e.g., hand open), the human user must attempt the hand motion and hold the posture of the phantom hand. During this period, the EMG signals are considered to be stationary, i.e., the distribution of the stochastic signals does not change, and therefore the EMG activation pattern is consistent for the classifier to identify the user intended motion for

continuous prosthesis control. In contrast, EMG signals in the lower limbs during walking are non-stationary over a full gait cycle. As a result, a different EMG pattern recognition strategy is necessary for lower limb prosthesis control compared to upper limb prosthesis control. If we assume that: (1) gait EMG is quasi-stationary within a gait phase, and (2) EMG patterns recorded from residual muscles are different between locomotion modes, but consistent within the same mode, then a phase-dependent EMG pattern recognition strategy can be implemented. This approach has been enacted with a system consisting of multiple pattern classifiers, each corresponding to a gait phase [37] (Figure 1).

In each phase, the pattern recognition includes feature extraction, dimension reduction (optional), pattern classification, and post processing of classification decisions (optional). Feature extraction is an important step for accurate pattern classification. Selected features from the input data sources should maximally extract information that can distinguish between locomotion modes (classes). Focusing on EMG features, time domain (e.g. number of zero crossings, mean absolute value, and slope sign change) [38, 41, 92, 102] and frequency domain (e.g. medium frequency [88], bi-spectrum [89]) features have been used previously. Additionally, adding autoregression coefficients for EMG features can account for potential signal degradation, fatigue, and motion artifacts [41, 85, 103-105]. Groups have also used dimension reduction techniques, such as principal component analysis, to reduce the dimension of feature vectors and prevent model overfitting [91, 95, 104, 106]. Other feature/source reduction methods explored in lower limb prosthesis control include sequential forward and backward selection and minimum-redundancy-maximum-relevance algorithms [90]. The extracted features were fed to a pattern classifier for locomotion mode recognition. A variety of commonly used classifiers have been used, e.g., Artificial Neural Networks, Support Vector

Machine (SVM), Linear Discriminant Analysis (LDA), Quadratic Discriminant Analysis (QDA), and Dynamic Bayesian Networks (DBN). DBN can be combined with LDA to provide time history and feed forward information to the classifier [104]. The DBN model predicts the future locomotion model, while LDA labels the previous stride. This structure is especially helpful with EMG inputs because the classifier can re-learn EMG patterns over time or across multiple training sessions. Finally, a post-processing method, such as majority vote [38], has been considered to further reduce classification errors, but increased the system delay for real-time applications.

1.4.1.3 EMG Pattern Recognition Based Prosthesis Control

In practice, EMG or data fusion-based decoders require model training before applying them to real-time prosthesis control. Model training requires collection of labeled training data (i.e., input data with class labels), followed by establishing the parameters in the classifiers. Collecting enough training data for multiple conditions, such as sit-to-stand, ramps, stairs, and level-ground walking across multiple speeds could take hours, on top of time needed for tuning/customizing prosthesis control parameters for each user [41]. In addition, daily recollection of EMG training data for each individual user is required for reliable performance [41, 90]. A means for efficient and automatic training data collection could minimize users' time and effort to calibrate the system [107].

During real-time operation, the trained EMG classifier estimates the locomotion mode, which triggers task state transitions in the finite-state machine for robotic leg control (Figure 1). One challenge is EMG pattern recognition approaches are sensitive to EMG signal variability caused by disturbances (like motion artifacts and electrode location shifts over time/multiple sessions) or physiological changes (such as muscle fatigue) [92, 105, 108-111], which threatens

the reliability of the supervisory EMG control system and user safety. Beyond re-training the pattern classifier, other solutions have been proposed to improve the robustness of locomotion mode recognition system [112]. For example, classifiers with redundant EMG sensors can detect abnormal signals, reject corrupted EMG channels, and only select viable EMG signals and mechanical sensor inputs for robust performance [108]. Adaptive pattern recognition, which can update the parameters in the classifier while using it in real-time, can be another promising solution to allow for robust classifiers better equipped to handle real-world settings [104, 113]. Another challenge for supervisory EMG control is the definition of timing to trigger the switch for low-level prosthesis control mode [114]. Although EMG pattern recognition provides real-time decisions regarding the user's locomotion mode, the low-level controller parameter only updates at one critical timing that is defined for each type of task transition. For example, Huang et al. defined the critical timing for transitions from level-ground walking to stair ascent at the prosthesis foot toe-off before stepping on the staircase to ensure a smooth and safe switch of walking terrain in amputee users [38]. Table 1 in the Appendix summarizes existing literature related to EMG-based locomotion mode recognition and supervisory control with detailed approaches used in each study. Note we only included the studies that tested the system on individuals with lower limb amputations in this table.

1.4.1.4 Performance/Evaluation Metrics

The performance of supervisory EMG control systems is typically evaluated by classification error/accuracy rate, the confusion matrix during steady state activity, and/or prediction accuracy of task transition and prediction time. The reported accuracy rate ranges from 75% to 99%. Usually, task transition can be predicted accurately before the defined critical timings [37, 38, 89, 104, 105]. The most common classification error is between ramps and

level-ground walking [41, 104, 115]. However, how these engineering performance metrics influence the amputee user's locomotion performance is unclear. Zhang et al. systematically studied the influence of errors and delays in supervisory EMG control of robotic knee prostheses on human walking stability [114, 116]. The research found that not all errors disturb measured dynamic stability and the user's perceived walking stability; it depends on the timing and cumulated mechanical work change around the prosthesis knee joint. The group also suggested a range of timing for switching prosthesis control mode that ensures user safety during terrain transitions [114].

Supervisory EMG controllers are inherently autonomous finite-state-machine-based controllers where the low-level autonomous control law dominates the joint mechanics. Even though the EMG signals are included in the control algorithm, the EMG control only functions during locomotion mode (i.e., state) transitions and the approach is inadequate to enable the prosthesis to assist tasks that have not been preprogramed in the low-level control. This approach is also problematic for tasks that do not readily conform to the autonomous finite-state-based controller (e.g., dancing, sports activities).

1.4.2 Direct EMG Control

While most lower limb prosthesis controllers measure prosthesis activity or human muscle activity to inform a state prediction for autonomous control, direct EMG control uses active and continuous input from the human user muscle activity to determine prosthesis dynamics. Thus, direct EMG control mimics the biological neural control pathway in an intact musculoskeletal system. The efferent neural signals (EMG) of the residual agonist-antagonist muscle pairs are used to directly modulate prosthesis joint mechanics (i.e., impedance, angle, and/or torque) (Figure 2). The prosthesis joint mechanics can be determined by the human

feedforward neural output. This method has shown increasing success in improving various activity performance and postural control in a recent study [117]. Note that direct EMG control here is defined as a neuromuscular control method for powered prostheses, which follows antagonistic muscle function around a joint for movement control. Therefore, non-biomimicry mappings of EMG signals to joint mechanics, such as neural networks, are not discussed in this section.

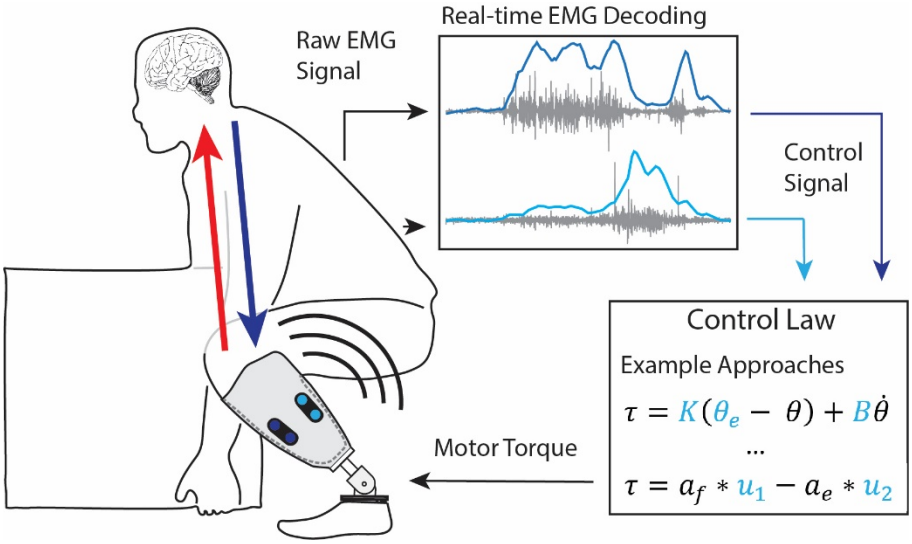

Figure 1-2 Direct EMG Control paradigm for robotic lower limb control. In the direct EMG control scheme, the magnitude of the envelope of EMG signals recorded from antagonistic residual muscles directly and continuously modulates the prosthesis joint dynamics. Various control laws are used to continuously map EMG activity to motor torque to drive prosthesis dynamics. Similar to normative joint function, the user is capable of continuously modulating efferent neuromuscular commands (blue arrow) in response to afferent feedback (red arrow) about the state of the prosthetic ankle joint, though this feedback is significantly altered compared with intact joints.

1.4.2.1 EMG Decoding Methods

The inputs of the decoder for direct EMG control are the EMG signals recorded from residual antagonistic muscles. Most commonly, the magnitude of the EMG signals

proportionally increases a prosthetic joint parameter [16, 118]. One challenge of this approach is that the antagonist residual muscle sometimes inadvertently contracts as the amputee intends to activate the agonist muscle only, causing a certain level of involuntary co-activation [39, 57]. Involuntary co-activation limits the ability of amputees to access portions of the control input space like isolated joint flexion or extension. To avoid this problem, one approach incorporates an EMG classifier in the direct EMG control scheme to identify the isolated intended joint motion (e.g. flexion vs. extension) first [106]. This approach has been evaluated on individuals with amputations in the sitting position, but not during walking. Another solution first transforms the multiple-channel EMG inputs via principal component analysis [39] or non-negative matrix factorization [83] to obtain the isolated "motor primitive" representing the voluntary control for each studied motion. These decoding algorithms may help amputees with involuntary co-activation [57]. However, it remains to be seen whether amputees are capable of generating more isolated residual muscle contractions given sufficient training.

A large portion of work has used impedance control laws, where neuromuscular activity modulates one or multiple joint impedance parameters (i.e., set stiffness, equilibrium position, etc.). Initial efforts with impedance control used residual muscle activity to proportionally modulate equilibrium velocity (i.e. rate of change of the equilibrium point) [39, 106]. Subsequent studies incorporated relative co-activity from residual muscles to additionally modulate the set stiffness value in the impedance control law [39, 40, 60, 83]. These studies have shown the ability for amputees to volitionally modulate both stiffness and position of the prosthesis, showing promise for its commercial use. Another common output of the decoder is joint torque. While using the impedance control law described above, Fite et al. also incorporated additional torque gain terms for the residual thigh flexors/extensors to proportionally generate control

torque for a prosthesis knee [118]. This allowed the direct torque terms to be weighted depending on phase of gait (stance vs. swing) and for the impedance control to be more responsible for limb kinematics during the swing. Using a pneumatically actuated prosthetic ankle, Huang et al. used EMG magnitude of the residual *gastrocnemius* to proportionally modulate plantar-flexor torque [16, 119], and this control method has been extended to two agonist-antagonistic residual muscles to control both dorsi- and plantar-flexor torques [69, 70].

Musculoskeletal models are another possible means of EMG decoding method for direct EMG control. The EMG magnitude, extracted from EMG signals of residual agonist-antagonist muscles, activates a virtual musculoskeletal model (similar to a human biological joint) to estimate the missing joint mechanics. However, this type of control has only been tested with a virtual ankle joint for transtibial amputees in a sitting position [93] and with able-bodied individuals walking with a bent-knee adapter [120].

1.4.2.2 Activity Evaluation

The gold-standard task to evaluate direct EMG control paradigms in the literature has been locomotion. For transfemoral amputees, direct EMG control has been tested for over-ground walking [39, 121] and stair ascent [118]. These preliminary studies with an individual amputee showed potential for amputees to adapt residual thigh muscles to control prosthetic knee torque during cyclic movements like walking. For transtibial amputees, direct EMG control has been tested in over-ground walking using the residual *gastrocnemius* [16, 119]. Amputees successfully adapted their residual muscle activation once given feedback of the prosthetic ankle state. Clites et al. incorporated multiple residual muscles into prosthesis control for stair ascent and descent for transtibial amputees [60]. Direct EMG control was also tested in stair ascent/descent and over-ground walking on a transtibial amputee after receiving an AMI surgery

[60]. The AMI recipient demonstrated restored reflexive muscle activity and improved prosthesis embodiment, compared to amputees without AMI procedures using direct EMG control.

One of the benefits for direct EMG control is that it is not constrained to rhythmic locomotor tasks. Instead, direct EMG enables prosthesis assistance for a variety of activities in daily living. Unfortunately, there has been limited work to understand amputees' ability to use direct EMG control for other daily activities. Rogers et al. demonstrated the ability for EMG control of a novel powered ankle prosthesis to augment rock climbing in a person with transtibial amputation [122]. One preliminary study investigated direct EMG control use during situations with expected perturbations [69]. This study showed a transtibial amputee could produce anticipatory postural adjustments on an EMG-controlled prosthetic ankle to significantly improve stability after a perturbation. They also studied the ability for a transtibial amputee to control a variety of standing postural control tasks like quiet standing on firm and compliant surfaces as well as load transfer tasks [70]. The results demonstrated the ability for an amputee to significantly improve bilateral EMG activation synchronization and standing postural control with direct EMG control of a prosthesis ankle after extended, guided training with a physical therapist. These aforementioned activities have never been demonstrated by autonomous or EMG supervisory prosthesis control. The existing designs of direct EMG control discussed in this section are summarized in Table 2 in the Appendix along with critical study components (i.e. measured muscle activity, EMG decoding methods, Control parameters, Level of amputation, and activity used for evaluation).

1.5 EMG Control for the Enhancement of Standing Stability

This review of EMG control of lower-limb prostheses demonstrates the potential for utilizing neuromuscular signals for improving prosthesis function, however several questions

remain which will serve as the structure and motivation for this thesis. From this review it is apparent that Supervisory EMG control is suitable for cyclic tasks, where the state of the user can be easily classified. However, this paradigm may not be suitable for other tasks such as standing postural control. There exists a vast number of contexts that affect standing postural control (i.e. support surface, perturbation, balance strategy) that would require supervisory EMG control to be trained for each individual task. Direct EMG control more closely mimics the natural limb neuromechanics by allowing neuromuscular signals to directly and continuously affect joint behavior. Thus, this paradigm takes advantage of the user's ability to perceive various contexts and adapt their muscle behavior accordingly. However, in order to realize the potential of restoring volitional, continuous control of a missing limb for the improvement of standing postural control, several questions must be systematically answered: a) What is the ability for transtibial amputees to adapt and coordinate residual muscle activity from muscles that significantly contribute to maintaining postural stability (i.e., previously antagonistic Tibialis Anterior and Gastrocnemius). (Chapter 2) b) What is the ability for transtibial amputees to coordinate antagonistic residual muscle activity using dEMG control of a prosthetic ankle to improve standing balance under perturbation? (Chapter 3) c) How do transtibial amputees adapt neural control strategies to integrate residual muscle activity with intact muscle groups while using dEMG control of a prosthetic ankle? (Chapter 4). Through this analysis we expect to improve our understanding of the potential neural mechanisms that individuals with amputation employ while adapting residual muscle activity for volitional, prosthesis control. Through the restoration of active ankle joint control, we also expect individuals with amputation to restore the ability to adapt postural control mechanisms to improve standing balance. Enhancements of amputee standing balance have the potential to drastically reshape the life of lower-limb

amputees, reduce fear of falling, and improve their overall quality of life and participation in their community.

CHAPTER 2: Proportional Myoelectric Control of a Virtual Inverted Pendulum using Residual Antagonistic Muscles: Toward Voluntary Postural Control

Fleming, Aaron, et al. "Proportional myoelectric control of a virtual inverted pendulum using residual antagonistic muscles: toward voluntary postural control." *IEEE Transactions on Neural Systems and Rehabilitation Engineering* 27.7 (2019): 1473-1482.

2.1 Introduction

Postural control is required for daily-life activities and the ability to control posture is significantly altered for lower-limb amputees. Commercially-available prostheses leave amputees unable to apply typical postural control strategies at the ankle joint in situations of expected and unexpected perturbations[123], quiet standing [124, 125], and surface translations [126], resulting in significantly larger amounts of postural sway and instability. Usually amputees compensate for the loss in standing stability by developing compensatory activation strategies of intact muscles [123] and asymmetrically loading the intact limb [125, 126]. The adoption of compensation from intact joints and muscles is still insufficient to fully compensate for the loss of postural control after amputation, which is evidenced by amputees being at higher risk to experience falls and having lower balance confidence [7, 10].

Limited effort has been put forward to develop lower-limb prostheses that enable amputee users to actively engage prosthetic joints for effective postural control. One group has developed a powered prosthesis control to assist stance on various slopes [127, 128]. This ground-adaptive control for a powered prosthetic ankle-joint uses inertial sensors to recognize when the user is standing, which *reactively* initiates slope detection to then modify joint impedances and equilibrium angle. However, for situations with perturbations, postural control mechanisms (e.g. anticipatory postural adjustments (APAs)) are generated by feedforward neural

commands before the perturbations occur [129], and reactive control is inherently limited in assisting stability. One potential avenue to enable amputees to engage prosthetic joints in postural control is through direct connection of neuromuscular control commands in humans with the prosthetic ankle joints.

Electromyography (EMG) is a commonly used neural control source for artificial limbs. There are several methods that have been used to incorporate descending neuromuscular commands (i.e. EMG signals) in lower limb prosthesis control [37, 92, 130-135]. Two predominate methods include EMG pattern recognition [37, 130-132] and proportional myoelectric control [134-136]. EMG pattern recognition in powered lower limb prostheses usually maps activation patterns of residual muscles to discrete locomotion modes (such as stair ascent, level ground walking, etc.). The detailed joint motion in each locomotion mode was, however, still operated by autonomous control, not human neuromuscular control signals. In addition, EMG pattern recognition would require the pre-definition of muscle activation patterns for APA and compensatory posture adjustments (CPA) [129] in various contexts in order to train the pattern classifier. Therefore, it is challenging to use EMG pattern recognition for prosthetic joint control to assist posture adjustments in changing contexts. Alternatively, proportional EMG control allows a user to continuously modulate prosthetic joint mechanics, proportional to the EMG magnitudes of the residual muscles. That is to say the prosthetic joint is directly operated by human efferent motor commands. This design potentially can enable a prosthesis to produce both APA and CPA together with the amputee and is adaptive to perturbations with different type, timing, magnitude in various environments. However, due to disruption of neuromusculoskeletal system and disuse of the residual muscles post amputation, it remains unclear whether amputees are capable of coordinating antagonistic residual muscle activations to

accomplish a highly-dynamic balancing task with requirements similar to postural control (i.e. maintaining upright posture, avoiding falls, and generating activations related to magnitude of perturbation/load).

An initial study of the ability of lower limb amputees to use their residual muscles for proportional EMG control has involved one residual muscle [133, 135, 137]. The EMG signal recorded from the residual gastrocnemius muscle has been used proportionally modulate prosthetic ankle torque during the push-off phase only in walking[133] and stair ascent [137]. Huang et al. demonstrated the ability for amputees to continuously modulate the activity of the residual gastrocnemius to control a powered ankle in walking [135]. Note that this reported design was free of autonomous control; the plantarflexion of the prosthetic ankle was completely determined by the EMG magnitude of the residual gastrocnemius muscle in real-time.

A very limited number of studies have been carried out to understand the capability for lower limb amputees to coordinate a residual agonist-antagonist muscle pair for proportional EMG control of a prosthetic joint. In our group, we showed the ability for transtibial amputees to generate ballistic-like activation patterns (an activation pattern observed in able-bodied quiet standing) of both antagonist muscles independently [138]. Another study highlighted the difference in ability across transtibial amputees to produce patterns of reciprocal and co-activation of residual antagonistic muscles [139]. These two studies were not tested in the context of dynamic tasks. Proportional EMG control has been implemented on a prosthetic knee for a single transfemoral amputee for over ground walking [136]. Over four training sessions, the subject adapted activation of antagonistic residual thigh muscles and generated consistent knee angle trajectories, including moderate stance flexion. These studies do not demonstrate the ability for amputees apply the observed patterns of antagonistic control (reciprocal and

coactivation) for postural control since these contexts did not contain a dynamic control goal (virtual) and were for a singular, cyclic activation pattern (walking). Whereas, postural control, specifically under perturbation, requires continuous, non-cyclic responses in order to accomplish the high-level goal of maintaining balance[129]. This gap in current knowledge motivated us to investigate the potential of amputees in using proportional EMG control to actively drive prostheses for restoration of other motor functions, such as posture control in standing.

Towards our long-term goal, we developed a virtual inverted pendulum system that was an unstable, dynamic system, emulating the dynamics of human dynamics in standing posture. The inverted pendulum can be balanced by two-input EMG control signals. The purpose of this study was to investigate whether and how transtibial amputees can continuously coordinate activation of agonist-antagonist residual ankle muscles to balance the virtual inverted pendulum. The use of a virtual system shows promise as a means of an initial investigation of the ability of amputees to coordinate residual muscle continuously for performing dynamic tasks as various studies have used virtual tasks as a platform to study motor control capability of both intact and residual lower limb muscles [138-143]. We compared the task performance of amputees and that of able-bodied persons. Information gathered from this study provides a basis for future studies, involving proportional antagonist EMG control for a powered prosthetic ankle to assist balance and postural control in transtibial amputees.

2.2 Methods

2.2.1 Participants and Measurements

We recruited 6 transtibial amputees (TT) and 6 able-bodied (AB) individuals to participate in this study. Each group was composed of 5 male and 1 female subjects. This experimental protocol was approved by the University of North Carolina at Chapel Hill

Institutional Review Board. All participants provided written informed consent before participating in the study. Amputee participants' details (age, years since amputation, etc.) are shown in Table I. Average age of AB participants was 36.67(±15.15) years.

To examine the coordination of residual ankle muscles, we monitored the EMG signals recorded from the residual *tibialis anterior* (TA) and the residual *lateral gastrocnemius* (GAS) muscles in the TT subject. For the AB subjects, we monitored their intact TA and GAS muscles of their dominant leg.

Table 2-1 Amputee Subject Demographics

Subject	Age	Post Amputation	Reason for amputation
TT1	73	10	Soft Tissue Sarcoma
TT2	58	3	Septic Shock
TT3	30	6	Failed Leg Salvage
TT4	62	5	Dysvascular
TT5	70	49	Trauma
TT6	29	11	Trauma

2.2.2 Virtual Inverted Pendulum Model

We adopted and modified an inverted pendulum virtual model (Fig. 1a), previously used to mimic human postural control [140, 141]. The model contained two linear stabilizing springs, which can be used either in unison or coordinated fashion to balance a virtual pendulum (Fig.1A) [144]. The equation of motion for the system and the equation for torque, T, about the base joint are defined below:

$$\mathbf{J}\ddot{\theta}(\mathbf{t}) = \boldsymbol{mgL\,sin}\,\theta\,(\boldsymbol{t}) + \boldsymbol{T}(t) \tag{2.1}$$

$$\boldsymbol{T}(\boldsymbol{t}) = -\boldsymbol{cmgL}\theta(\boldsymbol{t}) - \boldsymbol{b}\dot{\theta}(\boldsymbol{t}) + \boldsymbol{T_{active}}(\boldsymbol{t}) \tag{2.2}$$

where *J, θ, m, g, L* and their values are respectively the moment of inertia (77 kg m^2), angle from vertical, mass (70 kg), gravity (9.81m s^{-2}), and length of rod to the center of mass (0.92 m). These values are derived from the model reported in Loram et al. [141]. The two terms (cmgLθ and $\boldsymbol{b}\dot{\theta}$*)* are the passive components of rotational stiffness (i.e., k_p in Fig. 1a) and viscosity of the base joint, respectively. Wherein, *b*, passive base joint viscosity, is set at 2.9 Nm rad^{-1} and a constant *c* is set at 0.85. The *c* value sets passive stiffness to a normative value during standing, making the passive system (T_{active} = 0) unstable giving pendulum position growth an exponential time constant of 0.92s [141]. T_{active} represents the active portion of torque from the linear springs, whose stiffness is modulated by the subject using continuous proportional myoelectric control via the (residual) ankle muscles (TA and GAS). T_{active} is defined as

$$\boldsymbol{T_{active}(t) = nh\left[(EMG_{TA}(t)k_1s_1(t)\cos\left(\theta_{p1}(t)\right) - EMG_{GAS}(t)k_2s_2(t)\cos\left(\theta_{p2}(t)\right)\right]} \quad (2.3)$$

where *h* is the height of the spring attachment to the pendulum and is 0.25m. *n* denotes a constant gain. Based on our pilot test on an amputee, we selected *n*=2 because the subject can achieve the task while maintaining a certain level of challenge. The attachment points of each spring to the ground are set at 5cm from the origin. The spring stiffness k_1 and k_2 (Fig. 1A) have values of 47,575 N/m. s_1 and s_2 are the displacement of two springs, respectively; θ_{p1} and θ_{p2} denote the angular position the orientation of each supporting spring from normal to the pendulum rod. As this work is intended to inform future myoelectric prosthetic control, the torque generated by each spring was modulated by the muscle activation level of TA and GAS, respectively. The level of muscle activation (i.e., $EMG_{TA}(t)$ and $EMG_{GAS}(t)$) was computed as the percentage of the EMG magnitude relative to the signal magnitude recorded during maximum voluntary

contraction (MVC). For an activation of 100% (10V output of real-time control board) spring stiffness is multiplied by a factor of 1.

2.2.3 Real-Time Controller and Setup

We interfaced a real-time control board (dSPACE, CLP-1103, 0-10V output) to compute control signal inputs from surface EMG signals and output the control signal values to the simulation of the inverted pendulum model. We used Simulink in MATLAB (MathWorks Inc., US) to program the controller and implemented the simulation of the virtual inverted pendulum (Fig. 1). The EMG signals were acquired by SX230 sensors and the DataLINK acquisition system (Biometrics Ltd, UK) and were further sampled at 1000Hz. To compute the EMG signal magnitude in Simulink, we first high-pass filtered the raw EMG signals using a second-order Butterworth high pass filter with 20 Hz cut off frequency in order to remove motion artifacts and other low frequency interferences. The processed signal was full-wave rectified and then low-pass filtered by a second-order Butterworth low pass filter with 2Hz cut-off frequency. The control action was made every 10ms. We recorded input EMG signals at 1000Hz and the values for pendulum position and velocity at 100Hz. All the recordings were synchronized. We used a Vicon DataStream SDK (Vicon, UK) to display the inverted pendulum on the screen.

2.2.4 Experimental Protocol

In the experiment, we first placed EMG electrodes on a subject. To determine the sensor placement, we palpated the subject's (residual) TA and GAS while asking the subject to contract and relax their muscles and placed the EMG sensor over the muscle belly in line with the striation of the muscle [145]. A ground electrode was placed on the bony landmark at the distal end of the ulna at the wrist joint. For the TT subjects, the location of EMG sensor placement was

further fine adjusted to obtain high signal-to-noise ratio without cross-talk. In addition, we placed EMG sensors (6mm thickness) away from bony landmarks on the residual limb surface in a comfortable location. Amputees donned his/her prescribed gel liner, socks, and prosthetic socket overtop.

We seated subjects in front of a monitor at eye height, displaying the real-time visualization of the inverted pendulum model (Fig.1b). A limited acclimation period was provided to each subject before the experimental trials in which each element of the platform was shown (Fig. 1b, screen) and described (pendulum, scoring, reference lines, etc.). This limited exposure offered us an opportunity to observe self-selected control strategies that would emerge naturally. We instructed subjects that their goal was to keep the pendulum as close to vertical (reference line provided) as possible by contracting their TA and/or GAS. No visual feedback of EMG activity was provided to the subjects. Subjects were also instructed to prevent the pendulum from falling off of the screen (Fig. 1b). We implemented a scoring system to incentivize the task goal (Fig. 1b, yellow coins). Subjects earned virtual 'coins' at an increasing rate (1, 0.5, 0.25, 0.1 coin/sec) the closer they maintained pendulum position to vertical (within ±1, ±2.5, ±5, and ±10 degrees, respectively) where no coins were earned outside ±10 degrees. From pilot tests we determined these parameters sufficiently incentivized both low and high performers. If the pendulum fell beyond ±45 degrees, pendulum position was automatically reset 0.01 degrees from vertical and velocity was reset to zero. Ten trials were conducted. Each trial lasted 90 seconds. 3-minute breaks were given between trials.

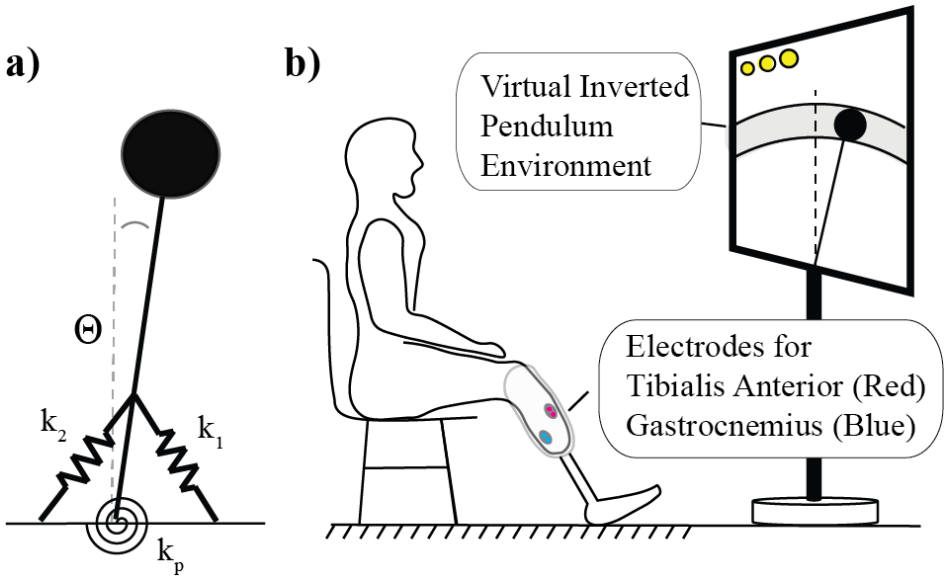

Figure 2-1 Inverted pendulum model and visualization. a) Inverted pendulum apparatus. θ represents angle from vertical. The torsional spring at the base of the pendulum (k_p) has a passive stiffness set to counteract of 85% the torque on the pendulum from gravity. Linear springs on either side of the pendulum have spring stiffnesses k_1 and k_2 which are multiplied by %MVC of TA and GAS muscle respectively. b) Experimental setup. Subject is seated in front of virtual pendulum display with electrodes attached and socket donned overtop. Display shows inverted pendulum with vertical (dashed) reference line and coins that add at a rate that increases as pendulum approaches vertical. When the pendulum falls off of screen (±45 deg) it is reset to 0.01deg with zero velocity. A high score is shown after each trial to aid subject engagement.

Note that all the subjects performed the task in a sitting posture rather than a standing posture. This was because (1) our previous study showed that the ability of amputees to coordination residual muscle contracts has no obvious difference between sitting and standing [138]; and (2) in the standing posture, intact muscle activation in AB subjects could cause postural destabilization, which required additional muscle contraction for posture corrections. Such muscle activities were not related to the virtual task performance. Nevertheless, residual muscle contractions in TT subjects cause no destabilizing effect on the posture. To compare the behavior of intact and residual ankle muscles, we had AB and TT subjects perform the virtual control task in different seated positions. We seated the AB subjects on an elevated chair so that

the foot was not in contact with the ground. With the ankle freely moving (i.e., without ground interaction forces), the antagonistic ankle muscles (i.e. TA, GAS) were in a relaxed state which was more comparable to the state (i.e. muscle tension) of residual muscles. We had the amputee subjects seated on a standard-height chair with their knee at a self-chosen angle so that the heel of the prosthetic foot was contacting the ground and preventing movement of the residual limb (Fig. 1b).

2.2.5 Task Performance and Data Analysis

The overall task performance was quantified by average position, average sway size, and number of falls (and direction), for initial (the 1st and 2nd trials) and final conditions (the 9th and 10th trials). Average position and sway size are chosen since they describe how closely subjects were able to maintain pendulum position near vertical, and number of falls describes how well subjects accomplished the goal of avoiding pendulum fall. Number of falls were split into forward (in the direction of the TA activation) and backward (in the direction of the GAS) directions, where a fall was defined as an instance where the pendulum fell outside of ±45 degrees. Average position was calculated as the mean of all data points of pendulum position in each condition. Average sway size of the inverse pendulum was calculated using all sways except for those leading to falls. Wherein a sway was defined as a trajectory between two reversals in direction of pendulum motion. Initial and final conditions were chosen in order to determine if task performance improved from the beginning to the end of testing. All proceeding evaluation metrics use data from only initial and final conditions.

EMG data was labeled into four categories in order to analyze muscle coordination strategy [140]. We quantified the amount a strategy is used by the percentage of initial and final trial separately. (1) We termed portions of the trials where neither muscle was activated above

2.5% MVC as ‘Inactive’. (2) We termed sections where Co-activation index [146] was higher than 75% as ‘Co-Active’. This threshold was empirically chosen to insure only voluntary co-contraction was placed in this category. (3) We termed portions of the trial where subjects activated the TA higher than 2.5% MVC as ‘TA Active’ and (4) portions where GAS activation exceeded 2.5% as ‘GAS Active’. For instances where both muscles are activated above 2.5% MVC and under 75% Co-activation Index we labeled the strategy based on the highest activated muscle.

We sought to understand the state-action (i.e., pendulum state - EMG activation) relationship to reveal the muscle activation policy used by amputees. We plotted and qualitatively analyzed combined EMG signal from both muscles against pendulum position and velocity (i.e., the system states). EMG signal was combined by taking the maximum value between the TA and GAS signal over initial and final conditions. We also analyzed torque applied at the beginning of pendulum sways in order to determine how subjects attempted to bring the pendulum back towards vertical. Beginning of pendulum sway was defined as the point where the pendulum reversed direction and the velocity was zero. Torque values at these instances were divided in a forward and backward direction, corresponding with torque generated from TA and GAS activations respectively. We averaged these torques over each condition (initial and final) for each subject. We then normalized this torque by the average of pendulum position at beginning of sways for the same conditions (forward-backward, initial-final). The resulting normalized torque was termed T_{norm}, which described the amount of torque input to the system with respect to the pendulum position.

Additionally, we sought to understand changes in performance from amputees by analyzing sections of relatively poor EMG control. We defined ‘relatively poor EMG control’

sections to be sways of the inverted pendulum that lead to failures (where pendulum position exceeded 45deg and was reset). From the extracted sways leading to failure, we observed patterns of EMG activations that were non-goal-oriented which we labeled as patterns of 'Confusion' (Fig. 2). The term goal-oriented implied that the EMG activity sought to bring pendulum position toward the center or to reduce velocity so as to slow pendulum momentum as it approaches center. These non-goal-oriented activations further destabilized the pendulum leading to failure.

As a summary, we tabulated all quantified measures in terms of their relation to pendulum control (Table 2.1).

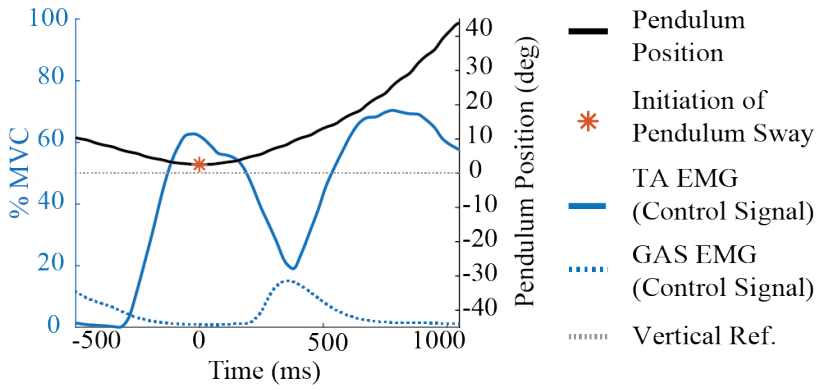

Figure 2-2 Representative pattern of 'Confusion' where, after the initiation of a sway, the TA is activated causing the pendulum to move further from vertical until failure (position reaches 45 degrees). Blue lines refer to percent of MVC (left axis) for each muscle: GAS (solid) and TA (dashed). Black solid lines refer to position (right axis) of the pendulum. The dashed horizontal line denotes the Vertical Reference at 0 degrees.

Table 2-2 Summarized pendulum control measures

Overall Performance Measures	EMG Activation Strategy	EMG Pattern Leading to Falls
1) Pendulum Position *2) Sway Size* *3) Number of Falls*	*1) Activation Type* *2)State-Activation Relationship*	*1) Number of occurrences of 'Confusion'*

2.2.6 Statistical Analysis

We used the statistical software (JMP, SAS, US) for statistical analysis of data. The overall performance outcome measures for analysis were *number of falls*, *average position*, *average sway size*. For analysis of *position* and *sway size*, we used two-way ANOVA to test for main and interaction effects between factors (population and trial), where subject was treated as a random blocking factor. Three-way ANOVA was used for *number of falls* with direction as an additional factor (population, trial, and direction). We also analyzed *activation strategy percentage* and *normalized applied torque*, i.e., T_{norm}. We used two-way ANOVA for activation strategy analysis with identical factors as the previous two-way analysis (population and trial) for position and sway size. For normalized applied torque we used a three-way ANOVA with the added factor of direction (population, trial, and direction).

We ran post-hoc Shapiro-Wilk tests to determine normality of residuals. All residuals were normally distributed, and no outliers were removed. We tested for statistical differences, post-hoc, in each outcome measure using Tukey's honestly significant difference test with $\alpha = 0.05$.

2.3 Results

2.3.1 Overall Performance Measures

Able-bodied individuals performed the task better than amputee participants, though both populations improved performance over time. Mean pendulum position and mean sway size are shown in Fig. 3. Position and sway size were compared across populations (AB vs. TT) and conditions (Initial vs. Final). Overall, AB participants maintained pendulum position closer to vertical than TT subjects ($p=0.041$) (Table III). AB subjects significantly reduced sway size

(Initial-Final, *p<0.001*), whereas TT subjects only slightly reduced the sway size (Initial-Final, *p=0.048*).

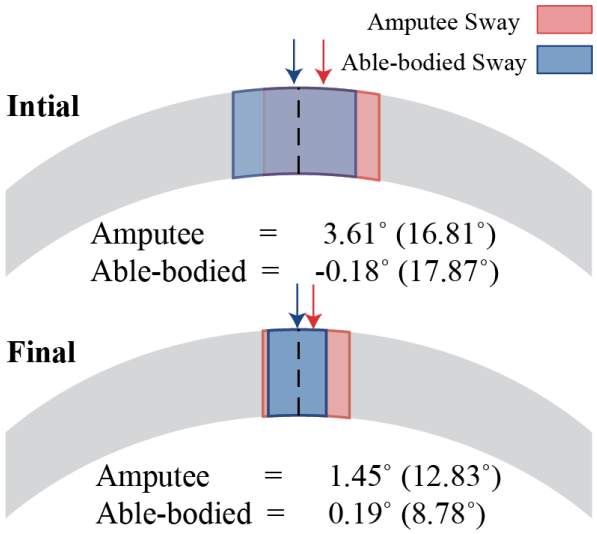

Figure 2-3 Mean position and sway size of the inverse pendulum. Plots show mean position (arrows) and mean sway size centered around mean position (red and blue shaded area). Grey shaded area represents total space pendulum can occupy (±45deg). Mean values are shown in each trial for each population, mean position (mean sway size).

Number of falls varied between the two populations depending on the direction of the fall (Fig. 4 and Table I). Significant differences were found for forward falls (AB-TT, *p=0.006*) but not backward falls (AB-TT, *p=0.405*). TT subjects committed more forward falls (Forward-Backward, *p<0.001*); however, there was no difference in the fall direction for AB subjects (Forward-Backward, *p=0.335*). Trial was significant as a main effect (*p=0.007*), though no interaction effects were significant with trial as a factor.

Table 2-3 p-values of fixed main and significant interaction effects on pendulum position, sway size, and number of falls.

Source	Position	Sway Size	Falls
Trial	0.396	**<0.001**	**0.007**
Population	**0.041**	0.757	0.219
*Trial * Population*	0.239	**0.068****	0.794
Direction	N/A	N/A	**0.020**
*Direction * Population*	N/A	N/A	**<0.001**

**Though Trial*Group interaction is not significant, it is included since it is near significance for sway size. Significant p-values are highlighted in bold.

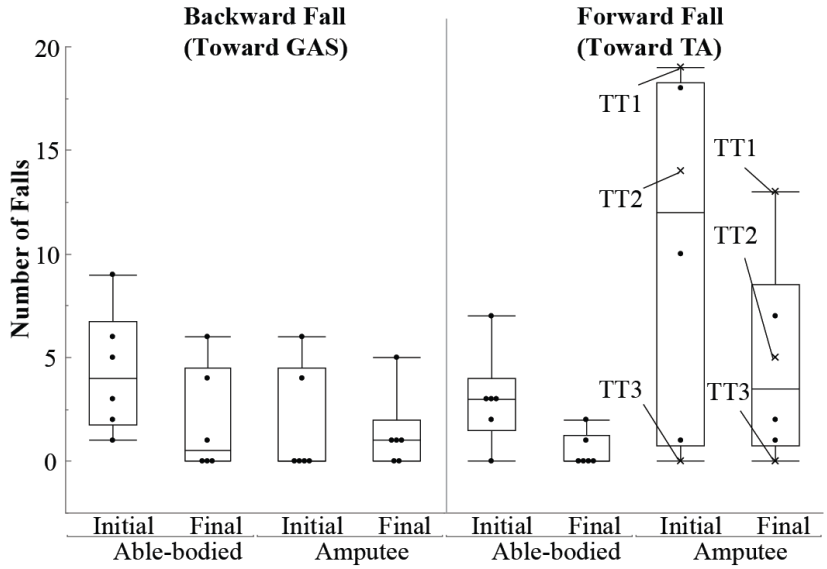

Figure 2-4 Number of pendulum falls. Fall occurs when pendulum passes (±45deg) and it reset. Direction is represented as backward and forward which are related to the GAS side and TA side respectively. Representative TT subjects are highlighted based on performance level in this outcome measure. TT1 presents the poorest performance (most falls), TT2 is an average performer (closest to mean # of falls), and TT3 is the highest performer (no falls). Amputees had a significantly higher number of forward falls compared any other condition.

2.3.2 EMG Activation Strategy

Subjects adopted various activation strategies using either single activation from the GAS or TA, Co-activation, or Inactivity. From the initial to final trials, mainly AB subjects altered the percentage to which they used activation strategies (Fig. 5). Mean and SD values are shown with significant factors (Table IV). AB subjects significantly reduced GAS activation strategy percentage (Initial-Final, *p=0.005*) though TT subjects did not (Initial-Final, *p=0.294*). Both AB and TT subjects showed a decreasing trend in TA activation strategy percentage (Table IV) though both were not significant, (Initial-Final, *p = 0.124*, *p=0.091* respectively). AB subjects increased percentage of inactivity (Initial-Final, *p=0.006*) and TT subjects did not.

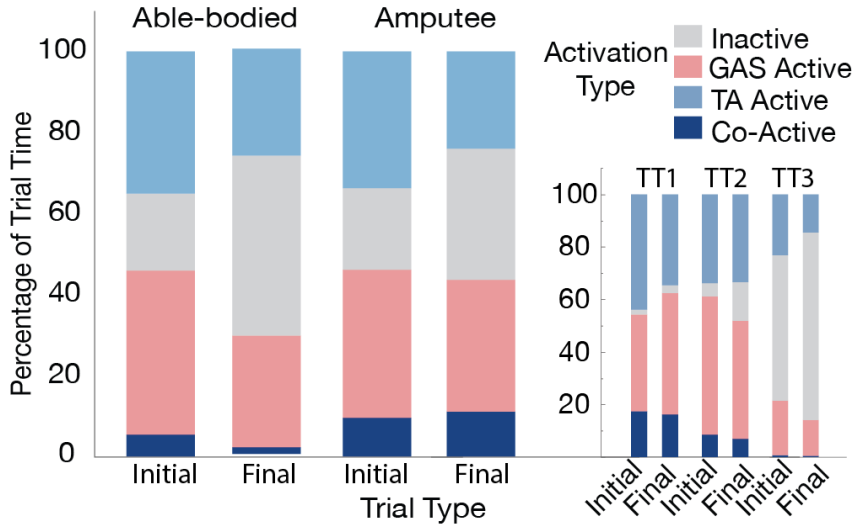

Figure 2-5 Self-selected activation strategy over the initial and final trials. **Co-active)** Portions of the trials with a Coactive Index higher than 75%. **Inactive)** activation of both muscles below 2.5% MVC. **TA Active)** Portions not already contained in previous groups, where TA activity is higher than GAS activity. **GAS Active)** Remaining portions where GAS activity is higher than TA activity. Representative TT subjects are plotted to demonstrate inter-subject variability.

Fig. 5 (right) also highlights the variability in muscle activation strategies in three representative TT subjects. TT1, a low performer (based on fall count Fig. 4), showed higher

levels of co-activation and smaller levels of inactivation than AB and other TT subjects. TT2's (middle performer) muscle activation strategy was most closely resembling average data collected from TT subjects. TT3 (high performer) used almost no co-contraction and seemingly higher levels of inactivity than even average data collected from AB subjects.

Table 2-4 Activation Strategy by percentage of trial

Activation Type	Able-bodied (AB)		Amputee (TT)		Trial Main Effect	Population Main Effect	Interaction Effect
	Initial (%)	Final (%)	Initial (%)	Final (%)			
Co-contraction	5.42 (±5.85)*	1.67 (±2.87)	9.57 (±9.08)	11.09 (±13.70)	0.425	0.198	0.078
Inactivity	18.98 (±13.08)	44.44 (±21.8)	20.13 (±21.58)	32.37 (±31.49)	**0.005**	0.664	0.231
TA Active	35.11 (±9.04)	26.33 (±11.27)	33.75 (±7.13)	24.00(±8.70)	**0.031**	0.636	0.897
GAS Active	40.49 (±8.64)	27.56 (±11.81)	36.54 (±11.22)	32.54 (±14.40)	**0.008**	0.936	0.111

***Mean% (±SD) for each population and main and interaction effects. Significant effects are in bold.**

Fig. 6 demonstrates the EMG activation (control action) at the different state of the pendulum (i.e. position and velocity). AB subjects, on average, appeared to maintain a consistent and efficient state-action relationship in order to use muscle activities to balance the virtual pendulum (Fig. 6). AB subjects activated TA muscle predominantly where pendulum position was negative; they activated the GAS when position was positive. The relationship between muscle activation and velocity appeared circular initially demonstrating high activations for either muscle at both negative and positive velocities. By the final trials, AB subjects further reduced the EMG activities and improved the performance of the virtual task by balancing the pendulum closer to vertical. Nevertheless, the state-action relationship observed in initial trials were seemingly maintained in the final trials.

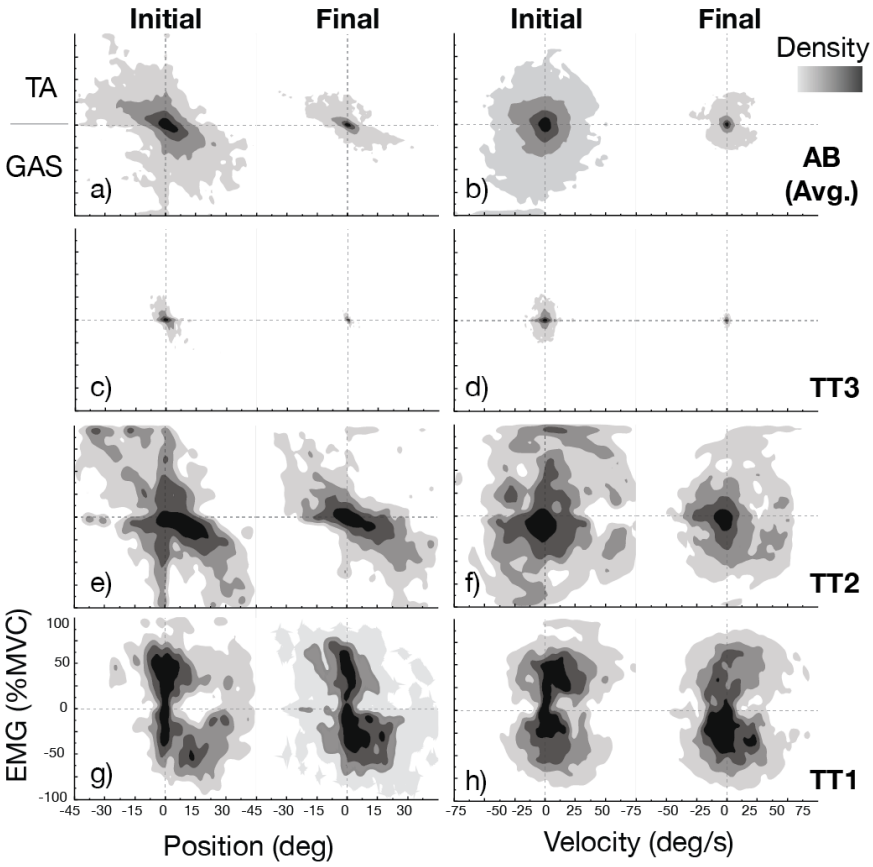

Figure 2-6 EMG activity versus pendulum position and velocity. a-b) Average AB subject data. c-e) representative TT subject data (chosen based on number of falls, Fig. 4). EMG values are normalized with respect to MVC. Negative EMG values are related to activation of the GAS, which generates torque in the backward (negative) direction, and positive EMG values are for activation of the 'TA'. During portions where both muscles are activated simultaneously only the highest magnitude is plotted, thus coactivation is not represented here.

TT subjects displayed varied EMG activations with respect to the state of the pendulum. Fig. 6 displays the data derived from 3 representative subjects selected based on performance in the pendulum balancing task from least number of falls (TT3), closest to mean number of falls (TT2), and the greatest number of falls (TT1). The highest performer, TT3, demonstrated state-action relationship closest to average AB subject data (Fig. 6c-d). Surprisingly, the magnitude of EMG activation was even smaller than averaged values observed from AB subjects. These magnitudes are also reduced from the initial to final trials. In the initial trials, the state-action

relationship obtained from the mean performer (TT2) demonstrated some similarity to that of AB subjects (Fig. 6e-f); however, there was an additional state-action relationship with high EMG activations when the pendulum position was close to zero (displayed as the covered areas around the vertical line when position is 0). By the final trials, TT2 reduced the latter relationship to more closely resemble the results in the initial trials observed in AB subjects. The state-action relationship for the worst performer (TT1) was dominated by the highly covered vertical line around 0 degree in position (Fig. 6g). By the final trials this relationship remains relatively unchanged. In addition, the EMG activity was not reduced significantly compared to that of the initial trials. Interestingly, the relationship between EMG activation and velocity differs from the circular pattern of other subjects in that there were not many points of low activations levels. This led to an hourglass-shaped pattern which was not observed in other subjects (Fig. 6h).

We sought to further characterize this state-action relationship of subjects by investigating how subjects applied torque with respect to pendulum position at the starting point of each sway, where the pendulum reverses direction. We compared population, trial, muscle, and their interaction as factors affecting normalized applied torque (Fig. 7). Significant main and interaction factors as well as means for each condition are shown in Table V. TT subjects showed significant differences in the normalized applied torque between torque direction (Forward-Backward, $p < 0.001$) whereas AB subjects showed no difference between direction (Forward-Backward, $p=0.472$). For the forward torques (TA) subjects showed significantly different normalized torques (TT-AB, $p =0.007$), whereas backward torques (GAS) showed no significant differences (TT-AB, $p = 0.850$). Overall TT subjects used more torque per degree at beginning points of sway, which translates in larger accelerations generated for these sways.

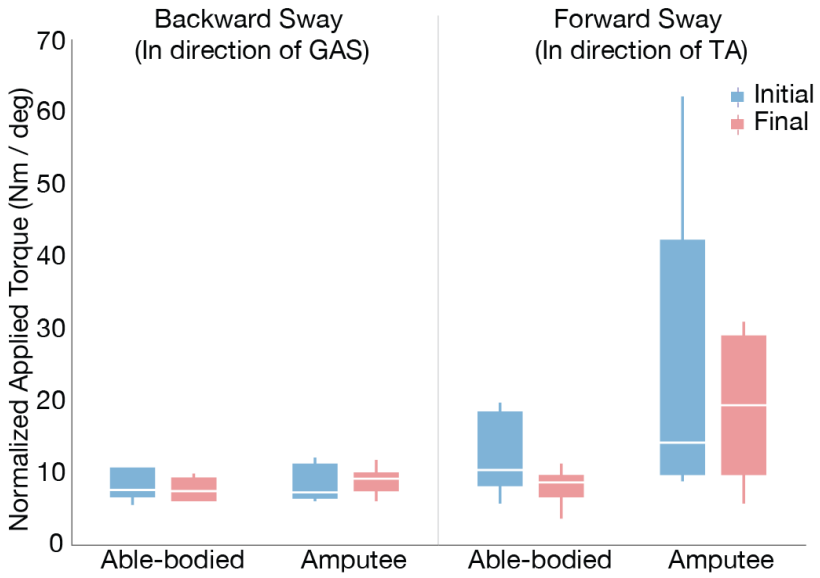

Figure 2-7 Normalized applied torque ($T_{norm,}$ by position) of beginning points of pendulum sways. Normalized Applied Torque is compared across AB and TT subject and initial and final conditions. Absolute torque is interchangeable with initial acceleration at sway starts, where sway start occurs at the moment pendulum trajectory reverses direction and velocity is zero. The absolute value is taken of backward sways for display purposes, though the torques generating sway in this direction are by definition negative.

Table 2-5 Normalized Applied Torque

Population	Sway direction	Trial	
		Initial (Nm/deg)	***Final (Nm/deg)***
Amputee (TT)	*Backward (GAS)*	8.34(±2.52)	8.91(±1.88)
	Forward (TA)	24.08(±21.06)	19.07(±9.95)
Able-bodied (AB)	*Backward (GAS)*	8.17(±2.14)	7.61(±1.57)
	Forward (TA)	12.12(±5.51)	8.15(±2.52)
Population Main Effect		*p = 0.081*	
Muscle Main Effect		***p = 0.001***	
Interaction Effect		***p = 0.019***	

2.3.3 EMG Pattern Leading to Falls

The amount amputees committed destabilizing EMG activation patterns (Confusion) varied widely. Representative low performer (TT1) committed some of the highest number of

'confusion' patterns (Fig. 8). This subject reduced this number by final trials. Middle performer (TT2) committed an average number of confusion patterns (Fig. 8), however did not noticeably alter the amount by final trials. The representative high performer (TT3) committed no patterns of confusion in either initial or final trials. These patterns of confusion accounted for 44% and 41% amputee pendulum falls in initial and final trials respectively.

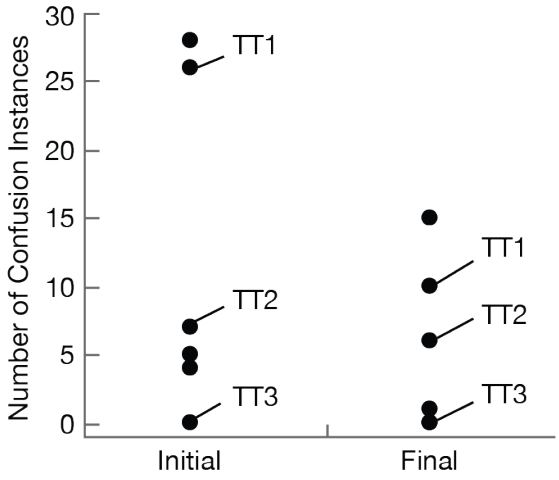

Figure 2-8 Number of instances of 'Confusion'. EMG activation patterns of Confusion are defined as points where activations further destabilize the pendulum resulting in a pendulum fall. Representative subjects (low (TT1), middle (TT2), high (TT3) performers) are displayed.

2.4 Discussion

In this study we demonstrated the capability of transtibial amputees to use EMG activity of residual agonist and antagonist ankle muscles to balance a virtual inverted pendulum, a highly unstable, dynamic system. This virtual task was designed and applied because balancing the inverted pendulum requires continuous control from both ankle muscles. Appropriate coordination pattern of two muscles and activation timing were necessary to prevent falls in the inverted pendulum. In addition, since our long-term goal is to design proportional EMG control

of powered prosthetic ankle for assisting posture control in amputees, the dynamics of inverted pendulum mimics the dynamics of human in standing postures. Overall, our study showed that all the recruited individuals with transtibial amputations were capable of understanding the dynamics of the inverted pendulum system and performed the virtual task at certain success rates. The outcome of this study implied that, in general, it was feasible to let amputees use their residual antagonistic muscle pair to control a highly dynamic, unstable system.

All the amputee subjects improved task performance after a limited time of practice in this study. In addition, most of the TT subjects essentially maintained or developed appropriate state-action relationship at the end of the experiment for improved task performance. This observation implied that even though most of the TT subjects had decreased ability to coordinate residual muscles, compared to able-bodied subjects, at the beginning of the study, once experienced with the dynamics of the control system and understood the consequence of their muscle activation on task performance, they can adapt the activation of antagonistic residual muscles for improved task performance. This was also supported by the observation reported by Dawley et. al [136]. The authors showed after using EMG controlled prosthetic knee in walking, a transfemoral amputee adapted residual muscle activation pattern and produced more reliable and repeatable antagonistic muscle coordination for prosthesis operation in cyclic walking. Together with the previous report, we hypothesize that lower limb amputees, after systematic training in myoelectric control of a powered prosthesis in different task contexts, are able to actively engage a prosthesis joint to assist anticipatory and compensatory postural adjustments in standing and walking. Testing this hypothesis will be our future work.

Given the similar amount of period for task practice, individual subjects showed different stages of task learning and different amounts of improvement of task performance. In human

motor learning, usually the initial learning involves identifying appropriate control solutions/policies that lead to success in task performance, followed by learning to reduce variations in motor control [147]. All the able-bodied subjects and some high-performing amputee (e.g. TT3) presented both steps of learning in this study, while many amputees only improved success rate of the task performance without reducing variations in EMG control (Fig. 3 and 6).

The rate of learning and amount of improvement seems to be pertinent to the initial capability of each individual to co-activate the agonist-antagonist muscle pair. For example, TT1 was also a participant in our previous study [139] (i.e. S09) where participants were asked to fill as much of a two-input co-activation space as possible with TA and GAS muscles. The upper boundary of this space was simultaneous activation of both muscles at 100% MVC, and participants were able to freely explore this space with no task-specific control goal. In this previous study of voluntary control of residual antagonistic muscles without a dynamic task context, TT1 demonstrated very limited coactivation patterns between two residual muscles (i.e., could only access parts of the coactivation space through rapid reciprocal activation). In this study when the muscle control was in a dynamic context, TT1 did not noticeably change state-action relationship, which was not accurate or effective control policy for task performance. Rather TT1 improved task performance by reducing number of occurrences of erroneous muscle activation pattern, such as confusion (Fig 8), resulting in fewer pendulum falls. That is to say, the low performers, like TT1, can only improve performance by locating appropriate executions within his limited muscle co-activation space (i.e., avoiding high activation of TA when pendulum is in positive position, see Fig. 6g, top right quadrant initial vs. final). For high performers, such as AB subjects and TT3, they quickly developed the appropriate state-action

policy (evidenced by no falls) and improve task performance by reducing variation of EMG activation, which saved the energy in task performance and increased the safety margin to maintain task success. Interestingly, TT3 was also a participant in the previous study [139] (i.e. S06), in which he showed the highest dexterity in co-activating two residual muscles (i.e. was able to access nearly all coactivation space with sustained coactivation). For middle-level performer, such as TT2, they gradually shaped state-action policy through practice and reduced the occurrence of erroneous activation that led to falls in order to improve the task performance. The results derived from our previous studies and this investigation suggested quantifying the amputee's co-activation capability between antagonistic residual muscles, such as the 2D muscle activation space used in [139], may serve as a predictor of amputee's performance in a complex, dynamic task context when using proportional myoelectric control. Future work testing proportional myoelectric control in a dynamic virtual system should incorporate the use of unexpected perturbations in order to more fully described the state-action policy of the human (amputee) operator through the quantification of the human sensorimotor loop delay [141]. In addition, it would be interesting to study whether the performance of low performers can be further improved if more training of muscle co-activation task is provided.

Amputees exhibited an interesting difference for both performance and behavior between the residual GAS and TA muscles. The performance measures showed more failure in the direction of the TA activation (Fig. 4) and behavior measures showed a larger amount of applied torque per degree by the TA activation (Fig. 7). This difference in control between two muscles might be driven by amount of use of residual muscle in current prostheses. Qualitatively, for example, both TT3 and TT6 indicated that they use their residual muscles for increased suspension during walking, and TT6 indicated using gastrocnemius flexion to improve

cushioning during running. Another potential explanation for this observation is the potential difference in pressure generated from residual muscle activations at the limb-socket interface, which led to different level of sensory feedback. Qualitatively, before donning the prosthetic socket, all the recruited amputees produced a visible change in residual limb volume when contracting GAS muscles, while the volume changes were barely noticeable when contracting TA. Therefore, GAS activation at different levels potentially led to graded pressure sensation against the socket to amputees. It is a worthwhile question then to study whether amputees were able to use this sensory feedback for control of the residual muscles for myoelectric prosthesis control. Application of flexible force and sheer sensors within the limb-socket interface [148] in future study might be helpful to quantify the change in pressure due to muscle activation, which further enable us to understand how amputees use this feedback to improve control of residual muscles. In addition, future work that incorporates the residual TA and GAS into proportional EMG control should aim to understand and address this observed disparity in level of control between the two antagonistic muscles.

Inter-subject variability in using (residual) ankle muscles for balancing a virtual inverted pendulum was noticeably higher for amputees than for AB subjects. Both physical and neural constraints caused by the limb amputation have the potential to drive the number of observed differences in muscle control and task performance. In this study there were no noticeable effects of either age or time since amputation on the amputees' level of performance, though a larger sample size is needed to validate this. This inter-amputee variability holds implications for introducing subjects a proportional EMG controlled prosthesis. It is possible that low performing subjects (TT1) may be unfit for proportional EMG control or would require extended training before using a device for dynamic tasks. This is due to incidences of 'Confusion' (Fig. 8) or an

inefficient state-action policy identified (Fig. 6g). For subjects that performed as well, if not better, as AB subjects (TT3 and TT6), it is also possible that only limited acclimation is required before introduction to a device.

Future work should investigate the relationship between performance in this virtual space and use of a physical prosthetic device. We have demonstrated the ability for amputees to improve antagonistic control in the virtual context, however it is unclear whether observed differences in control of a virtual task between amputees persist into control of a physical device. A relationship between virtual and physical performance would make this task a valuable predictor and potential training platform for proportional myoelectric control of lower limb prostheses. A limitation of this study is that amputee and able-bodied subjects are not age-matched. This experimental approach relies on visual feedback for control of the virtual pendulum, though future work should investigate the benefit of proprioceptive and vestibular feedback during postural control with proportional myoelectric control of an ankle prosthesis. Another limitation is a relatively small sample population in this study. It is possible there are many factors that contribute to observed differences in control such as time since amputation and reason for amputation, however our limited sample population is insufficient to study this. It is our future work to explore whether our observations hold for other frequent prosthesis users.

2.5 Conclusion

In this study, we demonstrated that transtibial amputees were capable of controlling an unstable dynamic system through coordinated antagonistic residual muscle activations via proportional myoelectric control. All the transtibial amputees improved their task performance over a limited time of practice, although the amount of improvement varied across amputees. The results of this study suggested that it may be feasible for amputees to actively engage a

powered prosthetic ankle via proportional EMG control in highly dynamic tasks, such as posture adjustment in standing and walking. However systematic training of amputees in coordinating the antagonistic residual muscles and dealing with dynamic systems are needed.

CHAPTER 3: Improved Standing Balance under Expected Postural Disturbances via Direct Electromyographic Control of a Powered Prosthetic Ankle

3.1 Introduction

Individuals with lower-limb amputation lose agency in their limb to interact with their everyday environments. Amputees relearn to navigate the world with prosthetic devices that are often mechanically passive, with a predetermined stiffness designed primarily for walking. Amputee daily life, however, contains many activities beyond steady-state walking and their prosthetic device provides no active support during these tasks (i.e., picking up a child, playing a game of soccer, shuffling in a line). Despite amputees' ability to adapt intact joint coordination strategies *around* their prosthetic device in these activities, they are at higher risk for falls, have lower balance confidence and participate significantly less in their community [6, 11]. Further, amputees often develop strategies such as relying more heavily on their intact limb, which create long-term consequences such as higher risk for osteoporosis and arthritis [149].

Recent advances in robotic lower limb prostheses present great promise to further address the mobility and stability in individuals with lower limb amputation. These devices can generate active torque to assist individuals [21, 22, 26, 27, 150]. A majority of existing research efforts have been spent on robotic prosthesis control in order to restore normative locomotion [21, 29]. These control paradigms often use finite-state machines, which use sensors on board the prosthetic device to determine the human-environment state and then *reactively* deliver a pre-determined joint mechanic. This control is well suited for cyclic conditions, where the state-action relationship is well defined, as demonstrated by improvements in amputee's ability to navigate across several terrain conditions and speeds [151, 152]. However, since autonomous control paradigms are only able to react to changes in state that can be sensed from the prosthesis

device, they are ill-suited to generate actions to contexts that require *preparatory* adjustments, such as anticipatory postural adjustments (APA), and require full body coordination, such as compensatory postural adjustments (CPA). Anticipatory and compensatory postural adjustments constitute the building blocks for many daily-life tasks. These postural control mechanisms are responsible for maintaining balance against perturbations that are generated externally (like catching an object) [153] or internally (like initiating a step) [154]. Anticipatory postural adjustments are crucial for balance maintenance, as evidenced by significant changes in stability when individuals know a perturbation is impending versus when they are blinded to the timing [155, 156]. Individuals develop these postural adjustments depending on the size, direction, and timing of perturbation [157-159]. These volitional, feedforward actions (i.e. not generated through reflexive neural commands) alleviate the burden on compensatory postural adjustments and improve overall stability [153, 156]. Hence, novel control mechanisms to further improve the function of robotic prostheses to address anticipatory and compensatory postural control for assisting versatile activities, beyond steady state walking, is needed.

One potential solution is to directly integrate the prosthesis control with feedforward neuromuscular commands of amputee users through electromyography (EMG) as amputees retain the ability to generate feedforward, volitional activations of their residual muscles (often eliciting a sensation of moving a 'phantom limb') [34]. This control paradigm, also called direct EMG control (dEMG) [160], uses neuromuscular activities of residual muscles (that originally controlled the amputated joint) to directly modulate an artificial joint's mechanics. It mimics the biological process for limb movement production, restores the biomechanical meaning of activation of residual muscle [16, 40, 118, 160], and enables individuals to continuously operate their prosthesis joint based on the neural control commands (including anticipatory and

compensatory postural control commands) in humans, just like control of an intact joint. Though this control paradigm is commercially used in upper-limb prostheses it has recently gained traction as being feasible for lower-limb prosthetic device control [160].

Although theoretically sound, research on dEMG control for robotic lower limb prosthesis has been limited, and initial feasibility studies still focused on walking [16, 44, 121]. One of the challenges, observed in these studies, is the significant changes in residual muscle activity after amputation, which is partly responsible for the initial difficulty of individuals to use dEMG controlled prostheses in locomotion. In addition, the dynamics of prosthetic limb is different from biological limb, which requires the prosthesis user to re-establish the relationship between neural control comments to the mechanics changes of prosthesis for a success use of dEMG prosthesis control. Two solutions were used to partially address these challenges. One study introduces a surgical technique, called agonist-antagonistic myoneural interface, to enhance the residual muscle coordinated activities [44]. A more practical and accessible approach is to train amputee users to adapt their muscle activation patterns for external device control. Huang et al. showed successful adaption of the residual gastronomes muscle for dEMG control of robotic prosthesis ankle plantarflexion in walking when training with visual feedback of their residual muscle activity [16]. When dEMG control was tested with two antagonistic muscle (responsible for plantar and dorsiflexion), amputees were able to adapt residual muscle activations to improve control of a virtual inverted pendulum after practice [34]. These results underscored the importance for amputee training in success use of dEMG controlled prosthesis.

Given the potential of dEMG prosthesis control to improve APAs and CPAs in daily activity and the importance of amputee training in successful use of dEMG control, the goal of this study is to systematically investigate the effects of training of transtibial amputees in using

dEMG controlled robotic ankle on postural control and balance under anticipated perturbations. Specifically, we implemented dEMG control on a pneumatic muscle driven robotic prosthesis ankle and trained multiple transtibial amputees in using this device. A specially designed anticipatory postural perturbation platform was designed to quantify the APA and CPA control strategy, kinematics and kinetics of bilateral lower limb, and EMG control signals across all the subjects when using dEMG controlled prosthesis, compared to their daily devices. To our knowledge, use dEMG controlled prothesis to assist daily activities that requires postural control has not been reported, except our previous single-subject case study [117]. The results of this systematic study can contribute important new knowledge on the benefit of dEMG control of robotic lower limb prosthesis on the postural stability and balance in lower limb amputees. We expect the improvement of standing stability and ability to accomplish daily-life activities via modern robotic prosthesis technology to have a dramatic effect on the quality of life for amputees by empowering them to participate in many more areas of life in the future.

3.2 Results

3.2.1 dEMG Control Enables Symmetrical, Synchronized Bilateral Ankle Control

In both pull and push perturbation conditions we observed significant improvements in stability measures when participants with transtibial amputation (TT) used dEMG control of a prosthetic ankle after training compared with their daily passive device. During these conditions participants generated anticipatory adjustments of their center of mass (CoM) against the direction of the perturbation. For reference, during the “Push” condition the able-bodied (AB) control participant moved their CoM in the anterior direction before the weight was released and continued to hold their center of mass forward in the following 2 seconds after perturbation (Fig. 1a). TT participants also generated anticipatory movements of their CoM before load release

using their passive device, however after perturbation they were unable to retain this CoM position, post-perturbation. While using dEMG control participants generated anticipatory CoM movement similar that of the AB participant and maintained CoM position after the perturbation.

Amputee participants more closely synchronized center of pressure (CoP) and ankle torque using dEMG control compared with their daily prosthetic device. In their daily device TT participants generated anticipatory CoP excursion in the posterior direction with their intact foot, however the CoP excursion under the prosthetic foot remained significantly less (Release: -31.35(±14.72mm) vs. 6.89(±8.53mm), $p=0.005$). However, post-perturbation this difference was not as noticeable (Hold: 61.15(±28.15mm) vs. 44.02(±17.41mm), $p = 0.121$). Hold is defined as the average value of the given measure during time, 1-2s, post-perturbation. Using dEMG control TT participants generated synchronized CoP excursion in timing and magnitude (Fig. 1b) (Release: 24.96(±18.29mm) vs. 20.05(±16.12mm), $p=0.509$; Hold: 48.66(±14.96mm) vs. 33.61(±23.40mm), $p=0.169$). This synchronized CoP excursion appeared to be similar to AB participant behavior between limbs (Fig. 1b). When TT participants used the dEMG control they generated dorsiflexion torque post-perturbation, noticeably similar to their intact limb. However, TT participants could not generate this dorsiflexion torque in their daily device, and only decreased their baseline plantarflexion (Fig. 1c).

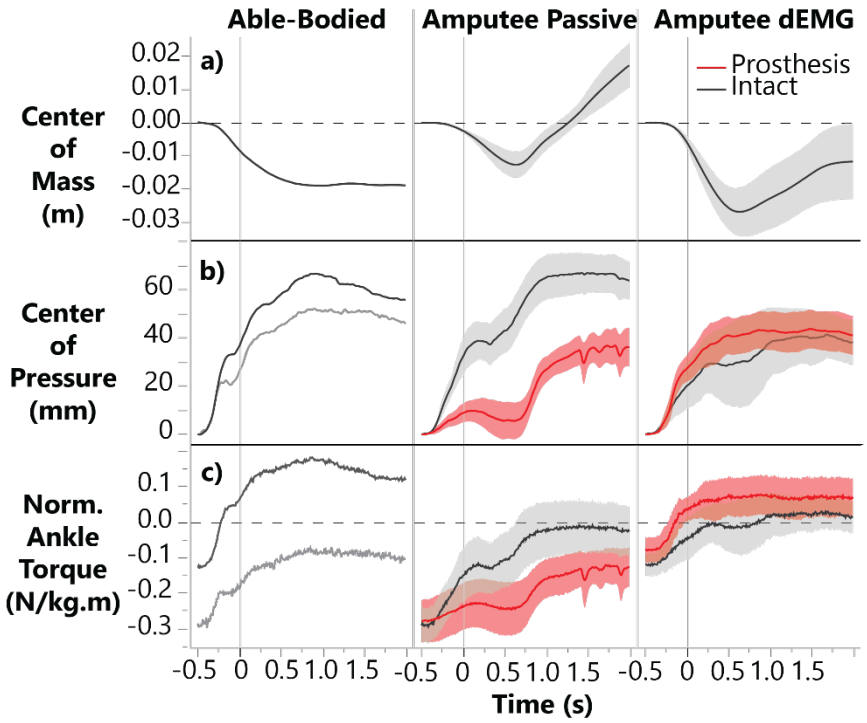

Figure 3-1. Able-Bodied and Amputee response to pushing perturbation with passive device and dEMG control prosthetic ankle. Individual leg contributions are graphed (dark line right limb, light line left limb) to show normative able-bodied response in CoP and Ankle Torque measures. Red) Prosthetic limb measurements for CoP and Normalized Ankle Torque. Grey) Intact limb measurements.

3.2.2 Amputees Improve Symmetry between Intact and Residual Limb Joint Excursions using dEMG Control

We observed TT participants modify postural configuration of their residual limb when using dEMG control to more closely match their intact limb in both "Push" and "Pull" conditions (Table 1 and 2). At the release of the "Push" perturbation (Table 1), TT participant's intact and prosthetic ankle joint flexion significantly differed using their daily device ($p<0.0001$). However, while using dEMG control ankle joint TT participants dorsiflexed their prosthetic ankle, resulting in no significant difference between intact and prosthetic ankle joint excursion post-training ($p=0.524$). During the perturbation hold we observed significant difference

between intact and prosthetic ankle joint excursion in both passive and dEMG control condition (Passive: *p<0.0001*; dEMG: *p=0.001*). However, TT participants significantly increased prosthetic ankle joint dorsiflexion during the perturbation hold using dEMG control compared with their passive device (*p<0.0001*). We observed significant difference between intact and residual knee joint excursion in the passive condition (*p = 0.010*), but not in the dEMG control (p=0.729). However, we observed significance difference between the intact limb knee joint and residual limb knee joint during the perturbation hold for both conditions (Passive: -1.57(±5.41deg) vs. 3.96(±2.44deg), *p<0.0001*; dEMG: 0.23(±4.97deg) vs. 3.20(±5.91deg), *p=0.007*). For hip joint comparison we only observed significant difference between the passive and dEMG control in the intact limb hip joint during release (-0.34(±0.66deg) vs. -0.46(±1.31deg), *p = 0.027*). However, no other comparisons were significantly different during perturbation hold. We also observed less hip flexion during perturbation hold when comparing the prosthetic limb hip excursions (*p<0.0001*) and intact limb hip excursions (*p<0.0001*).

Table 3-1 Joint Excursions ANOVA Results during "Push" Perturbation for Release and Hold Timepoints

	Joint Excursion*	Passive		dEMG Control		Device Main Effect	Side Main Effect	Interaction Effect
		Prosthesis (deg)	Intact (deg)	Prosthesis (deg)	Intact (deg)			
Release	Hip	-0.34(±0.66)	0.19(±1.11)	-0.46(±1.31)	-0.46(±1.55)	0.063	0.193	0.197
	Knee	1.27(±1.32)	-0.15(±1.34)	-0.30(±2.76)	-0.11(±2.51)	**0.049**	0.111	**0.0385**
	Ankle	-0.38(±0.54)	1.18(±1.19)	1.20(±1.97)	1.44(±1.60)	**0.001**	**0.0013**	**0.018**
Hold	Hip	1.48(±3.67)	1.72(±2.77)	-2.39(±2.21)	-1.27(±2.08)	**<0.0001**	0.178	0.379
	Knee	3.96(±2.44)	-1.57(±5.41)	3.20(±5.91)	0.23(±4.97)	0.493	**<0.0001**	0.094
	Ankle	-2.28(±1.62)	5.12(±5.27)	2.20(±5.41)	5.17(±4.96)	**0.0006**	**<0.0001**	**0.0008**

*Flexion directions are: Hip Flexion (+) Knee Extension (+) Ankle Dorsiflexion (+)

For the "Pull" perturbation we observed significant differences between intact and residual limb joints during the passive device, though these differences diminished while TT participants used the dEMG control (Table 2). For the ankle joints we observed significant difference in TT participant's average ankle joint excursion between their intact and residual limb (Release: $p = 0.014$; Hold: $p<0.0001$). We still observed significant differences in ankle joint excursion in the dEMG control condition during the perturbation release (Intact-Prosthetic, $p=0.018$), but not during the perturbation hold (Intact-Prosthetic, $p =0.173$). However, TT participants significantly increased prosthetic ankle joint plantarflexion using dEMG control compared with their passive prosthesis (Release: $p<0.0001$, Hold: $p<0.0001$).

Table 3-2 Joint Excursions ANOVA Results during "Pull" Perturbation for Release and Hold Timepoints

	Joint Excursion	Passive		dEMG Control		Device Main Effect	Side Main Effect	Interaction Effect
		Prosthesis (deg)	Intact (deg)	Prosthesis (deg)	Intact (deg)			
Release	Hip	0.83(±1.44)	0.52(±1.02)	0.01(±1.05)	0.71(±1.51)	0.184	0.420	**0.037**
	Knee	-1.30(±1.74)	-0.34(±0.94)	1.46(±2.59)	-0.17(±1.76)	**<0.0001**	0.308	**0.0001**
	Ankle	0.32(±0.59)	-0.55(±0.87)	-1.55(±2.18)	-0.72(±1.31)	**<0.0001**	0.936	**0.0008**
Hold	Hip	2.41(±2.92)	1.05(±2.26)	1.89(±2.37)	3.09(±3.33)	0.145	0.877	**0.015**
	Knee	-4.95(±3.00)	-1.64(±2.25)	2.05(±4.72)	-1.06(±2.52)	**<0.0001**	0.839	**<0.0001**
	Ankle	1.42(±0.99)	-1.36(±2.22)	-4.02(±4.81)	-3.21(±2.83)	**<0.0001**	**0.020**	**<0.0001**

*Flexion directions are: Hip Flexion (+) Knee Extension (+) Ankle Dorsiflexion (+)

We observed significant differences between intact and residual limb knee joint excursions in both passive (Release: $p=0.041$, Hold: $p<0.001$) and dEMG controlled conditions (Release: $p<0.0001$, Hold: $p<0.0001$). However, we observed TT participants change their residual limb knee excursion between the passive and dEMG control condition (Release: p<0.0001, Hold: p<0.0001). For hip joint excursions we only observed a significant difference between the intact and residual limb during the dEMG control condition release (p=0.041),

however all other hip joint comparisons had no significance. Further, hip joint excursion at perturbation appeared to be relatively small, 0.01(±1.05deg), compared to hip joint excursion after perturbation (1.89(±2.37deg), Table 2).

3.2.3 Amputees Reduce Falls and Compensatory Steps using dEMG control

We observed distinct changes in balancing strategies as TT participants use dEMG control compared with their passive device (Fig. 2). While using dEMG, 3 TT participants used predominantly ankle joint strategy, as evidenced by relatively small excursions from the knee and hip joint, and large, synchronized excursion from the ankle joints (Fig. 2a). We observed 2 participants used a mixed strategy, with simultaneous excursion from all joints (Fig. 2b). These participants still improved synchronization between prosthetic and intact limb ankle joint excursion compared with their passive device. Overall, nearly all participants failed to maintain static standing balance at least once (i.e., participant took a step or allowed handlebar to reach the end of the track) while using their passive device (Fig. 2c). While using dEMG control only 1 participant still required a stepping strategy to maintain balance, while all remaining participants were able to maintain static standing balance.

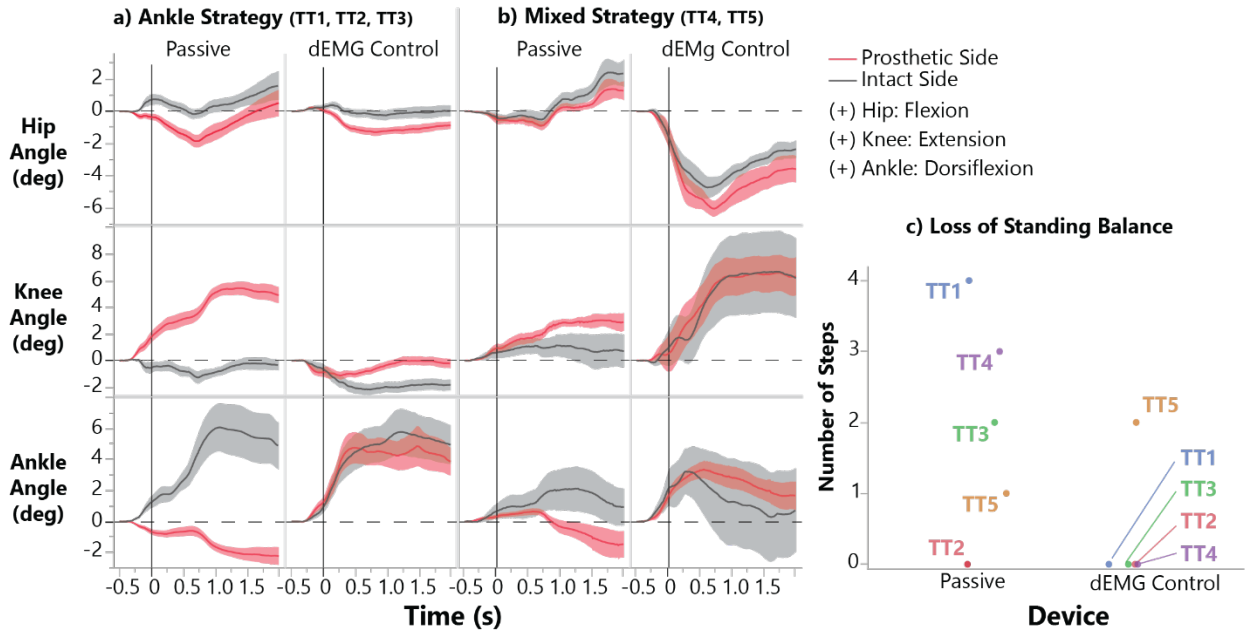

Figure 3-2 Balance strategies during pushing perturbation with passive and dEMG control prosthetic ankle. a) Participants significantly increase prosthetic ankle joint dorsiflexion using dEMG control and reduced flexion of hip and knee joint. b) Participants that significantly changed hip, knee, and ankle joint excursions. c) Number of trials where individual participants could not maintain balance resulting in a step or allowing the handlebar to reach the end of the provided track.

3.2.4 Amputees Shift Anticipatory Postural Adjustment Timing using dEMG control

During push and pull perturbations we observed patterns of muscle activations from TT participants (while using dEMG control) similar to previous work using with able-bodied individuals under expected perturbation [155]. Before perturbation release, TT participants activated/inhibited specific muscle groups in preparation for the oncoming perturbation depending on the direction. For the push condition (Fig. 3a) we observed anticipatory activation anterior muscle groups (TA, VL, and RF). In this condition we primarily saw inactivity from posterior muscles groups with some instances of tonic activity followed by anticipatory inhibition after the notification of load release (Fig. 3a Residual BF). For the pull perturbation

(Fig. 3b) we found anticipatory inhibition of anteriorly located muscle groupings (i.e. RF, VL) and anticipatory activation of posterior muscles group (i.e. BF, SOL, GAS). We also noticed reciprocal activation of these muscle groups close to the timing of load release (t=0s).

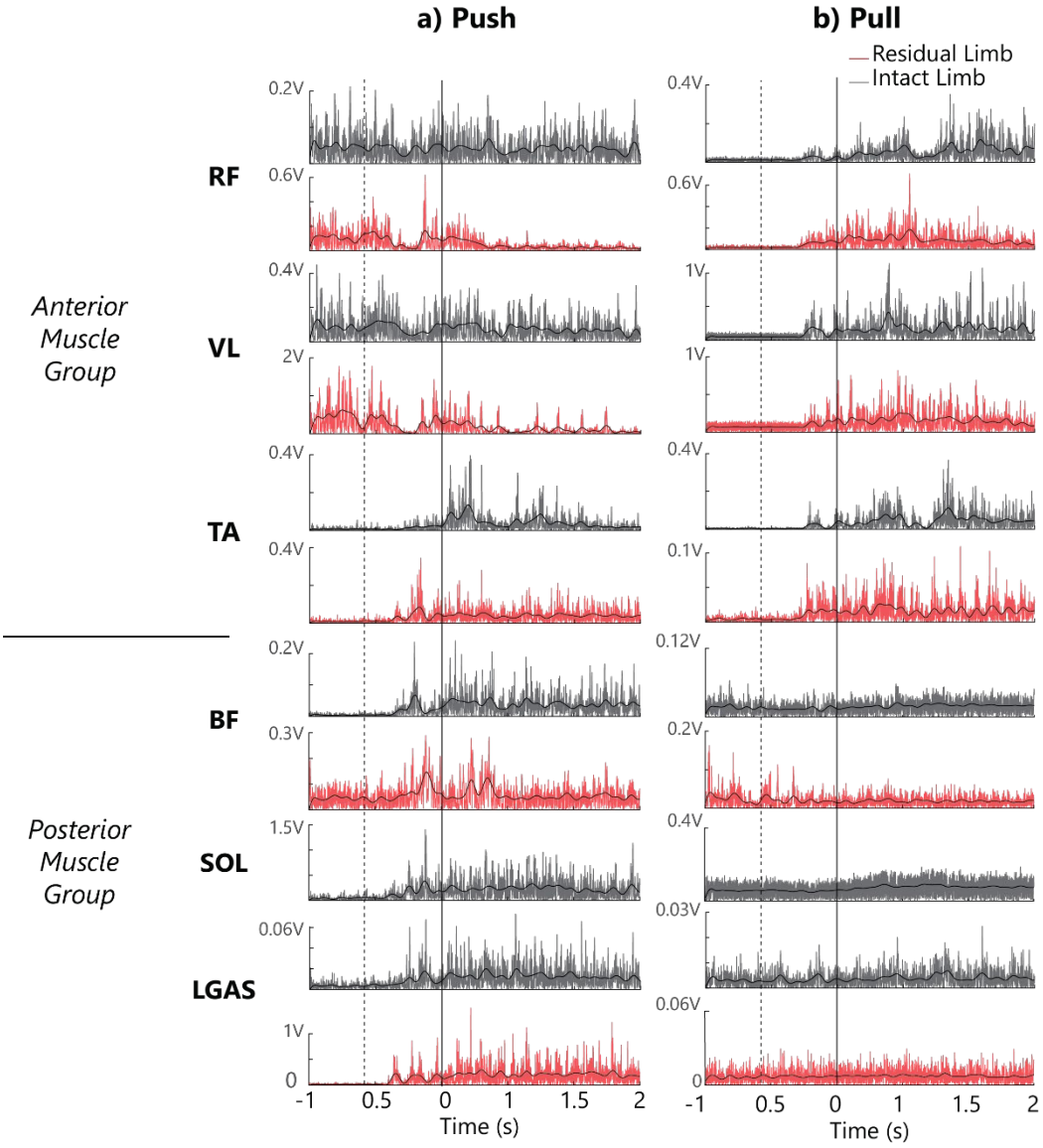

Figure 3-3 EMG activities during representative pull and push disturbances from all recorded muscles (TT3 and TT2 respectively). Rectified, raw EMG data and low-pass filtered EMG signals are shown. Dashed Line) Time of light switch notifying participant of oncoming perturbation. Solid Line) Moment of perturbation via load release. a) Pull condition EMG activity. b) Push condition EMG activity. Red Line) Activity of Residual Limb Muscles. Grey Line) EMG from intact muscle activity.

During push perturbation we spotted a change in anticipatory activation of relevant muscle groups (i.e. anterior muscles) between passive and dEMG control conditions (Fig. 4a). During the passive condition TT participants overall activation timings were quicker (i.e. closer to light switch) than in the dEMG control condition (Device, Pull: $p=0.005$, Push: $p=0.0003$). Between passive and dEMG control condition we observed muscle-specific changes in activation timing in the intact limb RF ($p=0.047$) and residual limb VL ($p=0.011$). We did not observe a significant difference between activation timings for any muscles within the passive and dEMG control condition. However, we observed a trend of ankle to thigh activation order (Fig. 4a) when participants used the dEMG control. When observing individual TT participant behavior, we noticed two activations strategy differences between representative subjects (Fig. 4b). TT3, who primarily used ankle joint strategy when we observed joint excursions, had similar activations timings of all recorded muscles. However, TT4, who lost balance more frequently in the dEMG control condition, had delayed activation of residual limb thigh muscles (Fig. 4c, rVL and rRF), whereas the remaining residual and intact muscles had similar activation timings.

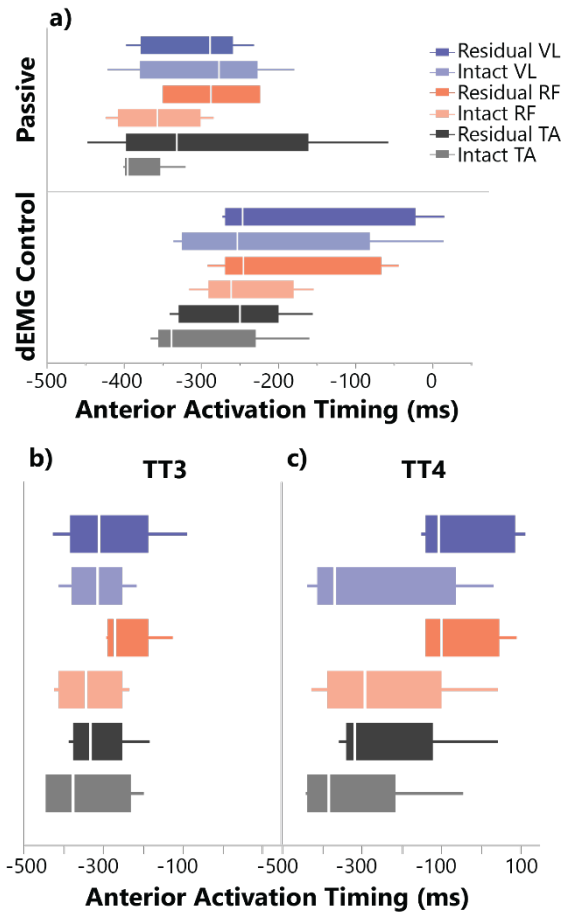

Figure 3-4 Onset of muscle activations from anterior muscles during push perturbation. A) Passive vs. dEMG control of muscle activations. Time zero represents the moment the perturbation occurs. B) Representative muscle activation timings using dEMG control from two participants TT3 (ankle strategy) and TT4 (mixed strategy).

3.3 Discussion

Here we have demonstrated the potential of transtibial amputees to coordinate antagonistic residual muscle activity using dEMG control of a prosthetic device to significantly improve standing stability after training. The main finding of this study is that amputees largely synchronized intact and residual limb behavior, in both anticipatory and compensatory responses, while using volitional control (i.e. dEMG control) resulting in improved standing stability under expected perturbation. This study extends the results of previous case study which

included only a singular participant, expanding the potential benefits of this control with a larger population of participants. Further we have broadened the analysis of standing stability from previous study using a novel perturbation platform capable of delivering expected disturbances at the shoulder level in multiple directions. By having control of *both* antagonistic residual muscle, participants were able to improve bilateral synchronization of joint excursions in multiple direction of perturbation. Further, this study is the first to demonstrate the potential for direct EMG control to restore normative control when comparing amputee behavior to an able-bodied control. Based on these works, future study should expand this work to evaluate the potential of this dEMG control, with guided training, on stability in a larger range of activities.

One of the primary findings of this study was that, by enabling neuromuscular control of a powered prosthetic ankle, amputees were 1) capable of eliciting motor commands that synchronized several measures between intact and residual limbs and 2) chose to use this synchronized interlimb behavior as a strategy during expected perturbation. This synchronization was apparent in several measures including CoP excursions, ankle joint torques and joint excursions in the ankle, knee and hip. We first observed drastically improved CoP excursions during the Push condition, where intact and residual limb did not differ while using the dEMG control. This CoP measure is a common measure related to postural control, where CoP excursion will begin to shift in anticipation of an oncoming disturbance, followed by changes in Center of Mass excursion [156]. This lack of synchronization in inter-limb CoP excursion from amputees while using a passive prosthetic device is a result of lack of active ankle joint control and has been observed previously in a variety of tasks [8, 117, 161]. Not only were participants capable of synchronizing inter-limb CoP excursion using dEMG control, but they also generated active, anticipatory dorsiflexion torque with the prosthesis during the ‘Push’ condition (Fig. 2c).

Lastly, differences in joint excursions between homologous joints largely disappear when participants used the dEMG control. This signals a shift by the TT participants to a more normative postural control strategy. Synchronized joint excursions are ubiquitous in the evaluation of normative postural control strategies to the extent that typically only kinematics from a single leg are reported. Here we present the first results demonstrating potentially normative postural control strategy used by amputees using dEMG control of a powered prosthetic ankle joint.

Interestingly, improvements in standing stability were evident in overall postural control strategies employed by participants when using the dEMG control. Participants struggled to maintain standing balance under the Push condition while using their passive device, as evidenced by the need for multiple steps or use of the safety rails on the perturbation platform (termed fall). While using the dEMG control participants were able to move their CoM position further against the direction of perturbation, resulting in no steps for nearly all participants (Fig. 3c). It is possible this increased excursion of CoM was made possible by the dorsiflexion torque (in the 'Push' condition) generated with the dEMG controlled prosthetic ankle compared with the lack of dorsiflexion torque from individuals' passive device. This improvement in stability was also evidenced by two postural control strategies in the dEMG control. TT1, TT2 and TT3 all employed an ankle joint strategy while TT4 and TT5 used a 'mixed' strategy. Ankle joint, hip joint and mixed strategies are well observed postural control strategies used by individuals to maintain standing balance, where hip and mixed strategies are typically employed during larger perturbations compared with ankle joint strategy [162]. The use of ankle joint strategy by TT1-TT3 demonstrates increased capacity of the individuals to handle larger perturbations using dEMG control. TT4 and TT5's use of a mixed strategy suggests this perturbation was still

difficult while using the dEMG control, however TT4 completed all trials with no steps use of guard rails. However, TT5 used both mixed strategy and had an additional step compared with using his passive prosthesis. In previous study we reported a similar spectrum of performance with residual muscle control across amputee participants, while all participants were able to improve performance [34]. Further, the amount of time provided for training was significantly less than previous study (3 sessions instead of 5). Thus, it is possible each participant may require different amounts of training to improve functionality with the dEMG control to surpass that of their passive device. We plan to investigate improvements of training-specific tasks to understand the potential differences in learning rates across amputees that could further explain this result.

We attempted to understand if amputee participants adapted their neuromuscular control strategy between their passive device and dEMG controlled device. Surprisingly, amputee participants had significantly delayed (closer to perturbation timing) muscle activations in the dEMG control compared with their passive device. Typically, delayed timing of anticipatory postural adjustments leads to decreases in stability [153], however in our results we see significant improvement despite later activation of muscles. This result appears to highlight the benefit of restored anticipatory postural adjustments at the prosthetic ankle joint that, despite all muscles activating later, allows for improved performance in this task. Surprisingly, we observed similar timing between residual and intact TA activity in the passive device during the Push condition. Since the order of testing was randomized, it is possible that participants learned to use their residual TA muscle during the dEMG controlled conditions and maintained this behavior in the passive device evaluation afterward.

Our study has demonstrated the exciting potential for amputees to improve control of their residual muscles to the extent that they can use both residual and intact limbs similarly towards the maintenance of standing postural control under expected perturbation. Although these results are promising, more participants are required to determine how these results can be generalized to the broader amputee population. It would be interesting to investigate the ability for amputees to use residual muscle activity to in dEMG control under other conditions of perturbation (i.e. unexpected, increased number of directions, etc.). While we observed improvements in most of the amputee participants it would be interesting to investigate individual participant improvement over training to understand the potential differences in learning rates across amputees. Ideally, future work should include the use of a motorized device in order to evaluate the benefit of this control in the myriad of daily activities in which amputees use their prosthetic device.

3.4 Material and Methods

3.4.1 Participants

We recruited 5 transtibial amputees (TT) and 1 able-bodied control (AB) to participate in this study. All participants were male. This experimental protocol was approved at the University of North Carolina at Chapel Hill Institutional Review Board. Each participant provided written consent before participating in this study. Information about the 5 TT participants is provided in Table 3. The average age of amputee participants was 43.4(±11.72) years, and the age of the AB participants was 29. All participants were active, community ambulators who wore their prosthesis at least 12 hours a day.

Table 3-3 Amputee Participant Demographics

Participant	Age (years)	Post Amputation (Years)	Reason for Amputation
TT1	58	8.5	Soft Tissue Sarcoma
TT2	41	18	Trauma
TT3	32	15	Trauma
TT4	53	6	Trauma / Failed Limb Salvage
TT5	33	0.75	Dysvascular

3.4.2 Pneumatic Actuated Ankle Prosthesis

For this study we fit a pneumatically actuated ankle prosthesis for each TT participant. Each participant fit their daily prosthetic socket to the pneumatic ankle, and the alignment for each participant was set by trained prosthetist while the prosthesis was locked in a 90deg position. This prosthetic ankle contained 4 pneumatic artificial muscles (PAM), 2 placed anteriorly to generate dorsiflexion moments and 2 posteriorly for plantarflexion moments. These PAMs are used to produce similar force-length dynamics of intact musculature and are actuated using EMG magnitude taken from the envelope of residual muscle activity. More details on the ankle prosthesis can be found in [119].

3.4.3 Direct EMG Control Setup

In this study we took the envelope of previously antagonistic residual muscle activity to drive prosthetic ankle dynamics directly and continuously. We calculated the envelope of the residual Tibialis Anterior (rTA) and residual Lateral Gastrocnemius (rGAS) activity in real-time (dSPACE, CLP-1103,0-10V output) to generate a smoothed control signal. We processed the residual muscle activity in real-time by first applying a high-pass filter (100Hz, 2^{nd} Order Butterworth) to reduce effect from potential signal artifacts. Our real-time filtering then rectified the EMG signal and applied a low-pass filter (2Hz, 2^{nd} Order Butterworth). Our system then sent

the filtered control signal from each muscle to the pressure regulators responsible for generating pressure proportional to the input voltage (0-10V for 0-90psi).

Without the presence of air pressure, the prosthetic ankle was completely loose, thus, to provide a set stiffness in the prosthetic ankle we personalized a baseline pressure to each pair of muscles for each participant. To determine the appropriate pressure, we asked participants to sit with their prosthesis unloaded while we sent a signal to each muscle ~2V such that the resting prosthetic ankle angle was between 5-7deg. We then asked participants to stand with this baseline pressure. We then adjusted the baseline signal based on the perceived stiffness of the prosthetic ankle as the participant compared this with their intact ankle joint. We then asked the participant to sit. We repeated the two procedures above until both resting ankle criteria and ankle stiffness met our criteria (i.e. 5-7deg resting position and similar perceived stiffness between intact and prosthetic ankle). The baseline stiffness of the prosthetic of each ankle remained close to 2V. To allow the participant true continuous control of the prosthetic ankle, we did not establish an EMG threshold that prevents low-level activity from modulating prosthetic ankle behavior. Finally, we applied a gain to each input control signal at the beginning of each session such that a maximum contraction from each muscle resulted in a control signal between 9 to 10V.

3.4.4 Experimental Protocol

Similar to our procedure in previous work [117] we introduced TT participants to the pneumatic ankle with several acclimation trials before the start of training and evaluation. During the first acclimation trial we asked participants to sit while the pneumatic ankle was held in place beside them. We instructed participants to freely move the ankle using residual muscle contractions. During this initial exploration we also provided visual feedback of residual muscle

activations via a 2D computer cursor and asked participants to fill in as much of the 2D input space as possible (where the x and y axis of this space were scaled to maximum rTA and rGAS activations) [57]. During the second acclimation session we fit and aligned the pneumatic ankle prosthesis for each TT participant under the supervision of a trained prosthetist while the ankle was locked at 90deg. During the third and final acclimation session, we asked each participant to don the prosthetic ankle and attempt weight bearing on the device while using a walker with the dEMG control active. We encouraged participants to freely explore interacting with the ground while using the dEMG control of the prosthetic ankle. We then instructed the participants to attempt to stand upright without the use of the walker. Once the participants were able to stand for 30 seconds without the assistance of the walker, we ended the final acclimation session. All participants were able to meet this criterion within one weight-bearing session.

After acclimation, our study consisted of a minimum of 3 training sessions and 2 evaluations sessions. The timeline for training and evaluation is outline in Table 4.

Table 3-4 Training and Evaluation Timeline

Day	***Day 1*** ***Day 2*** ***Day 3***	***Day 4***	***Day 5****
Session	dEMG Control Training	dEMG Control Evaluation	Passive Device Evaluation
Tasks	Load Transfer Sit-to-stand Arm raise Rocker Board Postural Sway	Expected Perturbation • Pull (10% BW) • Push (10%BW) Repeat Training Tasks	

*Passive evaluations occurred before or after all other training and evaluation sessions. The order of evaluations was randomized before testing commenced
**Body Weight (BW) percentage

For our training sessions we implemented a similar paradigm used for extended, PT-guided training of a single amputee with dEMG control [117]. We abbreviated this previous training protocol to three sessions which include several tasks relevant to daily life activities including: Postural Sway, Load Transfer, Sit-to-Stand, and Arm Raises. Many of these tasks (with the exception of the load transfer and postural sway) are a subset of clinical evaluation tasks in the BESTest [163]. Each participant conducted a minimum of 1 trial for each task where Load Transfer, Sit-to-Stand and Arm Raise trials contain a minimum of 5 repetitions and Postural Sway trials contained a minimum of 20 cycles.

To evaluate the ability of amputees to produce anticipatory postural adjustments under expected perturbation using dEMG control we developed a platform capable of delivering expected perturbations in 2 directions: Push and Pull (Fig. 5). In this setup we asked each participant to hold a handlebar placed at shoulder level while standing in a relaxed posture. We placed an LED strip at eye level of the participant. In order for the participant to know the perturbation timing we switched off the LED strip 0.6 seconds before the electromagnet is released via two relays (5V, Parallax, CA, USA) controlled using LabVIEW. In this setup, the perturbation was delivered by a hanging weight that is connected to the handlebars by two cords via a series of pulleys such that the vertical force of the weight is translated into a horizontal force on the handlebars. We placed an electromagnet in series with one of the cords to control its connection with the weight. Thus, when the electromagnet is released, all weight is transferred horizontally causing a force in the direction of the cord that remains attached to the handlebar. The location of the electromagnet is switched based on the desired perturbation direction (i.e. push or pull). We placed one load cell (Omega, Stamford, CT) on each side of the handlebar to measure the force each participants applied before and during perturbation. A trial will be

removed from the analysis if participants applied force to the handlebar before light switch. Before each repetition we visually confirmed participants stance to insure they had a vertical, relaxed posture with both feet place symmetrically and shoulder-width apart. We repeated each perturbation 5 times for each condition. We provided each participant with 5 practice trials for each condition before the beginning of testing in order to familiarize them with the task. The order of testing each weight and direction was randomized before the start of the evaluation session. The size of perturbation was chosen based on pilot testing since the magnitude of perturbation was sufficiently difficult that amputee participants would potentially be unable to maintain balance during either the push or pull condition.

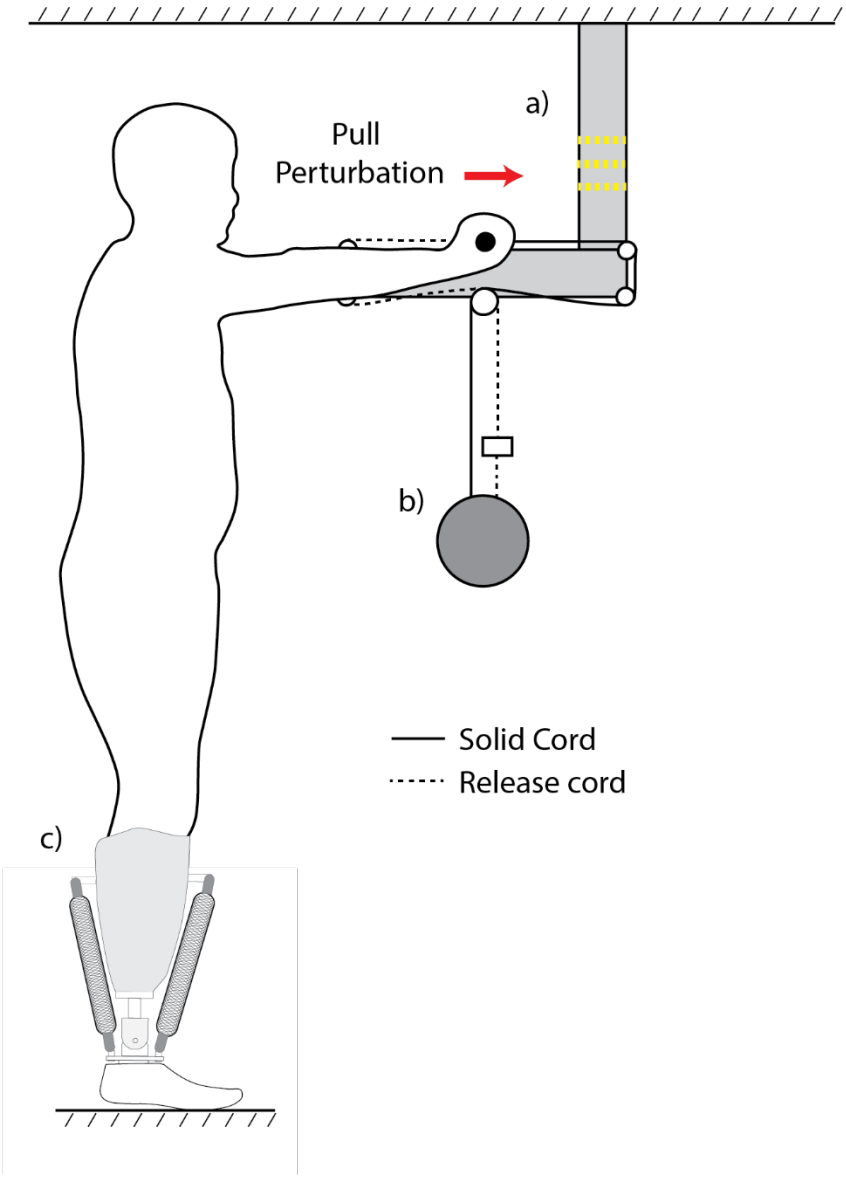

Figure 3-5 Experimental Platform Illustration. Participant stands upright while holding a handle bar at arm's length and shoulder height. The handlebar is attached to a suspended weight by two cords. One cord is directly attached to the weight (solid) and the other is attached to the weight with an electromagnet in series, that, when switched off severs the cord's connection with the weight (Release Cord). In this illustration the perturbation platform delivers a pulling perturbation on the participant. The direction of the perturbation is switched by changing the location of the solid and release cord. a) LED light. The LED light is switched off 0.6s before the electromagnet is released providing the participants with a notification of the impending perturbation. b) Perturbation load. Weight is normalized to the participants body weight (%BW). c) Pneumatic Artificial Prosthetic Ankle.

3.4.5 Measurements

During all sessions we collected EMG activity from intact and residual limb thigh and shank muscles. We placed EMG sensors (Motion Lab Systems, MA-420, Gainx20, Baton Rouge, LA) on the following muscles: Intact Tibialis Anterior (iTA), Intact Lateral Gastrocnemius (iGAS), Intact Soleus (iSOL), Intact and Residual Limb Rectus Femoris (iRF, rRF), Intact and Residual Limb Vastus Lateralis (iVL, rVL), Intact and Residual Limb Biceps Femoris (iBF, rBF). We determined the location of muscle via palpation and anatomical landmarks [164]. For residual Tibialis Anterior (rTA) and residual Lateral Gastrocnemius (rGAS), which are inside of the prosthetic socket, we placed low-profile EMG sensors (Neuroline 715, 1mm height, Ballerup, Denmark). We located muscles via palpation while participants contracted and relaxed muscles [58]. When residual muscle flexion was difficult to locate via palpation, we placed EMG sensors based on anatomical landmarks. We then iteratively shifted EMG sensor location to determine if other locations provided improved the observed signal-to-noise ratio. We routed cables to avoid bony landmarks and connected them to pre-amplifiers (Motion Lab Systems, MA-412, Gainx20, Baton Rouge, LA) outside of the prosthetic socket. We connected all sensors to an amplifier (MA300-XVI, Gain x1000).

In each session we collected ground reaction forces, moments under each foot using an instrumented split-belt treadmill (1,000Hz, BertecCorp, Columbus, OH). Center of pressure values are calculated under each foot using GRF and moments. We calculated overall CoP using the weighted average under each foot, weight by GRF [117]. We collected full-body kinematics (100Hz, 43 markers, VICON, Oxford, UK). We calculated center of mass (CoM) position using the analysis software (Visual 3D, C-Motion, Inc., Germantown, MD, USA). We low-pass filtered data from the treadmill (i.e. GRF, CoP), (20Hz, 4^{th} Order Butterworth).

From the perturbation setup we collected loading data from the handlebar via two tension load cells (Omega, Stamford, CT) placed on the anterior and posterior side. We recorded the control signal sent to each relay for light switch and electromagnet from the same DAQ as our split-belt treadmill (1000Hz).

3.4.6 Data Analysis

We processed data offline using MATLAB (Mathworks, Matick, MA). For evaluation trials we extracted and windowed each perturbation to 600ms prior to load release and 2000ms after release. To evaluate participant stability during each release perturbation we selected the CoM excursion, CoP excursion and ankle joint torque during each condition. For each repetition we calculated the average of each measure from 600-500ms prior to perturbation. We then subtracted this average value from each measure during each perturbation. We took the average of the 5 recorded trials for each condition, each device and each participant. For qualitative analysis we plotted the time series of each selected measure to compare behavior between the AB control, TT Passive, and TT dEMG control condition behavior. We plotted the push condition response since this was the most challenging condition for all participants (as evidence by frequent stepping responses required by TT participants with their passive device). For quantitative analysis we selected two time points from each repetition to understand the anticipatory and compensatory postural responses. For anticipatory responses we extracted the value of each measure at the moment of load release (t=0sec). Since the perturbation required participants to hold the load after release, we calculated the average value of each measure for 1000ms-2000ms after the load release, termed. We selected this time frame since CoP behavior changes only until ~1000ms after perturbation, demonstrating this time frame is representative of the final state of the participant under this perturbation.

To understand joint level strategy of participants when using their passive prosthesis compared with dEMG control we evaluated the ankle, knee and hip joint excursions during all perturbation repetitions with the same windowing described above. We subtracted the average joint angle of 600ms-500ms before load release from the full time series. For evaluation we then extracted values from "Release" and "Hold" time points.

For qualitative analysis of full-body strategies to maintain balance we qualitatively evaluated the combination of joint angle excursions from each participant using the dEMG control by observing two distinct joint excursions strategies. For 3 participants we spotted primarily ankle joint excursion when responding to the disturbance (where the hip and knee joint excursions did not exceed 2 degrees in either direction). For the remaining 2 participants we noticed a "mixed" strategy where participants move all joints more than 2 degrees for each joint simultaneously. We empirically defined these boundaries of excursions for strategies based on previous study of standing balance under perturbation [165]. During each condition we observed the number of instances where participants could not maintain balance. They either held onto the handlebar until it reached either the forward or backward stop (Fig. 1) or took a compensatory step. We counted the number of these situations and tabulated them.

We analyzed the neural control strategy through EMG activities from all intact and residual muscles. We first high-pass filtered the raw EMG signals (100Hz, 2^{nd} Order, Butterworth) then rectified it. For qualitative analysis of the neural strategy used while participants wore the dEMG controlled prosthetic ankle we plotted the EMG activities for each condition. To demonstrate this activity, we plotted representative activity from a single subject. For quantitative analysis of anticipatory postural adjustments between conditions we determined the moment of activation of relevant muscle during each condition. We determined the timing

muscle activations by first low-pass filtering all EMG signals (10Hz, 2nd Order, Butterworth). We then calculated the average and standard deviation of EMG signals during 600-500ms before the load release. We then determined the onset (or inhibition) of muscle activity as the moment where EMG signals exceeded either lower or higher than the average ±2SD within time window known for anticipatory postural adjustments (450ms pre-perturbation to 200ms post-perturbation). We then confirmed all activation timings of all muscles visually by observing raw and filtered EMG signals together for all muscles and all conditions. When muscle activity did not significantly change (either through quantitative or visual analysis) within the time window we did not tabulate a timing value for that muscle within that repetition. We then averaged each muscle's activation timings across all trials into one value within conditions, devices, and participants for further analysis.

3.4.7 Statistical Analysis

We conducted statistical analysis of the data using the statistical software (JMP, SAS, Cary, NC). We used a one-way ANOVA to compare CoM excursion and CoP excursion with Device (i.e., Passive vs. dEMG control) as the main effect. We used a two-way ANOVA for CoP excursion under each foot, joint angle excursions from "Release" and "Hold" time points with Device and Limb (i.e., intact vs. residual limb) as the main and interactions effects. We used a two-way ANOVA for activation timings of EMG activity using Device and Limb as the main and interaction effect. When the result indicates a significant effect, we tested for statistical difference within conditions using Tukey's honestly significant difference test. We set a threshold for significance at $a=0.05$. For each ANOVA analysis we included participant as a random effect. This effect was not significant in any outcome measure for any condition ($a<0.05$).

CHAPTER 4: Reorganization of Neural Control of Voluntary Postural Sway using Direct Electromyographic Control of a Powered Prosthetic Ankle

4.1 Introduction

The loss of a lower-limb drastically changes the movements and choices of individuals due to the limitations of a prosthetic limb. Current passive ankle prostheses (i.e. mechanically passive with set stiffness) do not behave like the intact limb it intends to replace, as individuals lack the ability to volitionally modulate ankle joint mechanics using descending motor commands. Individuals with amputation thus reorganize joint coordination strategies to compensate for the loss in function caused by the lack of volitional ankle joint control [8, 166, 167]. Naturally, this reorganization leads to asymmetry between the intact and residual limb behavior resulting in changes in weight-bearing [149, 168, 169] and other biomechanical features related to stability [8, 9, 161] (i.e. center of pressure, CoM excursions). These adaptations allow individuals with amputation to stand and ambulate with their prosthetic device, however the cost of these compensatory joint coordination strategies is poorer stability compared with able-bodied counterparts [6, 11]. Long-term, these asymmetric behaviors could also result in comorbidities such as osteoarthritis in continuously overloaded joints.

Despite the recent dawn of powered ankle prostheses (i.e., devices capable of generating net positive joint work like the intact limb), individuals with amputation are still challenged to generate normative multi-joint coordination to improve movement performance [170-172]. Researchers first implemented state-based autonomous control designs with powered prosthetic limbs, where movements of the amputees are sensed by the prosthesis and a predetermined joint torque is delivered to assist the individual [30, 152]. Early work with these autonomous paradigms with ankle prostheses showed promise for improving metabolic cost of walking [152].

However, recent study has shown this benefit is not consistent, potentially a result of poor coordination of prosthetic ankle joint behavior with intact joints [170].

What if we provide amputee users the potential to volitionally coordinate their own prosthesis behavior to restore normative function? Amputees retain the ability to volitionally contract residual muscles (i.e., muscles previously responsible for joint movement), and the efferent motor commands driving these muscles can be captured via electromyography (EMG). By using these neuromuscular signals, we can recreate a control paradigm like the intact limb where the joint mechanics are continuously and volitionally updated based on these efferent motor commands. Direct EMG (dEMG) control, also termed proportional myoelectric control, has been used primarily to restore function in locomotion using one or multiple residual muscle as sources [16, 39, 40]. One of the first generations of this control incorporated EMG control with autonomous control to control powered, push-off during walking [40]. Individuals lacked volitional control outside of this specific state, limiting the generalizability of this control to other daily-life tasks. Huang et. al used a single residual muscle to continuously control plantarflexion demonstrating the ability for amputees to restore positive ankle joint work during walking [16]. However, most individuals were unable to successfully adapt residual muscle activations without the presence of visual feedback of their muscle activations. Amputees could coordinate residual muscle activity with full-body movements (to restore positive ankle joint work), however they required additional feedback. Most recently, we investigated the effect of extended, PT-guided training to improve dEMG control using antagonistic residual muscle activations, demonstrating the ability for an amputees to closely synchronize residual muscle activity with homologous muscles resulting in improved stability during daily life tasks [117]. While this study demonstrated the improvement in joint and muscle coordination of the

prosthetic limb with intact limb mechanics with a single participant, it is unclear how multiple amputees might adapt residual muscle activity to improve standing balance. Further, this study did not provide significant information regarding the adaptations from other muscles besides those controlling the prosthetic ankle. Thus, we have not yet determined 1) if multiple individuals with amputation are capable of coordinating residual and intact muscle activity 2) what are the neural strategies used to coordinate these muscle groups and 3) what are the implications for overall movement control based on these neural adaptation strategies used by amputees. For example, by asking amputees to volitionally control prosthetic joint mechanics during postural control tasks, are additional attentional resources allocated when using dEMG control such that the cognitive load is significantly increased (i.e. potentially placing the individuals at a higher rate of falls [173, 174])? In order to improve our understanding of the mechanisms behind amputee neural control of movement while using dEMG control of a prosthetic ankle, systematic analysis of movement coordination is required.

A common method to investigate the potential neural underpinnings of coordinated movement production is through the use muscle module analysis. Muscle modules are theorized to be the method by which the human body simplifies the complex problem of simultaneously controlling of many individual muscles towards the completion of a given task [175, 176]. This theory postulates the central nervous system (CNS) groups individual muscles into set spatial structures with time varying activation profiles [177]. It is possible then for these muscle modules to be combined, scaled and co-varied to accomplish a various goal-oriented movements [178, 179]. This analysis has been implemented in neurologically impaired populations (i.e. stroke and Parkinson's) to understand the potential relationship between changes in neural coordination and movement performance over rehabilitation [180, 181]. In both cases

researchers found significant differences in muscle coordination structure were significantly correlated with task performance, suggesting that these intact neural structures were predictive of individual's performance and improvement during rehabilitation. Further, these studeis provided a window to see the strategies used by various populations during rehabilitation. This analysis might thus provide a fuller understanding of the neural resources available to improve function while using antagonistic residual muscle for continuous, volitional control of a prosthetic ankle [182].

We propose here to systematically analyze the changes in neuromuscular coordination strategies, via muscle mode analysis, of transtibial amputees from extended training with dEMG control of a powered prosthetic ankle. This analysis will allow us to understand: 1) if amputees adapt residual muscle activity in coordination with intact muscle groups to form new, goal-oriented muscle modules 2) If amputees are capable of improving consistency (i.e., reducing variability) of muscle module activations 3) Whether changes in neuromuscular coordination are correlated with changes in movement performance for a standing postural control task. Results from this study could set the foundation for future work to understand the ability for amputee to develop neuromuscular control strategies across residual and intact muscle groups that have the potential to be generalized across other tasks. Further, the results from this study could allow the use of muscle module analysis to elucidate the potential reasons for differences in performance across amputees with dEMG control based on the neural strategies available to coordinate residual muscle with intact muscles activity.

4.2 Results

Across training we observed individual changes in number of muscle modules employed during the voluntary postural sways, however these changes were not significant on average (p =

0.273) (Fig. 1). Pre-training, we observed 3±1 (*range: 2-4*) muscle modules used by participants while using the dEMG control prosthetic ankle. After training the participants either reduced or maintained the number of motor modules used (e.g., TT1 and TT5 respectively, Fig. 1) (2.4± 0.55). While using their daily device participants used a similar number of muscle modules (2.8 ± 0.45). We extracted results from TT1 and TT5 specifically to illustrate the general differences in participants who either maintained or reduced number of synergies used.

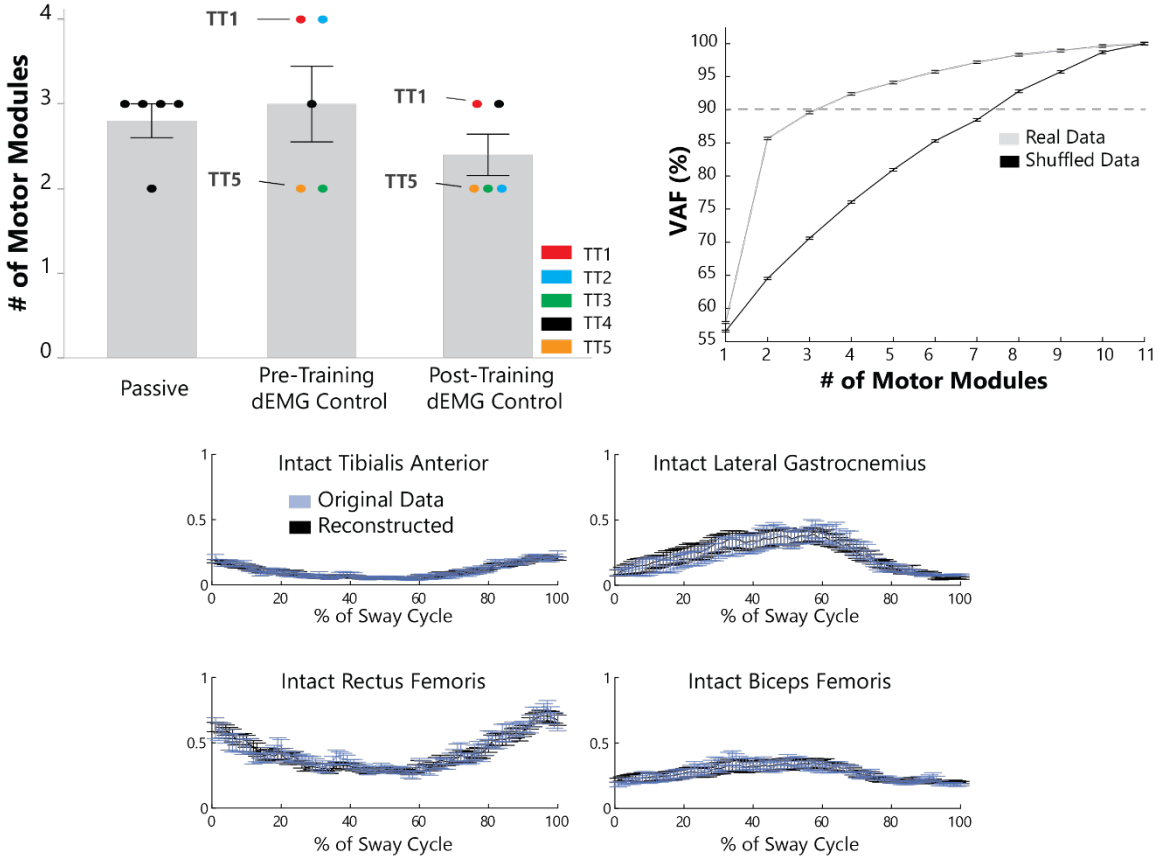

Figure 4-1 Number of motor modules and goodness of fit. Top Left) number of muscles modules required to sufficiently described original EMG activity with reconstructed EMG. Passive, and dEMG control conditions from pre and post-training are displayed. Top Right) Exampled VAF for each number of synergies used for a representative subject (TT1). VAF and 95% CI are constructed for real EMG data as well as shuffled EMG data. Bottom) Example

reconstructed EMG from a single subject (TT5) averaged across sways plotted with standard error bars.

4.2.1 Representative Participant Behavior Pre- vs. Post-Training

In our analysis we observed two representative behaviors based on number of muscle modules and extracted representative participants behavior for further evaluation: 1) Reduction in number of employed muscle modules (e.g., TT1) and 2) Preservation of number of muscle modules (TT5). For our representative participant TT1 we observed several changes in muscle module structure pre- vs. post-training (Fig. 2). Pre-training, TT1 primarily activated posterior muscle groups (i.e., GAS, BF, SOL) during the forward part of the sway (50% sway cycle) in effort to bring their body backward (Fig. 2a). However, the participant used multiple modules, where the first module contained activation primarily from the residual limb (i.e. rGAS and rBF) as well as coactivation from the residual TA. The remaining module contained activation from all posterior muscles as well as co-activation from the iRF, rVL and iVL (Fig. 2a). Post-training, the participant only employed a single muscle module with all posterior muscle groups during the forward part of the sway and eliminated co-activation from thigh muscles (Fig. 2c). We observed co-activation from the residual TA, however the scale of this activation was less than pre-training muscle modules (Fig. 2c). Similarly, we observed multiple modules used during the backward portion of the postural sway (i.e., 0% and 100% of sway cycle) (Fig. 2b). One muscle module contained rRF, iRF and rVL with co-activation from the SOL muscle. The remaining module contained iTA, iRF and iVL with co-contraction from the iBF muscle. We did not observe significant activation from the residual TA in either muscle module pre-training (Fig. 2b). Post-training, we observed a single muscle module containing residual TA along with all other anterior muscle group during the backward part of the sway (Fig. 2d). We also observed co-contraction in this muscle modules from the residual GAS (Fig. 2d.). Post-training, we also

observed a muscle module, whose activation remained relatively constant across the sway cycle, which we term as a 'Tonic' Muscle module (Fig. 2e). This module contained rRF, rVL and iVL muscles (Fig. 2e).

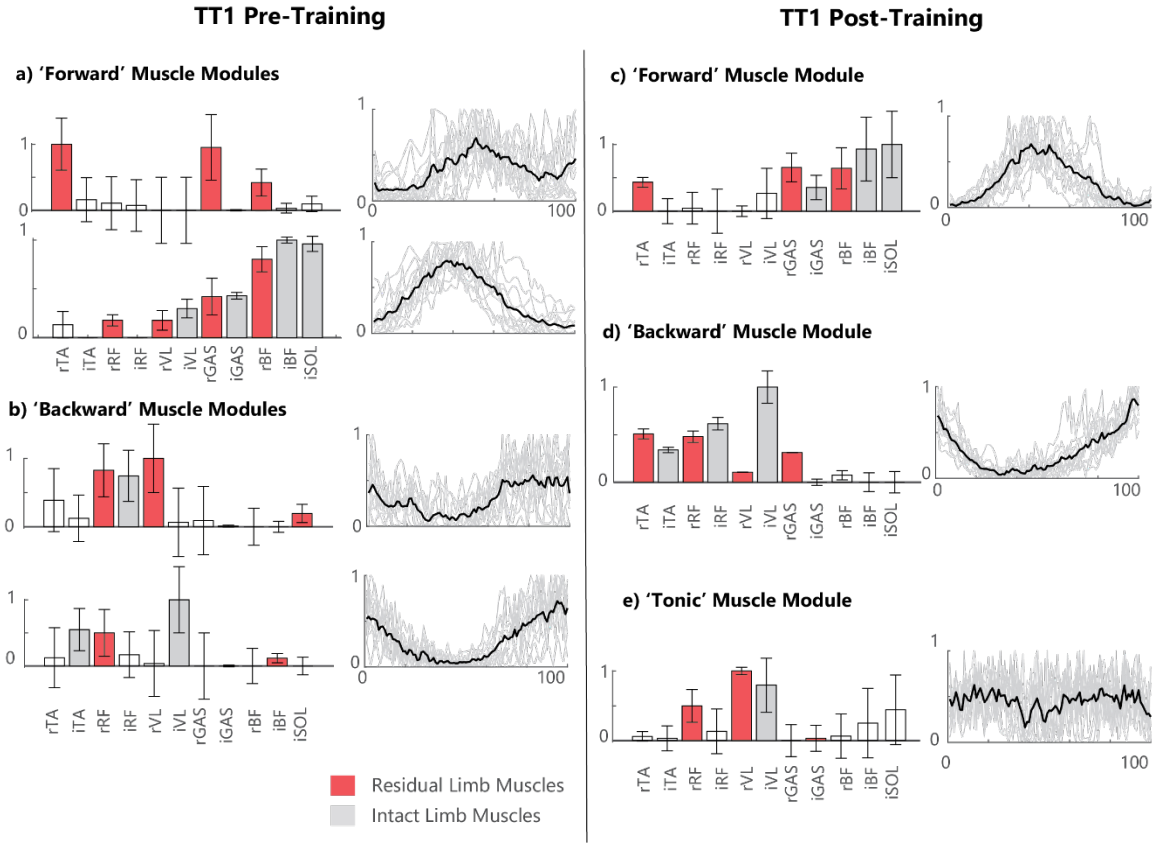

Figure 4-2 Extracted Muscle Module and Activation Coefficient from pre-training and post-training conditions with dEMG controlled ankle from TT1. Red Bar) residual limb muscles Grey Bar) Intact Limb Muscles. Empty bar) Muscles whose 95% CI (error bars) passes 0 bound and are considered inactive. Average time series of activation module is shown (black line) as well as individual time series for each repetition (grey line) Muscle modules are grouped based on motor module activation profiles where muscle modules activated at forward-most part of the sway (i.e. 50% of sway cycle) are 'Forward' modules (a, b). 'Backward' Muscle Modules consist primarily of anterior muscles and are activated predominantly at the backward-most part of the sway (i.e. 0 or 100% of sway cycle) (c, d). Tonic muscle modules are defined by the consistent, tonic activation of the motor module through the sway cycle (e).

We observed a strategy used by some participant to maintain the same number of motor modules pre- and post-training. We extracted and analyzed one representative participant from

these three, TT5 (Fig. 3). Pre-training, TT5 employed one motor module for each direction of sway (Fig. 3a, c) and maintained this behavior post-training (Fig. 3b, d). Pre-training, TT5 significantly activated all but one muscle (Fig. 3a) in the 'Forward' module demonstrating high co-activation. Post-training, TT5 reduced the number of co-active muscles in the 'Forward' muscle module (*Pre: 10 vs. Post: 8*). Further, TT5 clearly reduced the variability of the activation coefficient of the 'Forward' muscle module (Fig. 3c). Across training, TT5 reduced co-activation of residual muscles such that rTA activity was not present post-training (Fig. 3b). Pre-training, TT5 had high numbers of significantly active muscles in the 'Backward' module (Fig. 3c), however the participant reduced this number post-training (Fig. 3d) (*pre: 9 vs. post: 7*). Post-training, TT5 also notably reduced the variation of the activation coefficient of the 'Backward' module (Fig. 3d). Muscle modules and activation profiles for the remaining participants are located in Appendix B.

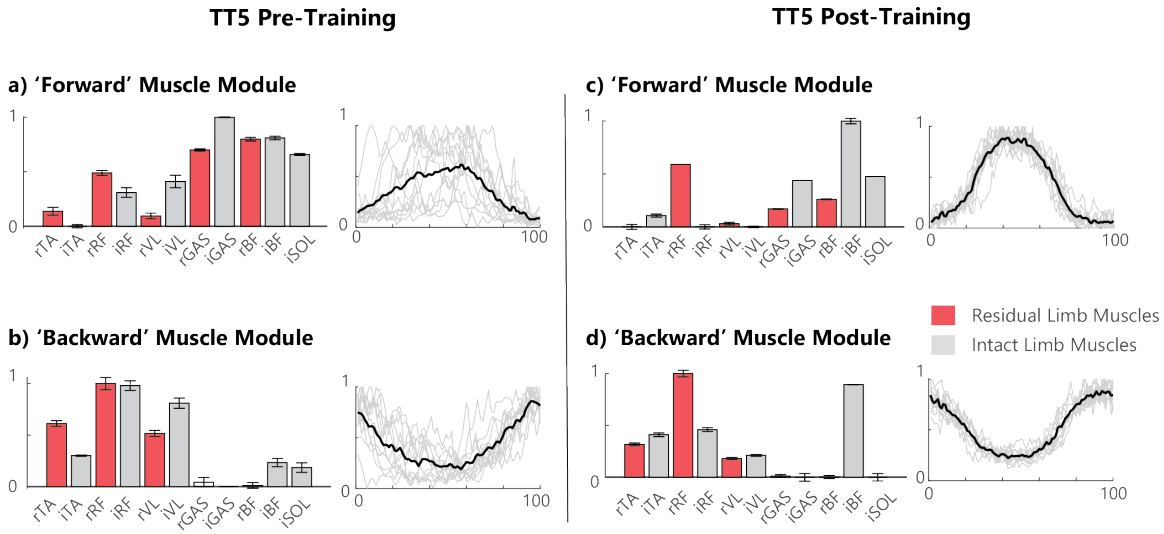

Figure 4-3 Extracted Muscle Module and Activation Coefficient from pre-training and post-training conditions from participant with same number of motor modules (TT5). *Red Bar)* residual limb muscles *Grey Bar)* Intact Limb Muscles. *Empty bar)* Muscles whose 95% CI (error bars) passes 0 bound and are considered inactive. Average time series of activation module is shown *(black line)* as well as individual time series for each repetition *(grey line)*.

4.2.2 Muscle Modules Similarity Pre- vs. Post-Training

From pre- to post-training, we observed low correlation between muscle module structures across participants, however activation coefficients were highly correlated across training. On average participants altered muscle module structure between pre- and post-training (Backward: $r = 0.51 \pm 0.30$, Forward: $r = 0.55 \pm 0.33$), less than the 0.735 correlation threshold (see methods, 4.4.4.3). Only TT4 maintained significantly similar muscle mode structure pre- and post-training (Backward: $r = 0.984$, Forward: $r = 0.886$) (Fig 4a, c). On average, participants did not significantly change activation coefficient profiles from pre- to post-training (Backward: $r = 0.91 \pm 0.05$, Forward: $r = 0.90 \pm 0.10$) (Fig. 4b).

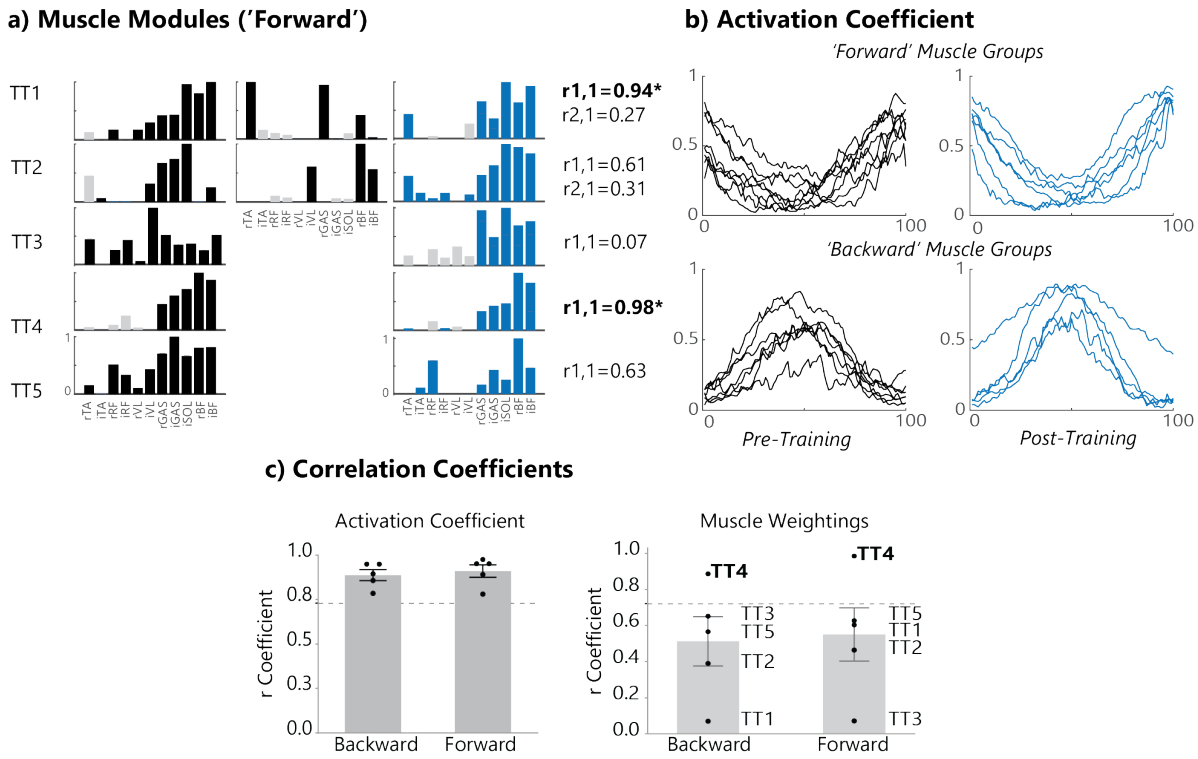

Figure 4-4 Comparison of muscle module structure and activation coefficient structure pre- vs. post-training. a) Pearson correlation coefficient between muscle module structures pre- vs. post-training for 'Posterior' muscle modules (i.e., muscle modules that contain primarily posterior muscle groups and are activated at the forwardmost parts of postural sway). Muscle modules that are significantly similar across training are shown in bold. b. Average temporal profile of muscle module activation (i.e., activation coefficient) across training for both 'Posterior' and 'Anterior' muscle modules for all participants. All muscle modules activation profiles are shown in this graph with the exception of one 'tonic' activation muscle module from TT1 (Fig. 2). c) Average Pearson correlation coefficients both activation coefficient profiles and muscle weightings. Dashed line represents threshold for correlation coefficients that have similarity that is statistically significant (see methods). Correlation coefficients are separated by timing of activation (i.e., during forward sway or backward sway).

4.2.3 Muscle Modules Measures

We observed changes in both the temporal structure and number of muscle modules used across participants. From pre- to post-training, we observed a significant improvement in the consistency (i.e., less variability) of the activation of muscle modules (Fig. 5a). That is, participants decreased the RMSE between the activation coefficient of individual sways and the

average of all sways (Pre-Training C_{rms}: *0.18(±0.03),* Post-Training C_{rms}: 0.12(±0.04), *p=0.014*). TT4 demonstrated the smallest change in C_{rms} across training (Pre-Training C_{rms}: *0.161*, Post-Training C_{rms}: *0.143*). Participants did not significantly change amount of muscle module activation (i.e., area under average activation coefficient curve for each module) (Pre-Training C_{area}: 35.64(±4.82), Post-Training C_{area}: 37.55(±5.75), *p=0.584)* (Fig. 5b). We did not observe significant change in duty cycle of muscle mode activation as well (Pre-Training C_{duty}: 81.47(±10.58), Post-Training C_{duty}: 75.83(±9.47), *p = 0.401)* (Fig. 5c). Over training, participants reduced the total number of significantly active muscle across all modules *(*Pre-Training: 18.2(±1.92), Post-Training: 15.6(±0.89), *p = 0.025)* (Fig. 5d).

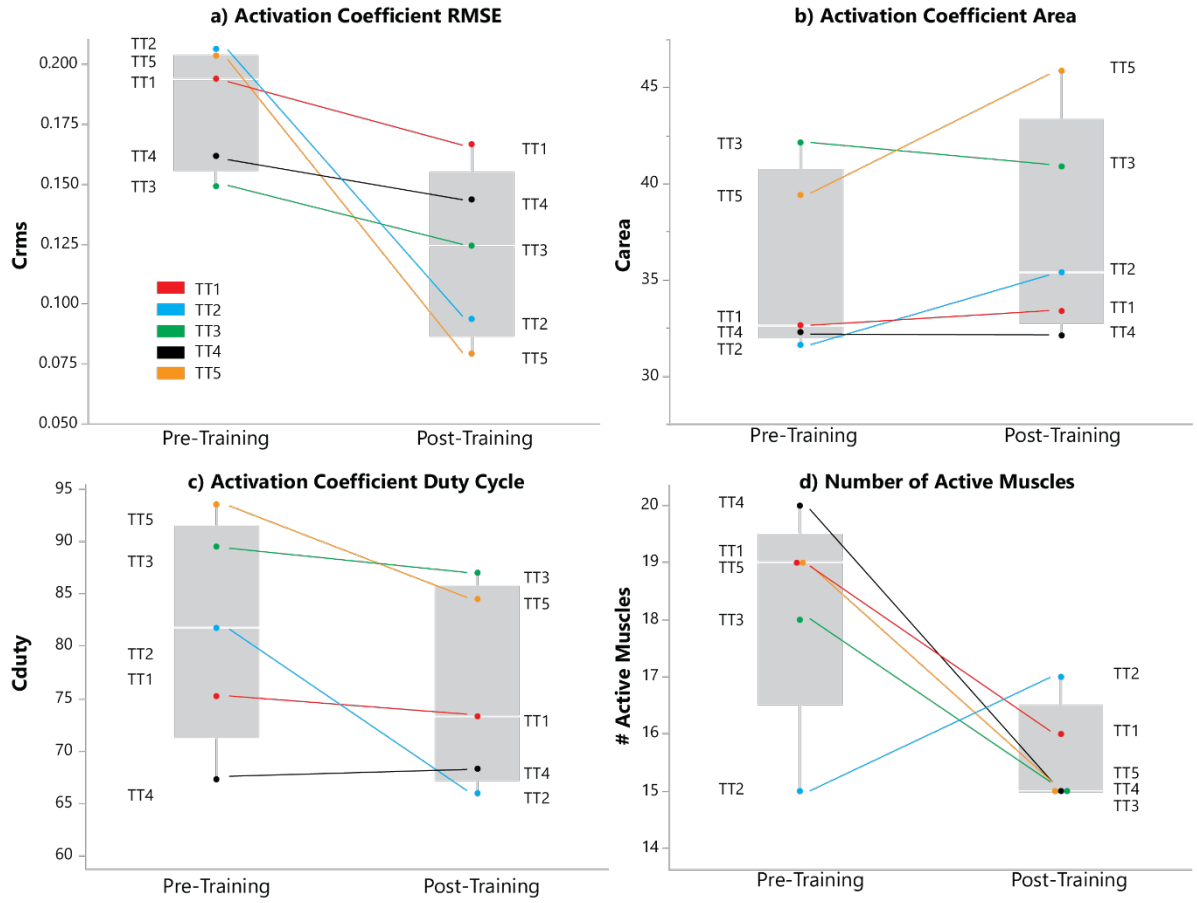

Figure 4-5 Muscle module spatial and temporal structural changes pre- vs. post-training. a) Average RMS of muscle module activation from individual sways with the mean muscle module activation over all sways (Crms). RMS values are averaged across all muscle modules for each participant. b) Area underneath mean muscle module activation across all modules for each participant (Carea). c) Duty cycle of muscle module activation (i.e., % of postural sway cycle muscle module activation spent about 0.15) (Cduty). d) Total number of significantly active muscle across all muscle modules for each participant. Individual participants are shown to highlight individual behavior changes across condition.

4.2.4 Postural Sway Outcome Measures

We observed several changes in postural sway measures across training and device. After training with the dEMG controlled ankle, participants significantly reduced the error in sway time (Pre-Training: 0.76(±0.35s), Post-Training: 0.25(±0.22s), $p=0.025$) (Fig. 6a). The error in sway time was not significantly different between devices (Passive: 0.16(±0.25s), $p = 0.554$).

We did not observe significant difference in CoP excursions between the intact and prosthetic feet before and after training (Pre-training: 47.45(±25.79), Post-training: 32.59(±6.44), $p = 0.247$). We also did not observe a significant difference between devices (Passive: 34.99(±4.93), $p = 0.526$). Most participants improved weight bearing symmetry after training with the dEMG controlled device (Fig. 6c), however this effect was not significant (Pre-training: 104.57(±11.2%), Post-training: 100.53(±9.39%), $p = 0.554$). Nearly all participants improved weight bearing symmetry with dEMG controlled device compared with their passive, however this comparison was not significant (Passive: 107.22(±11.86%), $p = 0.352$). In each comparison the only participant who did not improve weight bearing symmetry was TT4. We observed near significant change in the amount of postural sway participant made with the CoM in the Anterior-Posterior Direction using the dEMG control prosthetic ankle post-training (Pre-Training RMS: 0.86(±0.09), Post-Training RMS: 1.11(±0.24), $p = 0.095$). We observed a trending increase in the CoM sway compared with the passive condition, however this was not significant (Passive RMS: 0.93(±0.19), $p = 0.220$).

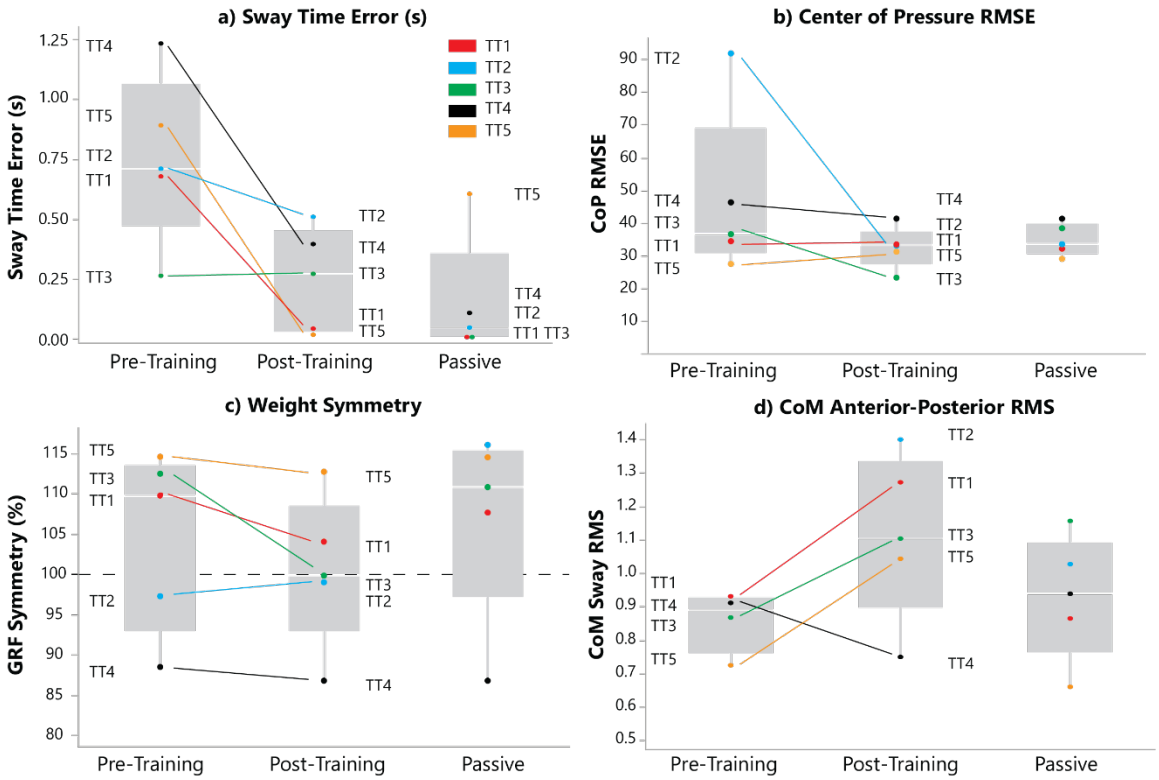

Figure 4-6 Postural Sway Outcome Measures between pre-training, post-training and passive device conditions. a) Average sway time across full trial for each participant. b) Root mean squared error for CoP excursions between prosthetic and intact foot for each participant. c) Weight bearing symmetry between intact and residual limb. d) Root mean squared of CoM sway over full trial.

4.3 Discussion

Here we present the first study to systematically investigate adaptions in neural control of movement while individuals with lower-limb amputation learn to use residual muscle activity to drive a dEMG controlled powered prosthetic ankle. In this study we observed several significant adaptations from amputees that demonstrate the capacity to incorporate residual muscle activity into task-oriented muscle groupings with intact muscle groups. These adaptations demonstrate the potential ability for amputees to 1) improve proficiency of neural control of movement (i.e., more consistent activation of muscle modules) 2) improve composition of muscle modules,

simplifying movement control in a standing postural sway task from multiple to singular modules 3) improve efficiency of muscle module composition demonstrating potential decrease in number of cortical resources involved in movement. Our results also demonstrate a potential relationship between the ability of amputees to adapt muscle module recruitment including residual muscles to the improvement in movement outcomes. These results are the first step in understanding the potential neural mechanisms amputee employ while adapting residual muscle activity as well as the potential for these individuals to reduce the cognitive burden involved while using dEMG control.

Interestingly, we observed several participants (TT1,TT2,TT4) who initially employed muscle modules that were abnormal compared with typical able-bodied behavior (see [183]), however these participants significantly altered muscle modules after training with the dEMG controlled ankle. Pre-training, several participants employed various muscle modules structures with either 1) isolated activity from the antagonistic residual muscles (TT1) 2) no activation of residual muscles (TT1, TT4) or 3) separate modules for the residual and intact muscles (TT2). Post-Training these participants successfully incorporated residual muscle activity with other muscle groups to form new modules with synchronized activation of homologous muscles from the residual and intact limb (see Fig. 2 and Appendices). These modules were linked to specific phases of the postural sway cycle, where activation of anterior muscles served to bring the CoM forward and activation of posterior muscle served to bring the CoM backward. It is possible that these participants grouped the activations of all posterior/anterior muscle groups into one task-level command, resembling able-bodied neural behavior [183]. This shift in the resulting individual muscle activation from an altered task-level command from the Central Nervous System (CNS) could simplify the amputees' control of movement while using the dEMG

controlled prosthetic ankle. The remaining participants already demonstrated grouped activation of residual and intact muscle groups before training, however they did reduce the number of coactivated muscle not related to the current movement (i.e. some posterior muscle activated while the anterior muscle group is primarily activated, see Fig. 3a,c). It would be interesting to further investigate the neural behavior of related standing postural control tasks to determine if participants developed neural strategies that can be generalized across tasks. Investigation toward this question would determine if common theories of muscle modules as building blocks for various movements [178] could hold true amputee participants. If true, this would demonstrate the possibility to improve the performance for multiple daily-life tasks through the training of select movements.

We also observed amputees improve proficiency of neural activity after training with the dEMG controlled prosthetic ankle (Fig. 3, 5a). Participants reduced variation of muscle module activations after training (Fig. 5a, C_{rms}), a trend similarly observed when comparing novices and experts during balance beam walking [178] and after targeted rehabilitation in individuals with Parkinson's disease [181]. The high initial variability of muscle module activations we observed from participants may be a result of several factors: 1) Amputees may be attempting to explore possible actions across all muscles to improve movement control [184]. 2) The muscle modules necessary to complete the task were outside the currently developed muscle modules [178], however this is unlikely as participants could complete the task with their passive device, and performance between the trained dEMG control device and passive device was not significantly different. 3) Amputees may have learned to interpret relevant sensory information (i.e. pressure at the limb-socket interface, vestibular, efferent motor signals [185, 186]) 4) Participants may have experienced greater instability initially with the dEMG control, leading to more discrete

activation of muscle modules to maintain balance [178, 187]. The only participant to not improve proficiency was TT4 (Fig. 5a), who also did not significantly change muscle module structure across training (Fig 4a). Interestingly, this participant also did not improve outcome measures for the postural sway task (Fig. 6), suggesting that the change in neural strategy of other participants resulted in improvements in task performance. Future study should investigate the potential mechanisms behind improvement in consistency observed here in the neural control structure while using dEMG of a prosthetic ankle.

We observed improved efficiency in muscle coordination after training with dEMG control. Post-training, participants had less co-activation of muscles, using less muscles overall to complete the voluntary postural sway task (Fig. 5d). This improvement in muscle coordination efficiency has been observed previously in long-term task training [178] and in rehabilitation of individuals with sensorimotor impairments [180]. It is suggested that this increase in efficiency reflects improved efficiency of movement generation at the primary cortex level [188] and represents an improved efficiency of the use of cortical resources [189]. Additionally, it is suggested that longer practice may begin to shift the role of coordinating motor patterns to subcortical circuits as well, alleviating the burden on the motor cortex [190, 191]. It would be interesting to further investigate whether the cognitive burden introduced by the restoration of volitional ankle joint control is reduced over long-term use with dEMG control with a powered prosthetic ankle.

This study highlights the potential for adaptations neural structure of coordinated muscle activity from residual and intact muscles due to targeted training with dEMG control of a prosthetic ankle device. Promisingly, all participants improved in one or more areas of muscle module generation, however there was separation in the amount of improvement, which

qualitatively seemed to correlate with improved task performance. Future study should include a greater population of participants in order to confirm these initial results. It would be exciting to expand this initial work through the inclusion of more evaluated tasks as well as a more thorough investigation into the potential relationship of neural structures with outcome measures like previous muscle mode work including uncontrolled manifold analysis [183]. While we observed minimal improvement in outcomes measures related to the task performance compared with individuals' passive device, we expect that more challenging tasks (i.e., situations of perturbation) would likely better illustrate the functional benefit of dEMG control of powered prosthetic ankles. In this study we conducted 3 guided training sessions with the dEMG control device, however previous study with a single transtibial amputee showed continued improvement over the course of 5 training sessions. Thus, future study might observe greater improvements given a more extended, guided training protocol. These results show promise for ability for amputees to meaningfully adapt residual muscle activations with intact muscles over guided training towards accomplishing daily-life tasks involving standing postural control.

4.4 Materials and Methods

We recruited 5 transtibial amputees to participate in this study. This study was approved by the IRB at UNC-Chapel Hill. All participants provided written, informed consent. We tabulated participants demographics (Table 1). The average age of participants was 43.4(±11.72) years. All participants were active individuals, who wore their prosthesis at least 12 hours a day.

Table 4-1 Amputee Participant Demographics

Participant	Age (years)	Post Amputation (Years)	Reason for Amputation
TT1	58	8.5	Soft Tissue Sarcoma
TT2	41	18	Trauma
TT3	32	15	Trauma
TT4	53	6	Trauma / Failed Limb Salvage
TT5	33	0.75	Dysvascular

4.4.1 Experimental Procedure

All participants completed a controlled postural sway task using 1) their daily passive prosthetic ankle, 2) dEMG control prosthetic ankle pre-training and 3) dEMG control, post-training. For the postural sway task, we instructed participants to sway as far forward and backward as possible repeatedly at a frequency of 0.25Hz [183] for a total of 20-25 sways. We instructed participants to keep both their prosthetic and intact foot flat on the ground during the entire task and provided a metronome to assist with timing. Participants stood at a comfortable stance with arms held by their side.

4.4.2 dEMG Control Training

To investigate the changes in motor coordination behavior for standing postural control with the dEMG controlled prosthetic ankle we conducted an extended, guided training with each participant using the dEMG control device. We adapted a previously developed training protocol, which was used specifically for dEMG control of a powered prosthetic ankle [117]. This training protocol contained several daily-life tasks (i.e., Sit-to-Stand, Load Transfers, Arm Raises, Quiet Standing). In this study we also included the postural sway task within the training protocol in order to directly train this task. During training days each participant completed a minimum of 5 repetitions of each training task. For postural sway trials participants completed

20-25 complete sways (forward moment to forward moment). We ask participants to repeat this task a minimum of two times each training session. We selected this number of repetitions for each task to avoid participant fatigue before all training tasks were completed at least one time each day. The timeline and training tasks are tabulated (Table 2).

Table 4-2 Training and Evaluation Timeline

Day	***Day 1***	***Day 2***	***Day 3***	***Day 4***	***Day 5****
Session	Training (dEMG control)			dEMG Control Evaluation	Passive Device Evaluation
Tasks	Load Transfer Sit-to-stand Arm raise Rocker Board Postural Sway			Expected Perturbation • Pull (10% BW) • Push (10%BW) Repeat Training Tasks	

*Passive evaluations occurred before or after all other training and evaluation sessions. The order of evaluations was randomized before testing commenced
**Body Weight (BW) percentage

During training we provided verbal feedback to each participant about their performance after completing a task [117]. Initially, we provided verbal feedback to participants regarding their joint level behavior with the dEMG controlled prosthesis (i.e., we encouraged synchronized muscle activity by informing participant whether they activated their residual muscle before, after, or simultaneously with their homologous muscle from the intact limb). As participants were able to consistently time residual muscles activations w.r.t. to intact muscles, we then began to provide verbal feedback to the participant concerning their whole-body symmetry. That is, at the end of each repetition of the task we informed participants whether they shifted their weight to the prosthetic or intact side significantly during task completion. This feedback replicated physical therapist feedback provided in previous study [117], similar also to typical feedback that would be available in a clinical setting.

4.4.3 Measurements

4.4.3.1 Kinematic Data

During all sessions we collected full-body kinematic data using 3D motion capture system (100Hz, 43 markers, VICON, Oxford, UK). We collected ground reaction forces and moments under each foot with an instrumented, split-belt treadmill (1,000Hz, BertecCorp, Columbus, OH).

4.4.3.2 Electromyographic Data

During each session we measured EMG activity from the intact and residual limb thigh and shank muscles. We placed EMG sensors (Motion Lab systems, MA-420, Gainx20, Baton Rouge, LA) on the intact Tibialis Anterior (iTA), intact Lateral Gastrocnemius (iGAS), intact Soleus (iSOL), intact and residual limb Biceps Femoris (iBF, rBF), intact and residual limb Rectus Femoris (iRF, rRF), intact and residual limb Vastus Lateralis (iVL, rVL). We determined muscle location via palpation and anatomical landmarks [164]. We placed low-profile EMG sensors (Neuroline 715, 1mm height, Ballerup, Denmark) on the residual Tibialis Anterior (rTA) and residual Lateral Gastrocnemius (rGAS). We determined residual muscle location via palpation while participants contracted and relaxed these muscles several times [58]. When residual muscle location was difficult to determine via palpation (due to small muscle volume) we initially placed EMG sensors based on anatomical landmarks. Then we observed the EMG signal-to-noise ratio while the participant contracted and relaxed the targeted muscle. We then shifted EMG sensor location in several locations proximal to distal as well as medial to lateral within a distance of 2cm from the original placement. After searching we then qualitatively selected the location that provided the highest signal-to-noise ratio for the intended muscle. After

placement, we routed EMG cables outside of the prosthetic liner and socket, while avoiding bony landmarks, and connected them to pre-amplifiers (Motion Lab Systems, MA-412, Gainx20, Baton Rouge, LA). We connected all pre-amplifiers to an amplifier (MA300-XVI, Gain x1000).

4.4.4 Data Analysis

We processed all data offline using MATLAB (Mathworks, Matick, MA). We first low-pass filtered all data from the instrumented split-belt treadmill (2^{nd} Order, 20Hz, Butterworth). We calculated Center of Pressure in the Anterior-Poster (CoP_{AP}) direction using GRF and Moment data from the treadmill [192]. We windowed each individual sway selecting the forward most extremes of CoP_{AP} as the beginning and end of the sway. For each trial we first removed any sways where the participant was unable to maintain balance and required a step forward or backward. For the muscle module analysis we selected the middle 12 sways [183] from the remaining data. For evaluation of kinematic and kinetic variables we included all sways from the remaining data.

4.4.4.1 EMG data

For all conditions we post-processed EMG data by high-pass filtering (3^{rd} order, 35Hz, Butterworth), rectifying, then low-pass filtering (3^{rd} order, 40 Hz, Butterworth) [178]. We down sampled the collected EMG by averaging data into 50-ms time bins [178]. We then concatenated EMG data from all sways for each condition and participant generating data matrices of m (# of muscles) x b (# of bins) [178]. We did not time normalize EMG data, which resulted in data matrices of different sizes between participants. EMG matrices for each condition and participant contained a minimum of 700 data points. We normalized EMG values of each muscle vector by the maximum observed value of that muscle across sways. We did this separately for each

condition and participant. We then scaled each muscle vector to have unit variance in order that equal weighting is applied to each muscle during the muscle mode analysis. After muscle module extraction, we removed this scaling for each muscle vector.

4.4.4.2 Muscle Module Extraction

We extracted motor modules from each condition and participant separately using nonnegative matrix factorization (NNMF) [178]. NNMF has been used in numerous studies evaluating muscle module presence in various tasks and patient populations [178, 180, 181]. NNMF extracts muscle modules with the assumption that individual activity from muscles, V_{mxb}, are the result of the linear combination of the multiplication of groupings of muscles, H_{nxm}, with a module recruitment coefficient, W_{bxn}:

$$V_{b,m} = \sum_{i=1}^{n} W_{b,n} * H_{n,m} \quad (1)$$

Where $V_{b,m}$ is the reconstructed EMG activity of all muscles, m, and n represents the number of muscle modules used to reconstruct the original EMG activity. Using this model, groupings of muscle modules, H, are fixed while the activation of these modules, W, varies with time. Thus, various motor behaviors can be generated through the combination of the activation of one or more muscle modules.

We determined the number of motor modules required to sufficiently reconstruct the original EMG data by running NNMF for 1 to 11 modules (i.e., number of muscles recorded) for each condition and participant. We calculated the goodness of fit for each number of selected motor modules using Variance Accounted For (VAF), which determines the amount of variability of the original EMG data accounted for by the reconstructed EMG [193]. We also determined the VAF for each reconstructed muscle vector compared with the corresponding original muscle vector (VAF_m). To ensure consistent determination of VAF across conditions

and participants we resampled each original EMG matrix using bootstrapping, a statistical method to determine the uncertainty of a measured variable, to determine 95% confidence intervals (CI). We thus bootstrapped each EMG matrix 500 times with replacement for each condition and participant. We then calculated the VAF of each iteration of the bootstrapped EMG data. We then sorted the bootstrapped VAF values and found the 97.5 and 2.5 percentile to determine the 95% CI of the VAF of the original EMG data set. We selected the number of modules that met the following criteria: 1) The minimum number of modules must have VAF and lower bound of 95% CI greater than 90% VAF [178, 194]. 2) VAF_m of each muscle vector must exceed 75% VAF, or the amount of improvement in VAF_m of the lowest muscle vector does not increase >5% VAF with the inclusion of an additional muscle module [194].

We then qualitatively compared the number of muscle modules selected against the number of modules that would be extracted by random chance. Thus, we shuffled each original EMG data set 500 time, however, for this analysis we shuffled all muscle vectors separately, effectively removing the relationship between muscle activations in the data set. We then calculated the VAF and 95% CI of the 500 shuffled data sets compared with the original data set and plotted each VAF curve of the shuffled data sets with the VAF of the reconstruction of the original data sets [178]. If the addition of a muscle module caused the CI of the of shuffled data and original reconstructed data to overlap, then the number of muscle modules was not increased [195].

4.4.4.3 Muscle Module Analysis

We analyzed the similarity between muscle modules pre- and post-training. We first empirically grouped muscle modules into three groups based on the activation coefficient profile. We observed three common muscle module activation profiles labeled ‘Forward’, ‘Backward’

and ‘Tonic’ modules. ‘Forward’ modules we characterized by two peaks in the activation profile for the given muscle modules located at the forward most part of the postural sway cycle (i.e., 0 and 100% of sway cycle). Similarly, modules were labeled ‘Backward’ if the activation profile contained a single peak, where the peak was located at the backward most part of the postural sway (i.e., 50% of the sway cycle) (Fig. 4b). Third, we labeled muscle modules that contained a constant activation of muscle across the sway cycle as ‘Tonic’ muscle modules. Across all conditions and participants, we observed only one ‘Tonic’ muscle module (i.e., TT1 Post-Training, Fig. 2e).

We determined similarity between muscle modules within groupings from pre- and post-training by calculating the correlation coefficient between conditions [196]. Specifically, for each participant we calculated the correlation coefficient between each ‘Forward’ muscle module pre-training with each ‘Forward’ muscle module post-training. For example, if a participant used two ‘Forward’ muscle modules pre-training and one ‘Forward’ muscle modules post-training, we calculated the correlation coefficient of each pre-training modules with the post-training module and averaged the two resulting coefficients. To demonstrate this, we plotted all muscle modules pre- and post-training of ‘Forward’ muscle modules and their correlation coefficients (Fig. 4a).

If a correlation coefficient between muscle modules (i.e., pre- vs. post-training) exceeded 0.735 we considered the muscle module structure similar, which corresponds to the critical r value 9 degrees of freedom (i.e., 11-2 muscles). However, NNMF is constrained to produce only positive values for each element in the muscle module, so we would expect a positive correlation by chance alone. Thus, we generated 1000 randomized permutations of the weightings from each muscle mode extracted. We calculated the r value of each possible pair-wise comparison between conditions and generated a distribution of r values (351 pairs x 1000 permutations). An r

value of 0.735 corresponds to the 99.1 percentile of the generated r value distribution. Thus, we expect muscle mode comparisons that produce an r value greater than 0.735 to be more similar than what we would expect to observe by chance. Therefore, muscle synergies with $r<0.735$ were considered different [197, 198]. We compared the similarity in average activation coefficient structure (temporal activation of each muscle module) by conducting the same pair-wise comparison within muscle modules groups across conditions (i.e. activation coefficient from 'Backward' motor module pre-training vs. Post-Training) for each participant using the same criteria for r value significance.

4.4.4.4 Activation Coefficient Temporal Patterns

We evaluated potential changes in several common features of the activation coefficient (temporal activation of muscle modules) due to training [178]. We calculated the magnitude of muscle module recruitment over time as the area under the curve of the average activation coefficient for each muscle module (C_{area}). We calculated the duration of muscle module recruitment as the percentage of the activation coefficient profile that exceeded 15% during each sway cycle (C_{duty}) [178]. We determined the consistency of the activation coefficient by calculating the RMSE of each activation coefficient profile for each sway with the average activation coefficient for that module (C_{rmse}). We averaged these values across all muscle modules for each condition for each participant.

4.4.4.5 Muscle Module Structure Analysis

We analyzed coactivity within muscle module structure by comparing the number of muscles significantly activated during each condition (W_{mus}) [178]. We determined if muscles were significantly activated within muscle modules by determining the 95% CI for each element

(i.e., muscle) of the muscle module using the 500 EMG data sets derived from bootstrapping. Specifically, we held the number of muscle modules constant (as already determined in the previous steps) and calculated the muscle module structures for each participant in each condition for each data set. We then determined the CI for each muscle within each muscle modules across all 500 iterations. Significantly active muscles were ones that had a 95% confidence interval that did not include zero [178]. We then counted the number of significantly active muscles across all modules for each condition for each participant.

4.4.4.6 Analysis of Muscle Module Structure of Representative Participants

We observed two behaviors of participants from pre- to post-training from the number of muscle modules used. All participants either retained the number of muscle modules (i.e. TT3, TT4, TT5) or reduced the number of modules across training (TT1, TT2). We selected two individuals from each group for qualitative analysis on the specific changes in muscle module structure and activation profiles.

4.4.4.7 Task Performance Measures

To determine if muscle module composition was related to task performance and overall biomechanics, we analyzed movement measures from the voluntary sway task. We determined the ability for participants to follow the paced voluntary sway task by calculating the time from one forwardmost reach to the next. We then subtracted the target sway time (4s) from each sway time. We averaged each sway time error for all sways within the trial for each condition and each participant. We calculated weight-bearing symmetry index (SI%) by subtracting vertical GRF under the residual limb from the intact limb divided by participant's total weight [169]. We calculated differences in center of pressure contribution from each limb by calculating the RMSE

between the two center of pressure excursions [199]. We compared the range of CoM excursions between conditions by calculating the root-mean-square of anterior-posterior (AP) CoM sway across each trial. We averaged SI%, CoP RMSE, CoM rms for each condition for each participant.

4.4.5 Statistical Analysis

We conducted statistical analysis of the data using the statistical software (JMP, SAS, Cary, NC). We used one way ANOVA to compare W_{mus}, C_{area}, C_{duty}, and C_{rmse} with training as the main effect (Pre- vs. Post-training). We analyzed movement measures of sway time error, SI%, CoP RMSE and CoM AP rms with training as the main effect (Pre- vs. Post-training). We compared movement outcome measures between the dEMG control and the participants' daily device with a one-way ANOVA with device as the main effect (Post-Training dEMG Control vs. Passive). When we found a significant effect, we tested for statistical difference within conditions using Tukey's honestly significant difference test. We set a threshold for significance at $a=0.05$.

CHAPTER 5: Contributions, Conclusions, and Future Work

5.1 Contributions

With recent advances in powered lower-limb prostheses, the time is opportune for the development of control paradigms that assist amputees with the many activities and contexts they experience daily. A vast majority of work with powered prosthesis control has significantly improved control of walking across using autonomous control paradigms, however these controllers provide no active assistance in standing postural control, leading to significant deficits in the standing stability of individuals with lower-limb amputation. Direct EMG control (also termed proportional myoelectric control) opens the door to potential improvements in prosthesis function by enabling the user to continuously and directly change their prosthesis mechanics, though the results from initial studies with this control have been limited. These studies gave amputees control of one only movement (i.e. plantarflexion with their residual gastrocnemius) during walking, or (for above-knee amputees) included residual knee flexors and extensors during walking with a single subject. Thus, it is unclear how an individual with amputation might coordinate multiple residual muscle activity for non-cyclic tasks (i.e. control of standing posture) and how direct EMG prosthesis control might improve standing stability over current prostheses. To our knowledge, these studies (Chapter 2-4) are the first studies to address these questions concerning previously antagonistic residual muscle control and standing postural control. Our results demonstrate that individuals with amputation can coordinate antagonistic muscle activity using dEMG control leading to distinct improvements in standing stability in situations of expected perturbation. We encourage further research of residual muscle control and other daily-life tasks to improve the community engagement and quality of life in individuals with lower-limb amputation by restoring normative stability.

5.2 Conclusions

In Chapter 2, we demonstrated that individuals with transtibial amputation could coordinate residual muscle activity to control a virtual inverted pendulum with human-like dynamics. We observed that, while all individuals improved control with their residual muscles, there were distinct learning strategies between participants. Future research should investigate the potential reasons for observed differences between individual's residual muscle control. Based on this study there is promise for individuals to coordinate residual muscle activity during standing postural control to control a prosthetic ankle using dEMG control.

In Chapter 3, we then investigated the ability for individuals to restore postural control mechanisms at the prosthetic ankle joint using dEMG control of a powered prosthetic ankle. We observed that individuals with amputation successfully generated APAs and CPAs with their residual muscle activity against multiple directions of perturbations, significantly improving stability compared with their daily-use device. Further, individuals adopted a more symmetric postural control strategy between their residual and intact limb. These results start to demonstrate the potential for dEMG control to enable symmetric control of standing posture under expected perturbation and should be further investigated for more contexts of disturbance and other daily-life tasks.

Lastly, we investigated the potential neural mechanisms used by individuals when learning to coordinate residual muscle activity with intact muscles for standing postural control. Individuals significantly improved neural coordination of movement over training 1) grouping residual and intact muscle activity 2) reducing variation of muscle module activation and 3) improving efficiency of muscle recruitment. These results suggest a possible reduction in the neural resources required for standing postural control by training with the dEMG control.

Further, by improving proficiency of muscle module recruitment, individuals may be able more reliably employ these muscle modules across other activities outside of trained task (voluntary postural sway). We suggest that future study could elaborate on these observations by evaluating the presence of muscle modules across similar tasks to determine if indeed muscle modules developed in one condition can be generalized across multiple tasks.

5.3 Future Work

In chapters 2-4, we demonstrated the ability for individuals with amputation to coordinate residual muscle activity on a local level (i.e., isolated control of a virtual inverted pendulum, generation of postural control mechanisms at the prosthetic ankle joint) and a global level (i.e., improved standing stability under expected perturbation, development of residual-intact muscle modules during voluntary postural sway). Given sufficient training, it seems reasonable to employ dEMG control of a powered prosthetic ankle to improve standing stability. It would be interesting for future study to investigate specific mechanisms within the guided training used in these studies to potentially improve prosthetic ankle control beyond what we observed in these studies. In the current studies, we employed an abbreviated training protocol for the dEMG control compared with previous study, thus it is possible that the measures observed here may be further improved given additional training time alone. Future work should also work to better understand the mechanisms behind variations in the level of performance of dEMG control between individual participants. In our study we qualitatively observed that individuals who flexed their residual muscle in their daily devices (i.e., to improve cushioning or suspension) had improved performance with dEMG control in our virtual pendulum study compared with individuals who did not use their residual muscles daily. Future study might benefit by quantitatively evaluating this relationship, which may lead to the development of additional

training strategies that do not require the user to be actively using dEMG control in order to train their residual muscles. Naturally, it would be interesting to evaluate more tasks using dEMG control of a prosthetic ankle to understand the full potential of this control to improve daily-life function for individuals with amputation. In the long-term, the improvements in standing stability observed here have the potential to improve amputee quality of life by increasing balance confidence and reducing the chance of falls leading to improved quality of life.

APPENDICES

6.1 Appendix A. Supplementary Information for Chapter 1

Table A 1 Supervisory EMG Control Review Summary [160]

*Author**	*Muscles Recorded**	*Classifier Type****	*EMG Features*	*Windowing/ Prediction Time*	*Training*	*Control Type*	*Amputation Type*	*Activity*
Au et al. [93]	TA, GAS, SOL	Neural Network	pre-processed EMG	Predictions at 0.5 Hz	Back propagation method with pre-processed EMG as input	None; Offline Classification only	Transtibial	Trajectory tracking sitting
Jin et al. [88]	ADDL, TFL, RF, VL, VM, BF, SM, ST	Distribution of different muscle features	mean absolute value, waveform length, mean square value, zero tangent number, median power frequency	Entire gait cycle	3-5 times along walkway for each condition	None	Transfemoral	Level-ground walking at varying speeds, stairs, and ramps
Huang et al. [15]	GME (both), GMA (both), SAR, RF, VL, VM, GRA, ST, BFL, BFS, PL, GASL, GASL, EDB, TA, SOL	LDA and Neural Network	3rd order autoregression coefficients, mean absolute value, zero crossings, waveform length, number of slope sign changes and root mean square	Range from 50 to 150 ms EMG window, 200 ms phase window	10 walking trials of all activities with own prosthesis	None; Offline Classification only	Transfemoral	Level-ground walking, stepping over and obstacle, stairs, ipsilateral and contralateral turning, and standing
Au et al. [22]	GASL, GASM, TA	Neural Network	Variance of EMG signals	100 ms EMG window	Matching imagined ankle position to virtual ankle	Impedance control	Transtibial (Bilateral)	Level-ground walking, stair descents
Ha et al. [106]	Quadriceps, Hamstring	LDA, QDA	Not Provided	Not Provided	100 seconds of knee flexion/extension visualizations	Online impedance control (prosthesis next to participant)	Transfemoral	Virtual tracking tasks (sitting)
Huang, et al. [38]	GME, GMA, SAR, RF, VL, VM, GRA, BFS, ADM	SVM, LDA	Zero crossings, signal direction change, mean absolute value, waveform length	150 ms sliding EMG window Prediction	15 times each activity	None; Online classification	Transfemoral	Walking, Stair/Ramp ascent and descent, stepping over obstacles (and transitions)

Table A 1 (continued).

Hargrove et al. [200]	ST, SAR, TFL, ADM, GAR, VM, RF, VL, BFL	LDA	Mean absolute value, zero crossings, waveform length, and number of slope sign change	150 ms sliding window, prediction time 300-650 ms for transitions	12 seconds of EMG data for each motion	Virtual joint velocity control in a sitting posture	Transfemoral	Knee flexion/extension, plantar flexion/dorsiflexion, internal/external tibial/femoral rotation, relaxation of 2 and 4 DOF virtual prosthesis
Simon et al. [201]	SM, SAR, TFL, ADM, GRA, RF, VL, BFL	2 LDA Classifiers	mean absolute value, zero crossings, waveform length, slope sign change number, 5-count majority vote	250 ms overlapping	10 sit-to-stand trials	Impedance control	Transfemoral	Sitting down, walking and transition between them, repositioning prosthesis while sitting
Hargrove et al. [41]	Two reinnervated muscle segments, proximal BF, RF, VL, VM, SAR, GRA, ADM, TFL	DBN	Mean absolute value, zero crossings, waveform length, slope sign changes, three-order autoregression coefficients, RMS	Not Provided	Offline, 20 reps of locomotor circuit	Impedance control	Transfemoral	Level-ground walking, ramps, stairs and outside stairs
Young et al. [202]	ST, BF, TFL, VM, SAR, ADM, GRA	2 LDA models	Mean absolute value, waveform length, zero crossings, slope sign change, first two coefficients of 3rd order autoregressive model	300 ms before heel contact and toe off	Offline, 20 reps of 2 locomotor circuits, train classifier on 3 subjects test 1 as novel user. Then add 5-10 minutes of level-ground walking for novel user to train classifier.	None; Offline classification	Transfemoral	Level-ground walking, ramps, stairs
Zhang et al. [90]	RF, VL, VM, TFL, BFL, BFS, ST, ADM	SVM	Zero crossings, slope change number, mean absolute value, waveform length	EMG window 150 ms Decision time between 45 and 28 ms	Offline Training, at least 5 reps of 30 seconds of data per condition	None; Online classification	Transfemoral	Ramp/stair ascent, descent, level-ground walking, sitting, standing
Tkach et al. [103]	TA, PL, GASL, GASM	LDA	Mean absolute value, zero crossings, slope sign change, and waveform length	250 ms window	12 trials of each ambulation mode (stairs and ramps), and 12 trials of level-ground walking	None; Offline classification only	Transtibial	Level-ground walking, stairs, ramps, and transitions
Tkach et al. [96]	TA, PL, GASL, GASM, VM, VL, RF, BF	LDA	6 coefficients from 6th order autoregressive model, mean absolute value, zero crossings, slope sign change, waveform length	250 ms prediction window 50 ms overlap	18 seconds for data for each movement class (1-DOF up to 3-DOF, including no movement flexion, rotation, in/eversion)	None; Offline classification only	Transtibial	Virtual tasks for varying DOF ankle movements (rotation, flexion, in/eversion)

Table A 1 (continued).

Hargrove et al. [203]	ST, SAR, TFL, ADM, GRA, VM, RF, VL, BFL	LDA	Mean absolute value, zero crossings, slope sign change, waveform length	250 ms window, decisions every 50 ms	EMG for virtual cases, 4 reps of 3 seconds for each movement, no feedback provided	Online impedance control and avatar feedback	Transfemoral	Virtual and non weight-bearing tasks knee and ankle flexion/extension
Miller et al. [92]	TA, GASM, VL, BF	LDA and SVM	Mean absolute value, variance, wavelength, number slope sign changes, zero crossings	3 subwindows with varying times based on heel strike and toe off	6 trials each activity, additional trials for different walking speeds	None; Offline classification only	Transtibial	Level-ground walking 3 speeds, ramp/stair ascent/descent
Du et al. [109]	SAR, RF, VL, VM, GRA, BFL, ST, BFS, ADM	LDA	absolute value, slope sign changes, waveform length, zero crossings	150 ms	15-10 trials of each activity	None; Offline Classification only	Transfemoral	Level-ground walking, ramps, stairs
Zhang et al. [204]	RF, VL, VM, BFL, SAR, ST, ADM	SVM	Not provided	Not Provided	Offline Training with 10 reps of walking level-ground and ramp course	Impedance control	Transfemoral	Standing, level-ground walking ramp ascent/ descent
Young et al. [205]	ST, BF, TFL, RF, VL, VM, SAR, ADM, GRA	DBN	Mean absolute value, waveform length, zero crossings, slope sign change, two autoregressive coefficients	Tested 0-450 ms windows with 20 ms sliding window	Offline Training with 20 reps of locomotor circuit	None; offline classification	Transfemoral	Level-ground walking, ramps, stairs
Zhang et al. [206]	SAR, RF, VL, VM, GRA, BFL, ST, BFS, ADM	LDA with prior probability	Zero crossings, mean absolute value, waveform length, slope sign change number	Error decisions 100-300 ms	10 hours practice with device, at least 120 trials per experiment	Impedance control	Transfemoral	Ramp Ascent, Descent, Level-ground walking, Sitting, Standing (and transitions)
Hargrove et al. [97]	ST, BF, TFL, RF, VL, VM, SAR, ADM, GRA	LDA + DBN	Not Provided	Not Provided	Offline Training, 20 reps of locomotor circuit, level-ground walking at variable speeds, stopping/starting/turning	Impedance control	Transfemoral	Walking, stairs, ramps
Spanias et al. [207]	ST, ADM, TFL, RF	DBN	mean absolute value, waveform length, zero crossings, slope sign changes, 6 autoregressive coefficients	300 ms window	20 reps of locomotion circuit	None; Offline classification only	Transfemoral	Level-ground walking, ramp/straight ascent/descent, turn around
Spanias et al. [115]	ST, BF, TFL, RF, VL, VM, SAR, ADM, GRA	LDA with Log-Likelihood	Mean absolute value, waveform length, zero crossings, slope sign change, first two coefficients of 3rd order autoregressive model	300 ms before toe off and heel strike	Offline Training with 20 reps of locomotor circuit	Impedance control	Transfemoral	Level-ground walking, ramps, stairs
Lui et al. [113]	RF, VL, VM, BFL, SM, TFL, BFS	EBA, TSVM	absolute value, signal length, slope sign changes, zero crossings	160 ms window avg processing time 45 ms	Four one minute trials of each locomotion mode	EBA online impedance control	Transfemoral	Level-ground walking, ramps, stairs, and their transitions

Table A 1 (continued).

Spanias et al. [104]	Pairs of electrodes over RF, TFL, ST, ADM	8 DBN classifiers + LDA	Mean absolute value, waveform length, zero crossings, slope sign changes, 6 autoregressive coefficients from 6th order model PCA and ULDA to features totals	Transition Modes 300 ms (210 ms before gait event 90 ms after gait event	Offline Training with first session data across locomotor modes Online Training second session through forward prediction	Impedance control	Transfemoral	Level-ground walking, ramps, stairs over multiple days
Hussain et al. [89]	GM, GASL, GASM, TFL, RF, VL, VM, BFL, SOL, TA	SVM and LDA	Bispectrum for high order frequency spectrum/ non-Gaussian info, RMS, zero crossings, Histogram, integrated EMG, sum of square Integral, waveform length, mean/median frequency, autoregression, and reduced with PCA	Non-overlapping 150 ms-300 ms windows	Offline Training 5 trials for each walking mode	None; Offline Classification only	Transtibial and Transfemoral	Slow, steady state, and fast walking, ramps

*Authors are listed in order of year published

**Muscle Abbreviations: Adductor Magnus (ADM), Adductor Longus (ADDL), Biceps Femoris (BF), Biceps Femoris Long Head (BFL) Biceps Femoris Short Head (BFS), Extensor Digitorum Brevis (EDB), Gastrocnemius (GAS), Gastrocnemius Medialis (GASM), Gastrocnemius Lateralis (GASL), Gluteus Maximus (GMA), Gluteus Medius (GME), Gracilis (GRA), Peroneus Longus (PL), Rectus Femoris (RF), Sartorius (SAR), Semimembranosus (SM), Semitendinosus (ST), Soleus (SOL), Tensor Fasciae Latae (TFL), Tibialis Anterior (TA), Vastus Lateralis (VL), Vastus Medialis (VM)

***Classifier Abbreviations: Support Vector Machine (SVM), Neural Network (NN), Linear Discriminant Analysis (LDA), Quadratic Descriminant Analysis (QDA), Dynamic Bayesian Network (DBN), entropy-based adaption (EBA), Transductive Support Vector Machine (TSVM)

Table A 2 Direct EMG Control Review Summary

*Author**	*Muscle***	*EMG Decoding Method*	*Modulated Control Parameters*	*Amputation Type*	*Activity*
Ha et al. [106]	Quadriceps, Hamstring (unspecified)	Envelope (2 Hz Cutoff) 20% MVC Threshold Quadratic Discriminant Analysis	Reference Angular Velocity	Transfemoral	Virtual Tracking Task (Sitting)
Hoover et al [121]	VL, VM, RF, BF	Envelope (5-10 Hz Cutoff).	Flexion / Extension Torque	Transfemoral	Level-ground Walking
Hoover et al. [118]	BF, RF, ST, VL, VM	Envelope (2.5 Hz Cutoff)	Flexion / Extension Torque	Transfemoral	Stair Ascent
Dawley et al. [39]	Quadriceps Hamstring, (unspecified)	Initial processing not described Principal Component Analysis (Flexion / Extension)	Reference Angular Velocity Joint Stiffness	Transfemoral	Level-ground Walking
Wang et al. [40]	GAS (unspecified head)	Low-pass Filtered (15 Hz), Rectified Envelope (200 ms Moving Average Window)	Plantar flexor Torque Gain (push-off only)	Transtibial	Level-ground Walking
Alcaide-Aguirre et al. [208]	TA	Envelope (10 Hz Cutoff)	Virtual Object Acceleration	Transtibial	Virtual Tracking Task (Sitting)
Chen et al. [209]	TA, GAS (unspecified head)	Envelope (2.5 Hz Cutoff) PCA (Flexion / Extension)	Reference Angular Velocity Joint Stiffness	Transtibial	Virtual Target Hitting (Sitting)
S. Huang et al. [119]	GASL	Envelope (2 Hz Cutoff)	Pneumatic Artificial Muscle Force	Transtibial	Level-ground Walking
S. Huang et al. [16]	GASM or GASL	Envelope (2 Hz Cutoff)	Pneumatic Artificial Muscle Force	Transtibial	Level-ground Walking
S. Huang et al. [210]	TA, GASM or GASL	Envelope (2 Hz Cutoff)	Virtual Object Position	Transtibial	Virtual Ballistic Target Hitting (Sitting)
Clites et al. [60]	TA, GASL, TP, PL	Envelope (100 ms Moving Average Window)	Flexion / Extension Torque	Transtibial	Virtual Target Hitting Stair Ascent / Descent Obstacle Walking
Fleming et al. [34]	TA, GASL	Envelope (2 Hz Cutoff)	Virtual Spring Stiffness	Transtibial	Virtual Balancing Inverted Pendulum
S. Huang et al. [57]	TA, GASL	Envelope (2 Hz Cutoff)	Virtual Cursor position	Transtibial	Virtual Control Input Space Filling (Sitting)
Dimitrov et al. [83]	TA, GASM, GASL	Envelope (5 Hz Cutoff) Non-negative Matrix Factorization (125ms windows)	Equilibrium Angle Joint Stiffness	Transtibial	Target Hitting (Standing) Walking (with passive device)
Fleming et al. [70]	TA, GASL	Envelope (2 Hz Cutoff)	Pneumatic Artificial Muscle Force	Transtibial	Quiet Standing (Vision, No Vision, Foam and Firm Surfaces) Sit-to-Stand, Load Transfer

Table A 2 (continued).

*Authors are listed in order of year published **Muscle Abbreviations: Biceps Femoris (BF), Gastrocnemius (GAS), Gastrocnemius Medialis (GASM), Gastrocnemius Lateralis (GASL), Peroneus Longus (PL), Rectus Femoris (RF), Semitendinosus (ST), Soleus (SOL), Tibialis Anterior (TA), Vastus Lateralis (VL), Vastus Medialis (VM), Tibialis Posterior (TP)

6.2 Appendix B. Supplementary Information for Chapter 4

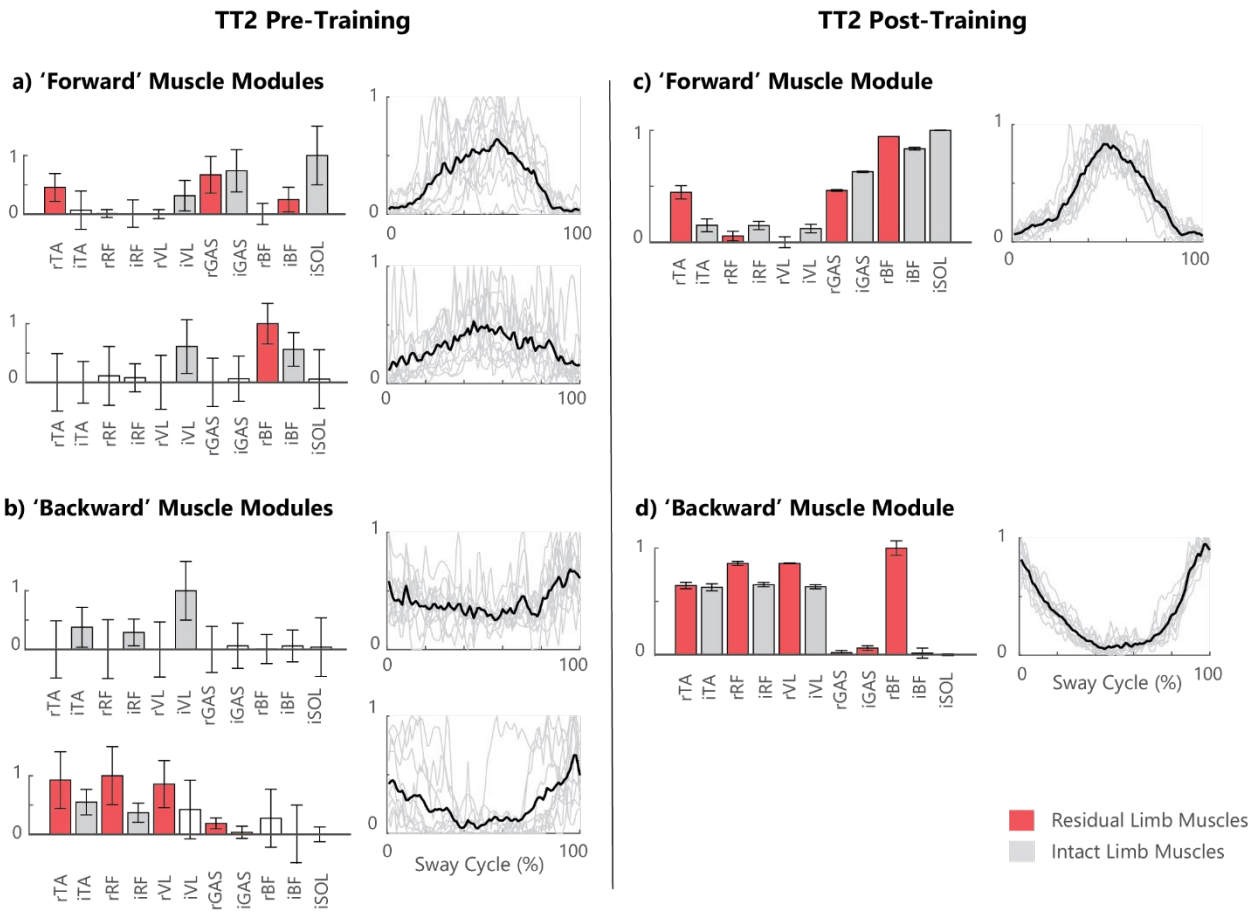

Figure B 1. TT2 Extracted Muscle Module and Activation Coefficient from pre-training and post-training conditions. *Red Bar)* residual limb muscles *Grey Bar)* Intact Limb Muscles. *Empty bar)* Muscles whose 95% CI (error bars) passes 0 bound and are considered inactive. Average time series of activation module is shown *(black line)* as well as individual time series for each repetition *(grey line).*

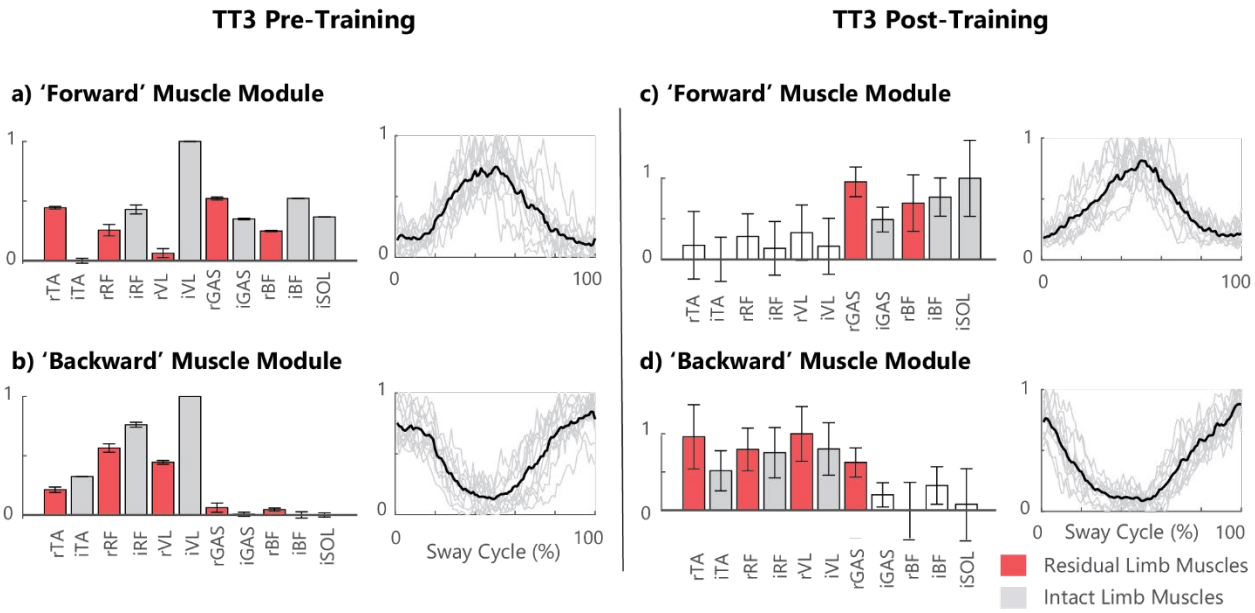

Figure B 2. TT3 Extracted Muscle Module and Activation Coefficient from pre-training and post-training conditions. *Red Bar)* residual limb muscles *Grey Bar)* Intact Limb Muscles. *Empty bar)* Muscles whose 95% CI (error bars) passes 0 bound and are considered inactive. Average time series of activation module is shown *(black line)* as well as individual time series for each repetition *(grey line).*

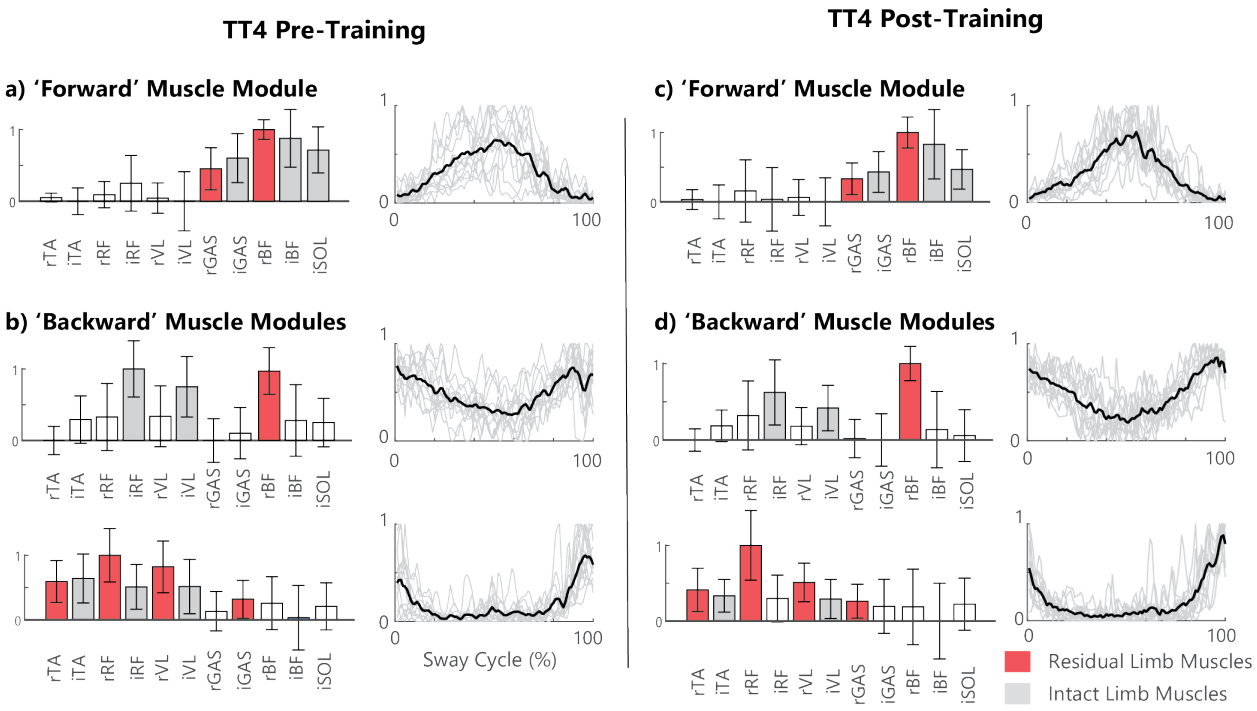

Figure B 3. TT4 Extracted Muscle Module and Activation Coefficient from pre-training and post-training conditions. *Red Bar)* residual limb muscles *Grey Bar)* Intact Limb Muscles. *Empty bar)* Muscles whose 95% CI (error bars) passes 0 bound and are considered inactive. Average time series of activation module is shown *(black line)* as well as individual time series for each repetition *(grey line)*.

REFERENCES

[1] H. Houdijk, E. Pollmann, M. Groenewold, H. Wiggerts, and W. Polomski, "The energy cost for the step-to-step transition in amputee walking," *Gait & posture,* vol. 30, no. 1, pp. 35-40, 2009.

[2] M.-J. Hsu, D. H. Nielsen, S.-J. Lin-Chan, and D. Shurr, "The effects of prosthetic foot design on physiologic measurements, self-selected walking velocity, and physical activity in people with transtibial amputation," *Archives of Physical Medicine and Rehabilitation,* vol. 87, no. 1, pp. 123-129, 2006.

[3] A. Geurts, T. W. Mulder, B. Nienhuis, and R. Rijken, "Dual-task assessment of reorganization of postural control in persons with lower limb amputation," *Arch Phys Med Rehabil,* vol. 72, no. 13, pp. 1059-64, 1991.

[4] S. J. Morgan, B. J. Hafner, D. Kartin, and V. E. Kelly, "Dual-task standing and walking in people with lower limb amputation: A structured review," *Prosthetics and orthotics international,* vol. 42, no. 6, pp. 652-666, 2018.

[5] C. B. Anderson, M. J. Miller, A. M. Murray, T. T. Fields, N. F. So, and C. L. Christiansen, "Falls after dysvascular transtibial amputation: a secondary analysis of falling characteristics and reduced physical performance," *PM&R,* vol. 13, no. 1, pp. 19-29, 2021.

[6] W. C. Miller, A. B. Deathe, M. Speechley, and J. Koval, "The influence of falling, fear of falling, and balance confidence on prosthetic mobility and social activity among individuals with a lower extremity amputation," *Archives of physical medicine and rehabilitation,* vol. 82, no. 9, pp. 1238-1244, 2001.

[7] W. C. Miller, M. Speechley, and B. Deathe, "The prevalence and risk factors of falling and fear of falling among lower extremity amputees," *Arch Phys Med Rehabil,* vol. 82, no. 8, pp. 1031-7, Aug 2001, doi: 10.1053/apmr.2001.24295.

[8] A. Aruin, J. Nicholas, and M. L. Latash, "Anticipatory postural adjustments during standing in below-the-knee amputees," *Clinical biomechanics,* vol. 12, no. 1, pp. 52-59, 1997.

[9] A. Vrieling *et al.*, "Balance control on a moving platform in unilateral lower limb amputees," *Gait & posture,* vol. 28, no. 2, pp. 222-228, 2008.

[10] W. C. Miller, M. Speechley, and A. B. J. P. t. Deathe, "Balance confidence among people with lower-limb amputations," vol. 82, no. 9, pp. 856-865, 2002.

[11] W. Miller and A. Deathe, "A prospective study examining balance confidence among individuals with lower limb amputation," *Disability and rehabilitation,* vol. 26, no. 14-15, pp. 875-881, 2004.

[12] G. Horn, "Electro-control: am EMG-controlled A/K prosthesis," *Medical and biological engineering,* vol. 10, no. 1, pp. 61-73, 1972.

[13] L. Peeraer, B. Aeyels, and G. Van der Perre, "Development of EMG-based mode and intent recognition algorithms for a computer-controlled above-knee prosthesis," *Journal of biomedical engineering,* vol. 12, no. 3, pp. 178-182, 1990.

[14] K. Englehart and B. Hudgins, "A robust, real-time control scheme for multifunction myoelectric control," *IEEE transactions on biomedical engineering,* vol. 50, no. 7, pp. 848-854, 2003.

[15] H. Huang, T. A. Kuiken, and R. D. Lipschutz, "A strategy for identifying locomotion modes using surface electromyography," *IEEE Transactions on Biomedical Engineering,* vol. 56, no. 1, pp. 65-73, 2008.

[16] S. Huang, J. P. Wensman, and D. P. Ferris, "Locomotor adaptation by transtibial amputees walking with an experimental powered prosthesis under continuous myoelectric control," *IEEE Transactions on Neural Systems and Rehabilitation Engineering,* vol. 24, no. 5, pp. 573-581, 2015.

[17] D. P. Ferris and B. R. Schlink, "Robotic devices to enhance human movement performance," *Kinesiology Review,* vol. 6, no. 1, pp. 70-77, 2017.

[18] R. Merletti and P. J. Parker, *Electromyography: physiology, engineering, and non-invasive applications*. John Wiley & Sons, 2004.

[19] E. Scheme and K. Englehart, "Electromyogram pattern recognition for control of powered upper-limb prostheses: state of the art and challenges for clinical use," *Journal of Rehabilitation Research & Development,* vol. 48, no. 6, 2011.

[20] E. C. Martinez-Villalpando and H. Herr, "Agonist-antagonist active knee prosthesis: a preliminary study in level-ground walking," *Journal of Rehabilitation Research & Development,* vol. 46, no. 3, 2009.

[21] F. Sup, A. Bohara, and M. Goldfarb, "Design and control of a powered transfemoral prosthesis," *The International journal of robotics research,* vol. 27, no. 2, pp. 263-273, 2008.

[22] S. Au, M. Berniker, and H. Herr, "Powered ankle-foot prosthesis to assist level-ground and stair-descent gaits," *Neural Netw,* vol. 21, no. 4, pp. 654-66, May 2008. [Online]. Available: http://www.ncbi.nlm.nih.gov/entrez/query.fcgi?cmd=Retrieve&db=PubMed&dopt=Citation&list_uids=18499394.

[23] B. Lambrecht and H. Kazerooni, "Design of a semi-active knee prosthesis," presented at the IEEE International Conference on Robotics and Automation, Kobe, Japan, Dec. 12-17, 2009.

[24] J. Hitt, R. Bellman, M. Holgate, T. Sugar, and K. Hollander, "The SPARKy (Spring Ankle With Regenerative Kinetics) Project: Design and Analysis of a Robotic Transtibial Prosthesis With Regenerative Kinetics," presented at the ASME 2007 International Design Engineering Technical Conferences and Computers and Information in Engineering Conference Las Vagas, NV, 2007.

[25] F. Sup, H. A. Varol, J. Mitchell, T. J. Withrow, and M. Goldfarb, "Preliminary Evaluations of a Self-Contained Anthropomorphic Transfemoral Prosthesis," (in Eng), *IEEE ASME Trans Mechatron,* vol. 14, no. 6, pp. 667-676, 2009, doi: 10.1109/TMECH.2009.2032688.

[26] A. F. Azocar, L. M. Mooney, L. J. Hargrove, and E. J. Rouse, "Design and characterization of an open-source robotic leg prosthesis," in *2018 7th IEEE International Conference on Biomedical Robotics and Biomechatronics (Biorob)*, 2018: IEEE, pp. 111-118.

[27] T. Lenzi, M. Cempini, L. Hargrove, and T. Kuiken, "Design, development, and testing of a lightweight hybrid robotic knee prosthesis," *The International Journal of Robotics Research,* vol. 37, no. 8, pp. 953-976, 2018.

[28] T. Elery, S. Rezazadeh, C. Nesler, J. Doan, H. Zhu, and R. D. Gregg, "Design and benchtop validation of a powered knee-ankle prosthesis with high-torque, low-impedance actuators," in *2018 IEEE International Conference on Robotics and Automation (ICRA)*, 2018: IEEE, pp. 2788-2795.

[29] M. Liu, F. Zhang, P. Datseris, and H. Huang, "Improving finite state impedance control of active transfemoral prostheses using Dempster-Shafer state transition rules," *Journal of Intelligent and Robotic Systems,* vol. 76, pp. 461-74, 2014.

[30] B. E. Lawson, H. A. Varol, A. Huff, E. Erdemir, and M. Goldfarb, "Control of stair ascent and descent with a powered transfemoral prosthesis," *IEEE Trans Neural Syst Rehabil Eng,* vol. 21, no. 3, pp. 466-73, May 2013, doi: 10.1109/TNSRE.2012.2225640.

[31] H. Zheng and X. Shen, "Design and Control of a Pneumatically Actuated Transtibial Prosthesis," *J Bionic Eng,* vol. 12, no. 2, pp. 217-226, Apr 2015, doi: 10.1016/S1672-6529(14)60114-1.

[32] T. Elery, S. Rezazadeh, C. Nesler, and R. D. Gregg, "Design and Validation of a Powered Knee-Ankle Prosthesis with High-Torque, Low-Impedance Actuators," *IEEE Trans Robot,* vol. 36, no. 6, pp. 1649-1668, Dec 2020, doi: 10.1109/TRO.2020.3005533.

[33] Y. Wen, J. Si, A. Brandt, X. Gao, and H. H. Huang, "Online Reinforcement Learning Control for the Personalization of a Robotic Knee Prosthesis," *IEEE Trans Cybern,* vol. 50, no. 6, pp. 2346-2356, Jun 2020, doi: 10.1109/TCYB.2019.2890974.

[34] A. Fleming, S. Huang, and H. Huang, "Proportional myoelectric control of a virtual inverted pendulum using residual antagonistic muscles: toward voluntary postural

control," *IEEE Transactions on Neural Systems and Rehabilitation Engineering,* vol. 27, no. 7, pp. 1473-1482, 2019.

[35] M. W. Legro, G. E. Reiber, J. M. Czerniecki, and B. J. Sangeorzan, "Recreational activities of lower-limb amputees with prostheses," *J Rehabil Res Dev,* vol. 38, no. 3, pp. 319-326, 2001.

[36] A. Brandt, Y. Wen, M. Liu, J. Stallings, and H. H. Huang, "Interactions Between Transfemoral Amputees and a Powered Knee Prosthesis During Load Carriage," *Sci Rep,* vol. 7, no. 1, p. 14480, Nov 3 2017, doi: 10.1038/s41598-017-14834-7.

[37] H. Huang, T. A. Kuiken, and R. D. Lipschutz, "A strategy for identifying locomotion modes using surface electromyography," *IEEE Trans Biomed Eng,* vol. 56, no. 1, pp. 65-73, Jan 2009. [Online]. Available: http://www.ncbi.nlm.nih.gov/entrez/query.fcgi?cmd=Retrieve&db=PubMed&dopt=Citation&list_uids=19224720.

[38] H. Huang, F. Zhang, L. J. Hargrove, Z. Dou, D. R. Rogers, and K. B. Englehart, "Continuous locomotion-mode identification for prosthetic legs based on neuromuscular–mechanical fusion," *IEEE Transactions on Biomedical Engineering,* vol. 58, no. 10, pp. 2867-2875, 2011.

[39] J. A. Dawley, K. B. Fite, and G. D. Fulk, "EMG control of a bionic knee prosthesis: exploiting muscle co-contractions for improved locomotor function," in *2013 IEEE 13th International Conference on Rehabilitation Robotics (ICORR)*, 2013: IEEE, pp. 1-6.

[40] J. Wang, O. A. Kannape, and H. M. Herr, "Proportional EMG control of ankle plantar flexion in a powered transtibial prosthesis," in *2013 IEEE 13th International Conference on Rehabilitation Robotics (ICORR)*, 2013: IEEE, pp. 1-5.

[41] L. J. Hargrove *et al.*, "Robotic leg control with EMG decoding in an amputee with nerve transfers," *New England Journal of Medicine,* vol. 369, no. 13, pp. 1237-1242, 2013.

[42] M. Donath, "Proportional EMG control for above knee pros-theses," Massachusetts Institute of Technology, 1974.

[43] R. J. Triolo, D. Nash, and G. D. Moskowitz, "The identification of time series models of lower extremity EMG for the control of prostheses using Box-Jenkins criteria," *IEEE transactions on biomedical engineering,* vol. 35, no. 8, pp. 584-594, 1988.

[44] T. R. Clites, H. M. Herr, S. S. Srinivasan, A. N. Zorzos, and M. J. Carty, "The Ewing amputation: The first human implementation of the agonist-antagonist myoneural interface," *Plastic and Reconstructive Surgery Global Open,* vol. 6, no. 11, 2018.

[45] T. A. Kuiken *et al.*, "Targeted muscle reinnervation for real-time myoelectric control of multifunction artificial arms," *Jama,* vol. 301, no. 6, pp. 619-628, 2009.

[46] J. M. Souza, N. P. Fey, J. E. Cheesborough, S. P. Agnew, L. J. Hargrove, and G. A. Dumanian, "Advances in transfemoral amputee rehabilitation: early experience with targeted muscle reinnervation," *Current Surgery Reports,* vol. 2, no. 5, p. 51, 2014.

[47] L. S. M. Tintle, C. J. J. Keeling, L. S. B. Shawen, L. J. A. Forsberg, and M. B. K. Potter, "Traumatic and trauma-related amputations: part I: general principles and lower-extremity amputations," *JBJS,* vol. 92, no. 17, pp. 2852-2868, 2010.

[48] E. Isakov, H. Burger, M. Gregorič, and Č. Marinčcek, "Stump length as related to atrophy and strength of the thigh muscles in trans-tibial amputees," *Prosthetics and orthotics international,* vol. 20, no. 2, pp. 96-100, 1996.

[49] V. Robinson, K. Sansam, L. Hirst, and V. Neumann, "Major lower limb amputation–what, why and how to achieve the best results," *Orthopaedics and Trauma,* vol. 24, no. 4, pp. 276-285, 2010.

[50] V. D. Sherk, M. G. Bemben, and D. A. Bemben, "Interlimb muscle and fat comparisons in persons with lower-limb amputation," *Archives of physical medicine and rehabilitation,* vol. 91, no. 7, pp. 1077-1081, 2010.

[51] D. Smith, "General principles of amputation surgery," *Atlas of amputations and limb deficiencies: surgical, prosthetic, and rehabilitation principles. 3rd ed. Rosemont, IL: American Academy of Orthopaedic Surgeons,* pp. 21-30, 2004.

[52] E. C. Ranz, J. M. Wilken, D. A. Gajewski, and R. R. Neptune, "The influence of limb alignment and transfemoral amputation technique on muscle capacity during gait," *Computer methods in BiomeChaniCs and BiomediCal engineering,* vol. 20, no. 11, pp. 1167-1174, 2017.

[53] P. F. Pasquina, P. R. Bryant, M. E. Huang, T. L. Roberts, V. S. Nelson, and K. M. Flood, "Advances in amputee care," *Archives of physical medicine and rehabilitation,* vol. 87, no. 3, pp. 34-43, 2006.

[54] B. J. Brown *et al.*, "Outcomes after 294 transtibial amputations with the posterior myocutaneous flap," *The international journal of lower extremity wounds,* vol. 13, no. 1, pp. 33-40, 2014.

[55] J. Eidt and V. Kalapatapu, "Lower extremity amputation: Techniques and Results," *Rutherford's Vascular Surgery,* vol. 2, 2010.

[56] G. Murdoch, "Knee-disarticulation amputation," *Bull Prosthet Res,* vol. 10, pp. 14-18, 1968.

[57] S. Huang and H. Huang, "Voluntary Control of Residual Antagonistic Muscles in Transtibial Amputees: Reciprocal Activation, Coactivation, and Implications for Direct Neural Control of Powered Lower Limb Prostheses," *IEEE Transactions on Neural Systems and Rehabilitation Engineering,* vol. 27, no. 1, pp. 85-95, 2018.

[58] S. Huang and D. P. Ferris, "Muscle activation patterns during walking from transtibial amputees recorded within the residual limb-prosthetic interface," *Journal of NeuroEngineering and Rehabilitation,* vol. 9, no. 1, p. 55, 2012.

[59] E. C. Wentink, E. C. Prinsen, J. S. Rietman, and P. H. Veltink, "Comparison of muscle activity patterns of transfemoral amputees and control subjects during walking," *Journal of neuroengineering and rehabilitation,* vol. 10, no. 1, p. 87, 2013.

[60] T. R. Clites *et al.*, "Proprioception from a neurally controlled lower-extremity prosthesis," *Science Translational Medicine,* vol. 10, no. 443, p. eaap8373, 2018.

[61] T. R. Clites, M. J. Carty, S. Srinivasan, A. N. Zorzos, and H. M. Herr, "A murine model of a novel surgical architecture for proprioceptive muscle feedback and its potential application to control of advanced limb prostheses," *Journal of Neural Engineering,* vol. 14, no. 3, p. 036002, 2017.

[62] S. Srinivasan *et al.*, "Polyimide electrode-based electrical stimulation impedes early stage muscle graft regeneration," *Frontiers in Neurology,* vol. 10, p. 252, 2019.

[63] S. Srinivasan *et al.*, "On prosthetic control: A regenerative agonist-antagonist myoneural interface," *Science Robotics,* vol. 2, no. 6, 2017.

[64] J. M. Souza, J. E. Cheesborough, J. H. Ko, M. S. Cho, T. A. Kuiken, and G. A. Dumanian, "Targeted muscle reinnervation: a novel approach to postamputation neuroma pain," *Clinical Orthopaedics and Related Research®,* vol. 472, no. 10, pp. 2984-2990, 2014.

[65] T. A. Kuiken, A. K. Barlow, L. Hargrove, and G. A. Dumanian, "Targeted muscle reinnervation for the upper and lower extremity," *Techniques in orthopaedics (Rockville, Md.),* vol. 32, no. 2, p. 109, 2017.

[66] L. A. Miller *et al.*, "Control of a six degree of freedom prosthetic arm after targeted muscle reinnervation surgery," *Archives of physical medicine and rehabilitation,* vol. 89, no. 11, pp. 2057-2065, 2008.

[67] M. S. Gart, J. M. Souza, and G. A. Dumanian, "Targeted muscle reinnervation in the upper extremity amputee: a technical roadmap," *The Journal of hand surgery,* vol. 40, no. 9, pp. 1877-1888, 2015.

[68] G. M. Hefferman, F. Zhang, M. J. Nunnery, and H. Huang, "Integration of surface electromyographic sensors with the transfemoral amputee socket: a comparison of four differing configurations," *Prosthet Orthot Int,* vol. 39, no. 2, pp. 166-73, Apr 2015, doi: 10.1177/0309364613516484.

[69] A. Fleming and H. H. Huang, "Proportional Myoelectric Control of a Powered Ankle Prosthesis for Postural Control under Expected Perturbation: A Pilot Study," in *2019 IEEE 16th International Conference on Rehabilitation Robotics (ICORR)*, 2019: IEEE, pp. 899-904.

[70] A. Fleming, S. Huang, E. Buxton, F. Hodges, and H. H. Huang, "Direct Continuous EMG control of a Powered Prosthetic Ankle for Improved Postural Control after Guided Physical Training: a Case Study," *Wearable Technologies,* vol. 2, 2021.

[71] T. Reissman, E. Halsne, R. Lipschutz, L. Miller, and T. Kuiken, "A novel gel liner system with embedded electrodes for use with upper limb myoelectric prostheses," *Plos one,* vol. 13, no. 6, p. e0198934, 2018.

[72] S. H. Yeon *et al.*, "Flexible Dry Electrodes for EMG Acquisition within Lower Extremity Prosthetic Sockets," in *2020 8th IEEE RAS/EMBS International Conference for Biomedical Robotics and Biomechatronics (BioRob)*: IEEE, pp. 1088-1095.

[73] H. A. Dewald *et al.*, "Stable, three degree-of-freedom myoelectric prosthetic control via chronic bipolar intramuscular electrodes: a case study," *Journal of neuroengineering and rehabilitation,* vol. 16, no. 1, p. 147, 2019.

[74] A. K. Vaskov *et al.*, "Surgically Implanted Electrodes Enable Real-Time Finger and Grasp Pattern Recognition for Prosthetic Hands," *medRxiv,* 2020.

[75] M. Ortiz-Catalan, R. Brånemark, B. Håkansson, and J. Delbeke, "On the viability of implantable electrodes for the natural control of artificial limbs: review and discussion," *Biomedical engineering online,* vol. 11, no. 1, pp. 1-24, 2012.

[76] J. Sigurðardóttir, "EMG as a Control Parameter In Lower Limb Prosthetics: Surface Vs. Implanted Electrodes," 2015.

[77] S. Salminger *et al.*, "Long-term implant of intramuscular sensors and nerve transfers for wireless control of robotic arms in above-elbow amputees," *Science Robotics,* vol. 4, no. 32, 2019.

[78] D. R. Merrill, J. Lockhart, P. R. Troyk, R. F. Weir, and D. L. Hankin, "Development of an implantable myoelectric sensor for advanced prosthesis control," *Artificial organs,* vol. 35, no. 3, pp. 249-252, 2011.

[79] P. Zhou *et al.*, "Decoding a new neural machine interface for control of artificial limbs," *J Neurophysiol,* vol. 98, no. 5, pp. 2974-82, Nov 2007, doi: 10.1152/jn.00178.2007.

[80] H. Huang, P. Zhou, G. Li, and T. A. Kuiken, "An analysis of EMG electrode configuration for targeted muscle reinnervation based neural machine interface," *IEEE Trans Neural Syst Rehabil Eng,* vol. 16, no. 1, pp. 37-45, Feb 2008, doi: 10.1109/TNSRE.2007.910282.

[81] B. R. Schlink, A. D. Nordin, and D. P. Ferris, "Comparison of Signal Processing Methods for Reducing Motion Artifacts in High-Density Electromyography During Human Locomotion," *IEEE Open Journal of Engineering in Medicine and Biology,* vol. 1, pp. 156-165, 2020.

[82] B. R. Schlink and D. P. Ferris, "A Lower Limb Phantom for Simulation and Assessment of Electromyography Technology," *IEEE Transactions on Neural Systems and Rehabilitation Engineering,* vol. 27, no. 12, pp. 2378-2385, 2019.

[83] H. Dimitrov, A. Bull, and D. Farina, "Real-Time Interface Algorithm for Ankle Kinematics and Stiffness from Electromyographic Signals," *IEEE Transactions on Neural Systems and Rehabilitation Engineering,* 2020.

[84] S. K. Au and H. M. Herr, "Powered ankle-foot prosthesis," *IEEE Robotics & Automation Magazine,* vol. 15, no. 3, pp. 52-59, 2008.

[85] A. J. Young, A. M. Simon, N. P. Fey, and L. J. Hargrove, "Intent recognition in a powered lower limb prosthesis using time history information," *Annals of biomedical engineering,* vol. 42, no. 3, pp. 631-641, 2014.

[86] Z. Liu, W. Lin, Y. Geng, and P. Yang, "Intent pattern recognition of lower-limb motion based on mechanical sensors," *IEEE/CAA Journal of Automatica Sinica,* vol. 4, no. 4, pp. 651-660, 2017.

[87] H. A. Varol and M. Goldfarb, "Real-time intent recognition for a powered knee and ankle transfemoral prosthesis," in *2007 IEEE 10th International Conference on Rehabilitation Robotics*, 2007: IEEE, pp. 16-23.

[88] D. Jin, J. Yang, R. Zhang, R. Wang, and J. Zhang, "Terrain identification for prosthetic knees based on electromyographic signal features," *Tsinghua Science and Technology,* vol. 11, no. 1, pp. 74-79, 2006.

[89] T. Hussain, N. Iqbal, H. F. Maqbool, M. Khan, M. I. Awad, and A. A. Dehghani-Sanij, "Intent based recognition of walking and ramp activities for amputee using sEMG based lower limb prostheses," *Biocybernetics and Biomedical Engineering,* 2020.

[90] F. Zhang and H. Huang, "Source selection for real-time user intent recognition toward volitional control of artificial legs," *IEEE J Biomed Health Inform,* vol. 17, no. 5, pp. 907-14, Sep 2013, doi: 10.1109/JBHI.2012.2236563.

[91] D. Joshi and M. E. Hahn, "Terrain and direction classification of locomotion transitions using neuromuscular and mechanical input," *Annals of biomedical engineering,* vol. 44, no. 4, pp. 1275-1284, 2016.

[92] J. D. Miller, M. S. Beazer, and M. E. Hahn, "Myoelectric walking mode classification for transtibial amputees," *IEEE Trans Biomed Eng,* vol. 60, no. 10, pp. 2745-50, Oct 2013, doi: 10.1109/TBME.2013.2264466.

[93] S. K. Au, P. Bonato, and H. Herr, "An EMG-position controlled system for an active ankle-foot prosthesis: an initial experimental study," in *9th International Conference on Rehabilitation Robotics, 2005. ICORR 2005.*, 2005: IEEE, pp. 375-379.

[94] B. H. Nakamura and M. E. Hahn, "Myoelectric activation pattern changes in the involved limb of individuals with transtibial amputation during locomotor state transitions," *Archives of physical medicine and rehabilitation,* vol. 98, no. 6, pp. 1180-1186, 2017.

[95] B. Hu, E. Rouse, and L. Hargrove, "Fusion of bilateral lower-limb neuromechanical signals improves prediction of locomotor activities," *Frontiers in Robotics and AI,* vol. 5, p. 78, 2018.

[96] D. Tkach, R. D. Lipschutz, S. B. Finucane, and L. J. Hargrove, "Myoelectric neural interface enables accurate control of a virtual multiple degree-of-freedom foot-ankle prosthesis," in *2013 IEEE 13th International Conference on Rehabilitation Robotics (ICORR)*, 2013: IEEE, pp. 1-4.

[97] L. J. Hargrove *et al.*, "Intuitive control of a powered prosthetic leg during ambulation: a randomized clinical trial," *Jama,* vol. 313, no. 22, pp. 2244-2252, 2015.

[98] M. A. Oskoei and H. Hu, "Support vector machine-based classification scheme for myoelectric control applied to upper limb," *IEEE transactions on biomedical engineering,* vol. 55, no. 8, pp. 1956-1965, 2008.

[99] A. E. Schultz and T. A. Kuiken, "Neural interfaces for control of upper limb prostheses: the state of the art and future possibilities," *PM&R,* vol. 3, no. 1, pp. 55-67, 2011.

[100] D. Madusanka, L. Wijayasingha, R. Gopura, Y. Amarasinghe, and G. Mann, "A review on hybrid myoelectric control systems for upper limb prosthesis," in *2015 Moratuwa Engineering Research Conference (MERCon)*, 2015: IEEE, pp. 136-141.

[101] N. Jiang, H. Rehbaum, I. Vujaklija, B. Graimann, and D. Farina, "Intuitive, online, simultaneous, and proportional myoelectric control over two degrees-of-freedom in upper limb amputees," *IEEE transactions on neural systems and rehabilitation engineering,* vol. 22, no. 3, pp. 501-510, 2013.

[102] H.-B. Xie, H. Huang, J. Wu, and L. Liu, "A comparative study of surface EMG classification by fuzzy relevance vector machine and fuzzy support vector machine," *Physiological measurement,* vol. 36, no. 2, p. 191, 2015.

[103] D. Tkach and L. J. Hargrove, "Neuromechanical sensor fusion yields highest accuracies in predicting ambulation mode transitions for trans-tibial amputees," in *2013 35th Annual International Conference of the IEEE Engineering in Medicine and Biology Society (EMBC)*, 2013: IEEE, pp. 3074-3077.

[104] J. Spanias, A. Simon, S. Finucane, E. Perreault, and L. J. Hargrove, "Online adaptive neural control of a robotic lower limb prosthesis," *Journal of neural engineering,* vol. 15, no. 1, p. 016015, 2018.

[105] A. M. Simon *et al.*, "Delaying ambulation mode transition decisions improves accuracy of a flexible control system for powered knee-ankle prosthesis," *IEEE Transactions on Neural Systems and Rehabilitation Engineering,* vol. 25, no. 8, pp. 1164-1171, 2016.

[106] K. H. Ha, H. A. Varol, and M. Goldfarb, "Volitional control of a prosthetic knee using surface electromyography," *IEEE Transactions on Biomedical Engineering,* vol. 58, no. 1, pp. 144-151, 2010.

[107] X. Zhang, D. Wang, Q. Yang, and H. Huang, "An automatic and user-driven training method for locomotion mode recognition for artificial leg control," *Annu Int Conf IEEE Eng Med Biol Soc,* vol. 2012, pp. 6116-9, 2012, doi: 10.1109/EMBC.2012.6347389.

[108] H. Huang, F. Zhang, Y. L. Sun, and H. He, "Design of a robust EMG sensing interface for pattern classification," *J Neural Eng,* vol. 7, no. 5, p. 056005, Oct 2010, doi: 10.1088/1741-2560/7/5/056005.

[109] L. Du, F. Zhang, H. He, and H. Huang, "Improving the performance of a neural-machine interface for prosthetic legs using adaptive pattern classifiers," in *2013 35th Annual International Conference of the IEEE Engineering in Medicine and Biology Society (EMBC)*, 2013: IEEE, pp. 1571-1574.

[110] J. Doud and J. Walsh, "Muscle fatigue and muscle length interaction: effect on the EMG frequency components," *Electromyography and clinical neurophysiology,* vol. 35, no. 6, p. 331, 1995.

[111] D. Tkach, H. Huang, and T. A. Kuiken, "Study of stability of time-domain features for electromyographic pattern recognition," *J Neuroeng Rehabil,* vol. 7, p. 21, May 21 2010, doi: 10.1186/1743-0003-7-21.

[112] L. Hargrove, K. Englehart, and B. Hudgins, "A training strategy to reduce classification degradation due to electrode displacements in pattern recognition based myoelectric control," *Biomedical signal processing and control,* vol. 3, no. 2, pp. 175-180, 2008.

[113] M. Liu, F. Zhang, and H. H. Huang, "An Adaptive Classification Strategy for Reliable Locomotion Mode Recognition," *Sensors (Basel),* vol. 17, no. 9, Sep 4 2017, doi: 10.3390/s17092020.

[114] F. Zhang, M. Liu, and H. Huang, "Investigation of Timing to Switch Control Mode in Powered Knee Prostheses during Task Transitions," *PLoS One,* vol. 10, no. 7, p. e0133965, 2015, doi: 10.1371/journal.pone.0133965.

[115] J. A. Spanias, E. J. Perreault, and L. J. Hargrove, "Detection of and compensation for EMG disturbances for powered lower limb prosthesis control," *IEEE Transactions on Neural Systems and Rehabilitation Engineering,* vol. 24, no. 2, pp. 226-234, 2015.

[116] F. Zhang, M. Liu, and H. Huang, "Effects of locomotion mode recognition errors on volitional control of powered above-knee prostheses," *IEEE Trans Neural Syst Rehabil Eng,* vol. 23, no. 1, pp. 64-72, Jan 2015, doi: 10.1109/TNSRE.2014.2327230.

[117] A. Fleming, S. Huang, E. Buxton, F. Hodges, and H. H. Huang, "Direct continuous electromyographic control of a powered prosthetic ankle for improved postural control after guided physical training: A case study," *Wearable Technologies,* vol. 2, 2021.

[118] C. D. Hoover, G. D. Fulk, and K. B. Fite, "Stair ascent with a powered transfemoral prosthesis under direct myoelectric control," *IEEE/ASME Transactions on Mechatronics,* vol. 18, no. 3, pp. 1191-1200, 2012.

[119] S. Huang, J. P. Wensman, and D. P. Ferris, "An experimental powered lower limb prosthesis using proportional myoelectric control," *Journal of Medical Devices,* vol. 8, no. 2, 2014.

[120] S.-K. Wu, G. Waycaster, and X. Shen, "Electromyography-based control of active above-knee prostheses," *Control Engineering Practice,* vol. 19, no. 8, pp. 875-882, 2011.

[121] C. D. Hoover, G. D. Fulk, and K. B. Fite, "The design and initial experimental validation of an active myoelectric transfemoral prosthesis," *Journal of Medical Devices,* vol. 6, no. 1, 2012.

[122] E. A. Rogers, M. E. Carney, S. H. Yeon, T. R. Clites, D. Solav, and H. M. Herr, "An Ankle-Foot Prosthesis for Rock Climbing Augmentation," *IEEE Transactions on Neural Systems and Rehabilitation Engineering: a Publication of the IEEE Engineering in Medicine and Biology Society,* 2020.

[123] A. S. Aruin, J. J. Nicholas, and M. L. Latash, "Anticipatory postural adjustments during standing in below-the-knee amputees," (in eng), *Clinical biomechanics (Bristol, Avon),* vol. 12, no. 1, pp. 52-59, Jan 1997.

[124] J. G. Buckley, D. O'Driscoll, and S. J. Bennett, "Postural sway and active balance performance in highly active lower-limb amputees," *Am J Phys Med Rehabil,* vol. 81, no. 1, pp. 13-20, Jan 2002. [Online]. Available: https://www.ncbi.nlm.nih.gov/pubmed/11807327.

[125] P. X. Ku, N. A. Abu Osman, and W. A. Wan Abas, "Balance control in lower extremity amputees during quiet standing: a systematic review," *Gait Posture,* vol. 39, no. 2, pp. 672-82, Feb 2014, doi: 10.1016/j.gaitpost.2013.07.006.

[126] A. H. Vrieling *et al.*, "Balance control on a moving platform in unilateral lower limb amputees," *Gait Posture,* vol. 28, no. 2, pp. 222-8, Aug 2008, doi: 10.1016/j.gaitpost.2007.12.002.

[127] B. E. Lawson, H. A. Varol, and M. Goldfarb, "Standing stability enhancement with an intelligent powered transfemoral prosthesis," *IEEE Trans Biomed Eng,* vol. 58, no. 9, pp. 2617-24, Sep 2011, doi: 10.1109/TBME.2011.2160173.

[128] A. H. Shultz, B. E. Lawson, and M. Goldfarb, "Variable Cadence Walking and Ground Adaptive Standing With a Powered Ankle Prosthesis," *IEEE Trans Neural Syst Rehabil Eng,* vol. 24, no. 4, pp. 495-505, Apr 2016, doi: 10.1109/TNSRE.2015.2428196.

[129] M. J. Santos, N. Kanekar, and A. S. Aruin, "The role of anticipatory postural adjustments in compensatory control of posture: 1. Electromyographic analysis," *J Electromyogr Kinesiol,* vol. 20, no. 3, pp. 388-97, Jun 2010, doi: 10.1016/j.jelekin.2009.06.006.

[130] L. J. Hargrove, A. M. Simon, R. D. Lipschutz, S. B. Finucane, and T. A. Kuiken, "Real-time myoelectric control of knee and ankle motions for transfemoral amputees," *JAMA,* vol. 305, no. 15, pp. 1542-4, Apr 20 2011, doi: 10.1001/jama.2011.465.

[131] H. Huang, F. Zhang, L. J. Hargrove, Z. Dou, D. R. Rogers, and K. B. Englehart, "Continuous locomotion-mode identification for prosthetic legs based on neuromuscular-mechanical fusion," *IEEE Trans Biomed Eng,* vol. 58, no. 10, pp. 2867-75, Oct 2011, doi: 10.1109/TBME.2011.2161671.

[132] L. J. Hargrove *et al.*, "Robotic leg control with EMG decoding in an amputee with nerve transfers," *N Engl J Med,* vol. 369, no. 13, pp. 1237-42, Sep 26 2013, doi: 10.1056/NEJMoa1300126.

[133] J. Wang, O. A. Kannape, and H. M. Herr, "Proportional EMG control of ankle plantar flexion in a powered transtibial prosthesis," *IEEE Int Conf Rehabil Robot,* vol. 2013, p. 6650391, Jun 2013, doi: 10.1109/ICORR.2013.6650391.

[134] G. D. F. Carl D. Hoover, Kevin B. Fite, "Stair Ascent With a Powered Transfemoral Prosthesis Under Direct Myoelectric Control," *IEEE/ASME Transactions on Mechatronics,* vol. 18, no. 3, 2012.

[135] S. Huang, J. P. Wensman, and D. P. Ferris, "Locomotor Adaptation by Transtibial Amputees Walking With an Experimental Powered Prosthesis Under Continuous Myoelectric Control," *IEEE Trans Neural Syst Rehabil Eng,* vol. 24, no. 5, pp. 573-81, May 2016, doi: 10.1109/TNSRE.2015.2441061.

[136] J. A. Dawley, K. B. Fite, and G. D. Fulk, "EMG control of a bionic knee prosthesis: exploiting muscle co-contractions for improved locomotor function," *IEEE Int Conf Rehabil Robot,* vol. 2013, p. 6650389, Jun 2013, doi: 10.1109/ICORR.2013.6650389.

[137] O. A. Kannape and H. M. Herr, "Volitional control of ankle plantar flexion in a powered transtibial prosthesis during stair-ambulation," *Conf Proc IEEE Eng Med Biol Soc,* vol. 2014, pp. 1662-5, 2014, doi: 10.1109/EMBC.2014.6943925.

[138] S. Huang and H. Huang, "Voluntary Control of Residual Antagonistic Muscles in Transtibial Amputees: Feedforward Ballistic Contractions and Implications for Direct Neural Control of Powered Lower Limb Prostheses," *IEEE Trans Neural Syst Rehabil Eng,* vol. 26, no. 4, pp. 894-903, Apr 2018, doi: 10.1109/TNSRE.2018.2811544.

[139] S. Huang and H. H. Huang, "Voluntary Control of Residual Antagonistic Muscles in Transtibial Amputees: Reciprocal Activation, Coactivation, and Implications for Direct Neural Control of Powered Lower Limb Prostheses," *IEEE Trans Neural Syst Rehabil Eng,* Dec 7 2018, doi: 10.1109/TNSRE.2018.2885641.

[140] Y. Asai, S. Tateyama, and T. Nomura, "Learning an intermittent control strategy for postural balancing using an EMG-based human-computer interface," *PLoS One,* vol. 8, no. 5, p. e62956, 2013, doi: 10.1371/journal.pone.0062956.

[141] I. D. Loram, H. Gollee, M. Lakie, and P. J. Gawthrop, "Human control of an inverted pendulum: is continuous control necessary? Is intermittent control effective? Is intermittent control physiological?," *J Physiol,* vol. 589, no. Pt 2, pp. 307-24, Jan 15 2011, doi: 10.1113/jphysiol.2010.194712.

[142] R. E. Alcaide-Aguirre, D. C. Morgenroth, and D. P. Ferris, "Motor control and learning with lower-limb myoelectric control in amputees," *J Rehabil Res Dev,* vol. 50, no. 5, pp. 687-98, 2013. [Online]. Available: https://www.ncbi.nlm.nih.gov/pubmed/24013916.

[143] K. E. Gordon and D. P. Ferris, "Proportional myoelectric control of a virtual object to investigate human efferent control," *Exp Brain Res,* vol. 159, no. 4, pp. 478-86, Dec 2004, doi: 10.1007/s00221-004-1970-6.

[144] A. Fleming, S. Huang, and H. H. Huang, "Coordination of Voluntary Residual Muscle Contractions in Transtibial Amputees: a Pilot Study," *Conf Proc IEEE Eng Med Biol Soc,* vol. 2018, pp. 2128-2131, Jul 2018, doi: 10.1109/EMBC.2018.8512674.

[145] S. Huang and D. P. Ferris, "Muscle activation patterns during walking from transtibial amputees recorded within the residual limb-prosthetic interface," *J Neuroeng Rehabil,* vol. 9, p. 55, Aug 10 2012, doi: 10.1186/1743-0003-9-55.

[146] J. R. Franz and R. Kram, "How does age affect leg muscle activity/coactivity during uphill and downhill walking?," *Gait Posture,* vol. 37, no. 3, pp. 378-84, Mar 2013, doi: 10.1016/j.gaitpost.2012.08.004.

[147] H. Muller and D. Sternad, "Motor learning: changes in the structure of variability in a redundant task," *Adv Exp Med Biol,* vol. 629, pp. 439-56, 2009, doi: 10.1007/978-0-387-77064-2_23.

[148] T. Agcayazi, M. McKnight, P. Sotory, H. Huang, T. Ghosh, and A. Bozkurt, "A scalable shear and normal force sensor for prosthetic sensing," in *2017 IEEE SENSORS*, 29 Oct.-1 Nov. 2017 2017, pp. 1-3, doi: 10.1109/ICSENS.2017.8233977.

[149] N. Vanicek, S. Strike, L. McNaughton, and R. Polman, "Postural responses to dynamic perturbations in amputee fallers versus nonfallers: a comparative study with able-bodied subjects," *Archives of physical medicine and rehabilitation,* vol. 90, no. 6, pp. 1018-1025, 2009.

[150] T. Elery, S. Rezazadeh, C. Nesler, and R. D. Gregg, "Design and Validation of a Powered Knee–Ankle Prosthesis With High-Torque, Low-Impedance Actuators," *IEEE Transactions on Robotics,* 2020.

[151] M. F. Eilenberg, H. Geyer, and H. Herr, "Control of a powered ankle–foot prosthesis based on a neuromuscular model," *IEEE transactions on neural systems and rehabilitation engineering,* vol. 18, no. 2, pp. 164-173, 2010.

[152] S. K. Au, J. Weber, and H. Herr, "Powered ankle--foot prosthesis improves walking metabolic economy," *IEEE Transactions on robotics,* vol. 25, no. 1, pp. 51-66, 2009.

[153] N. Kanekar and A. S. Aruin, "Improvement of anticipatory postural adjustments for balance control: effect of a single training session," *Journal of Electromyography and Kinesiology,* vol. 25, no. 2, pp. 400-405, 2015.

[154] C. D. MacKinnon *et al.*, "Preparation of anticipatory postural adjustments prior to stepping," *Journal of neurophysiology,* vol. 97, no. 6, pp. 4368-4379, 2007.

[155] M. J. Santos, N. Kanekar, and A. S. Aruin, "The role of anticipatory postural adjustments in compensatory control of posture: 1. Electromyographic analysis," *Journal of Electromyography and Kinesiology,* vol. 20, no. 3, pp. 388-397, 2010.

[156] M. J. Santos, N. Kanekar, and A. S. Aruin, "The role of anticipatory postural adjustments in compensatory control of posture: 2. Biomechanical analysis," *Journal of Electromyography and Kinesiology,* vol. 20, no. 3, pp. 398-405, 2010.

[157] A. S. Aruin, "The effect of asymmetry of posture on anticipatory postural adjustments," *Neuroscience letters,* vol. 401, no. 1-2, pp. 150-153, 2006.

[158] T. Shiratori and M. L. Latash, "Anticipatory postural adjustments during load catching by standing subjects," *Clinical neurophysiology,* vol. 112, no. 7, pp. 1250-1265, 2001.

[159] S. De Wolf, H. Slijper, and M. L. Latash, "Anticipatory postural adjustments during self-paced and reaction-time movements," *Experimental Brain Research,* vol. 121, no. 1, pp. 7-19, 1998.

[160] A. Fleming, N. Stafford, S. Huang, X. Hu, D. P. Ferris, and H. H. Huang, "Myoelectric control of robotic lower limb prostheses: a review of electromyography interfaces, control paradigms, challenges and future directions," *Journal of Neural Engineering,* 2021.

[161] D. F. Rusaw and S. Ramstrand, "Validation of the Inverted Pendulum Model in standing for transtibial prosthesis users," *Clinical Biomechanics,* vol. 31, pp. 100-106, 2016.

[162] F. B. Horak and L. M. Nashner, "Central programming of postural movements: adaptation to altered support-surface configurations," *Journal of neurophysiology,* vol. 55, no. 6, pp. 1369-1381, 1986.

[163] F. B. Horak, D. M. Wrisley, and J. Frank, "The balance evaluation systems test (BESTest) to differentiate balance deficits," *Physical therapy,* vol. 89, no. 5, pp. 484-498, 2009.

[164] A. O. Perotto, *Anatomical guide for the electromyographer: the limbs and trunk*. Charles C Thomas Publisher, 2011.

[165] C. Runge, C. Shupert, F. Horak, and F. Zajac, "Ankle and hip postural strategies defined by joint torques," *Gait & posture,* vol. 10, no. 2, pp. 161-170, 1999.

[166] N. Vanicek, S. Strike, L. McNaughton, and R. Polman, "Gait patterns in transtibial amputee fallers vs. non-fallers: Biomechanical differences during level walking," *Gait & Posture,* vol. 29, no. 3, pp. 415-420, 2009.

[167] A. K. Silverman and R. R. Neptune, "Muscle and prosthesis contributions to amputee walking mechanics: a modeling study," *Journal of biomechanics,* vol. 45, no. 13, pp. 2271-2278, 2012.

[168] M. J. Nederhand, E. H. Van Asseldonk, H. van der Kooij, and H. S. Rietman, "Dynamic Balance Control (DBC) in lower leg amputee subjects; contribution of the regulatory activity of the prosthesis side," *Clinical Biomechanics,* vol. 27, no. 1, pp. 40-45, 2012.

[169] V. Agrawal, R. Gailey, I. Gaunaurd, R. Gailey III, and C. O'Toole, "Weight distribution symmetry during the sit-to-stand movement of unilateral transtibial amputees," *Ergonomics,* vol. 54, no. 7, pp. 656-664, 2011.

[170] B. L. Fylstra, I.-C. Lee, S. Huang, A. Brandt, M. D. Lewek, and H. H. Huang, "Human-prosthesis coordination: A preliminary study exploring coordination with a powered ankle-foot prosthesis," *Clinical Biomechanics,* vol. 80, p. 105171, 2020.

[171] J. R. Montgomery and A. M. Grabowski, "Use of a powered ankle–foot prosthesis reduces the metabolic cost of uphill walking and improves leg work symmetry in people with transtibial amputations," *Journal of The Royal Society Interface,* vol. 15, no. 145, p. 20180442, 2018.

[172] R. E. Quesada, J. M. Caputo, and S. H. Collins, "Increasing ankle push-off work with a powered prosthesis does not necessarily reduce metabolic rate for transtibial amputees," *Journal of Biomechanics,* vol. 49, no. 14, pp. 3452-3459, 2016.

[173] M. Woollacott and A. Shumway-Cook, "Attention and the control of posture and gait: a review of an emerging area of research," *Gait & posture,* vol. 16, no. 1, pp. 1-14, 2002.

[174] A. C. Geurts and T. W. Mulder, "Attention demands in balance recovery following lower limb amputation," *Journal of Motor Behavior,* vol. 26, no. 2, pp. 162-170, 1994.

[175] M. C. Tresch, P. Saltiel, and E. Bizzi, "The construction of movement by the spinal cord," *Nature neuroscience,* vol. 2, no. 2, pp. 162-167, 1999.

[176] L. H. Ting and J. L. McKay, "Neuromechanics of muscle synergies for posture and movement," *Current opinion in neurobiology,* vol. 17, no. 6, pp. 622-628, 2007.

[177] G. Torres-Oviedo and L. H. Ting, "Muscle synergies characterizing human postural responses," *Journal of neurophysiology,* vol. 98, no. 4, pp. 2144-2156, 2007.

[178] A. Sawers, J. L. Allen, and L. H. Ting, "Long-term training modifies the modular structure and organization of walking balance control," *Journal of neurophysiology,* vol. 114, no. 6, pp. 3359-3373, 2015.

[179] T. Flash and B. Hochner, "Motor primitives in vertebrates and invertebrates," *Current opinion in neurobiology,* vol. 15, no. 6, pp. 660-666, 2005.

[180] D. J. Clark, L. H. Ting, F. E. Zajac, R. R. Neptune, and S. A. Kautz, "Merging of healthy motor modules predicts reduced locomotor performance and muscle coordination complexity post-stroke," *Journal of neurophysiology,* vol. 103, no. 2, pp. 844-857, 2010.

[181] J. L. Allen, J. L. McKay, A. Sawers, M. E. Hackney, and L. H. Ting, "Increased neuromuscular consistency in gait and balance after partnered, dance-based rehabilitation in Parkinson's disease," *Journal of Neurophysiology,* vol. 118, no. 1, pp. 363-373, 2017.

[182] S. Safavynia, G. Torres-Oviedo, and L. Ting, "Muscle synergies: implications for clinical evaluation and rehabilitation of movement," *Topics in spinal cord injury rehabilitation,* vol. 17, no. 1, pp. 16-24, 2011.

[183] A. Danna-dos-Santos, K. Slomka, V. M. Zatsiorsky, and M. L. Latash, "Muscle modes and synergies during voluntary body sway," *Experimental Brain Research,* vol. 179, no. 4, pp. 533-550, 2007.

[184] A. M. Haith and J. W. Krakauer, "Model-based and model-free mechanisms of human motor learning," in *Progress in motor control*: Springer, 2013, pp. 1-21.

[185] C. D. Frith, S.-J. Blakemore, and D. M. Wolpert, "Abnormalities in the awareness and control of action," *Philosophical Transactions of the Royal Society of London. Series B: Biological Sciences,* vol. 355, no. 1404, pp. 1771-1788, 2000.

[186] E. Todorov, "Optimality principles in sensorimotor control," *Nat Neurosci,* vol. 7, no. 9, pp. 907-15, Sep 2004, doi: 10.1038/nn1309.

[187] S. A. Chvatal and L. H. Ting, "Voluntary and reactive recruitment of locomotor muscle synergies during perturbed walking," *Journal of Neuroscience,* vol. 32, no. 35, pp. 12237-12250, 2012.

[188] N. Picard, Y. Matsuzaka, and P. L. Strick, "Extended practice of a motor skill is associated with reduced metabolic activity in M1," *Nature neuroscience,* vol. 16, no. 9, pp. 1340-1347, 2013.

[189] L. Jäncke, N. Shah, and M. Peters, "Cortical activations in primary and secondary motor areas for complex bimanual movements in professional pianists," *Cognitive Brain Research,* vol. 10, no. 1-2, pp. 177-183, 2000.

[190] R. Kawai *et al.*, "Motor cortex is required for learning but not for executing a motor skill," *Neuron,* vol. 86, no. 3, pp. 800-812, 2015.

[191] R. L. Routson, D. J. Clark, M. G. Bowden, S. A. Kautz, and R. R. Neptune, "The influence of locomotor rehabilitation on module quality and post-stroke hemiparetic walking performance," *Gait & posture,* vol. 38, no. 3, pp. 511-517, 2013.

[192] D. A. Winter, F. Prince, J. Frank, C. Powell, and K. F. Zabjek, "Unified theory regarding A/P and M/L balance in quiet stance," *Journal of neurophysiology,* vol. 75, no. 6, pp. 2334-2343, 1996.

[193] J. H. Zar, *Biostatistical analysis*. Pearson Education India, 1999.

[194] H. B. Hayes, S. A. Chvatal, M. A. French, L. H. Ting, and R. D. Trumbower, "Neuromuscular constraints on muscle coordination during overground walking in persons with chronic incomplete spinal cord injury," *Clinical Neurophysiology,* vol. 125, no. 10, pp. 2024-2035, 2014.

[195] S. A. Chvatal, G. Torres-Oviedo, S. A. Safavynia, and L. H. Ting, "Common muscle synergies for control of center of mass and force in nonstepping and stepping postural behaviors," *Journal of neurophysiology,* vol. 106, no. 2, pp. 999-1015, 2011.

[196] S. A. Chvatal, J. M. Macpherson, G. Torres-Oviedo, and L. H. Ting, "Absence of postural muscle synergies for balance after spinal cord transection," *Journal of neurophysiology,* vol. 110, no. 6, pp. 1301-1310, 2013.

[197] S. A. Safavynia and L. H. Ting, "Task-level feedback can explain temporal recruitment of spatially fixed muscle synergies throughout postural perturbations," *Journal of neurophysiology,* vol. 107, no. 1, pp. 159-177, 2012.

[198] J. Frère and F. Hug, "Between-subject variability of muscle synergies during a complex motor skill," *Frontiers in computational neuroscience,* vol. 6, p. 99, 2012.

[199] A. Mansfield, C. J. Danells, E. Inness, G. Mochizuki, and W. E. McIlroy, "Between-limb synchronization for control of standing balance in individuals with stroke," *Clinical Biomechanics,* vol. 26, no. 3, pp. 312-317, 2011.

[200] L. Hargrove, A. M. Simon, S. B. Finucane, and R. D. Lipschutz, "Myoelectric control of a powered transfemoral prosthesis during non-weight-bearing activities," in *Proceedings of the 2011 MyoElectric controls/powered prosthetics symposium, Fredericton. Myoelectric Symposium*, 2011, pp. 1-41.

[201] A. M. Simon, N. P. Fey, K. A. Ingraham, A. J. Young, and L. J. Hargrove, "Powered prosthesis control during walking, sitting, standing, and non-weight bearing activities using neural and mechanical inputs," in *2013 6th International IEEE/EMBS Conference on Neural Engineering (NER)*, 2013: IEEE, pp. 1174-1177.

[202] A. J. Young, A. M. Simon, N. P. Fey, and L. J. Hargrove, "Classifying the intent of novel users during human locomotion using powered lower limb prostheses," in *2013 6th International IEEE/EMBS Conference on Neural Engineering (NER)*, 2013: IEEE, pp. 311-314.

[203] L. J. Hargrove, A. M. Simon, R. Lipschutz, S. B. Finucane, and T. A. Kuiken, "Non-weight-bearing neural control of a powered transfemoral prosthesis," *Journal of neuroengineering and rehabilitation,* vol. 10, no. 1, p. 62, 2013.

[204] F. Zhang, M. Liu, S. Harper, M. Lee, and H. Huang, "Engineering platform and experimental protocol for design and evaluation of a neurally-controlled powered transfemoral prosthesis," *JoVE (Journal of Visualized Experiments),* no. 89, p. e51059, 2014.

[205] A. Young, T. Kuiken, and L. Hargrove, "Analysis of using EMG and mechanical sensors to enhance intent recognition in powered lower limb prostheses," *Journal of neural engineering,* vol. 11, no. 5, p. 056021, 2014.

[206] F. Zhang, M. Liu, and H. Huang, "Effects of Locomotion Mode Recognition Errors on Volitional Control of Powered Above-Knee Prostheses," *IEEE Transactions on Neural Systems and Rehabilitation Engineering,* vol. 23, no. 1, pp. 64-72, 2015, doi: 10.1109/TNSRE.2014.2327230.

[207] J. A. Spanias, A. M. Simon, K. A. Ingraham, and L. J. Hargrove, "Effect of additional mechanical sensor data on an EMG-based pattern recognition system for a powered leg prosthesis," in *2015 7th International IEEE/EMBS Conference on Neural Engineering (NER)*, 2015: IEEE, pp. 639-642.

[208] R. E. Alcaide-Aguirre, D. C. Morgenroth, and D. P. Ferris, "Motor control and learning with lower-limb myoelectric control in amputees," *J. Rehabil. Res. Dev,* vol. 50, no. 5, pp. 687-698, 2013.

[209] B. Chen, Q. Wang, and L. Wang, "Promise of using surface EMG signals to volitionally control ankle joint position for powered transtibial prostheses," in *2014 36th Annual International Conference of the IEEE Engineering in Medicine and Biology Society*, 2014: IEEE, pp. 2545-2548.

[210] S. Huang and H. Huang, "Voluntary control of residual antagonistic muscles in transtibial amputees: Feedforward ballistic contractions and implications for direct neural control of powered lower limb prostheses," *IEEE Transactions on Neural Systems and Rehabilitation Engineering,* vol. 26, no. 4, pp. 894-903, 2018.